REPUBLIC OF TURKEY

YILDIZ TECHNICAL UNIVERSITY

GRADUATE SCHOOL OF NATURAL AND APPLIED SCIENCES

INVESTIGATION OF ENERGY GENERATION POTENTIAL OF REVERSE ELECTRODIALYSIS FED WITH SYNTHETIC AND REAL SOLUTIONS

Ali ZOUNGRANA

DOCTOR OF PHILOSOPHY THESIS

Department of Environmental Engineering

Environmental Engineering Program

Advisor

Prof. Dr. Mehmet ÇAKMAKCI

December, 2020

REPUBLIC OF TURKEY

YILDIZ TECHNICAL UNIVERSITY

GRADUATE SCHOOL OF NATURAL AND APPLIED SCIENCES

INVESTIGATION OF ENERGY GENERATION POTENTIAL OF REVERSE ELECTRODIALYSIS FED WITH SYNTHETIC AND REAL SOLUTIONS

A thesis submitted by Ali ZOUNGRANA in partial fulfillment of the requirements for the degree of DOCTOR OF PHILOSOPHY is approved by the committee on 22.12.2020 in Department of Environmental Engineering, Environmental Engineering Program.

Prof. Dr. Mehmet ÇAKMAKCI

Yıldız Technical University

Advisor

Approved By the Examining Committee

Prof. Dr. Mehmet ÇAKMAKCI, Advisor
Yıldız Technical University _____

Prof. Dr. Doğan KARADAĞ, Jury Member
Yıldız Technical University _____

Prof. Dr. Mahir İNCE, Jury Member
Gebze Technical University _____

Prof. Dr. YAŞAR AVŞAR, Jury Member
Yıldız Technical University _____

Prof. Dr. ERKAN ŞAHİNKAYA, Jury Member
İstanbul Medeniyet University _____

I hereby declare that I have obtained the required legal permissions during data collection and exploitation procedures, that I have made the in-text citations and cited the references properly, that I haven't falsified and/or fabricated research data and results of the study and that I have abided by the principles of the scientific research and ethics during my Thesis Study under the title of Investigation of Energy Generation Potential of Reverse Electrodialysis Fed with Synthetic and Real Solutions supervised by my supervisor, Prof. Dr. Mehmet ÇAKMAKÇI. In the case of a discovery of false statement, I am to acknowledge any legal consequence.

Ali ZOUNGRANA

Signature

This study was supported by Yildiz Technical University Scientific Research Projects Grant No: FDK-2020-3860.

Dedicated to my family

and

my dearest friend

ACKNOWLEDGEMENTS

Above all, I would like to express my gratitude to Prof. Dr. Mehmet ÇAKMAKCI, who, in addition to being my advisor and project leader was a friend on whom I could count at any time. I appreciate his assistance, his valuable and precious advice during the preparation of my thesis; I could not have imagined having a better advisor for my Ph.D. study. I would also like to thank my jury members who guided, read, and corrected my work, and the professors and staff of the Department of Environmental Engineering YTU for giving me adequate education and for letting me feel at home. I will not forget all those values given to me.

I would like to express my thanks to Assoc. Prof. Süreyya AYDIN YÜKSEL and to the laboratory staff, especially to Research Assistant Oruç K. TÜRK, İsmail Hakkı ZENGİN, for their collaboration and support during the experimental study of my thesis. My sincere appreciation goes also to Z40 office graduate students for their assistance, advice, and memorable time spent together during this investigation.

Most of all, my mother and Father, Salimata ZOUNGRANA and Saga ZOUNGRANA deserve the biggest appreciation and gratitude. Your blessings, support, encouragement, and loves gave me strength during my studies. Finally, my thanks go towards my dearest Eunice F.B. OUALI, my sisters, brother, relatives, and friends who have actively supported me and have been present at all times with ideas, advice, and encouragement.

Ali ZOUNGRANA

TABLE OF CONTENTS

LIST OF SYMBOLS

A	Ampere
E	Energy
g	Gravity
I	Intensity
J	Joule
P	Power
Q	Volumetric flow
TW	Terrawatt
V	Volt
W	Watt
Wh	Watt-heure
ρ	Density
Ω	Ohm

LIST OF ABBREVIATIONS

ABT	Advanced biological Treatment
AEM	Anion Exchange Membrane
BMED	Bipolar Membrane Electrodialysis
CEM	Cation Exchange Membrane
COD	Chemical Oxygen Demand
DD	Diffusion Dialysis
ED	Electrodialysis
EDX	Energy-Dispersive X-ray Spectroscopy
EPA	Environmental Protection Agency
EROI	Energy Return on Investment
ERS	Electrode Rinse Solution
FC	Fuel Cells
FO	Forward Osmosis
FTIR	Fourier-Transform Infrared Spectroscopy
GHG	Greenhouse Gasses
HC	High Compartment
IEC	Ion Exchange Capacity
IEM	Ion Exchange Membrane
LC	Low Compartment
MBR	Membrane Bioreactor
MCDI	Membrane Capacitive Deionization
MD	Membrane Distillation
MF	Microfiltration

MT	Mechanochemical Turbine
NF	Nanofiltration
NOM	Natural Organic Matter
OCV	Open-Circuit Voltage
PD	Power Density
PRO	Pressure Retarded Osmosis
RCD	Reversal of the Capacitive Deionization
RE	Renewable Energy
RED	Reverse Electrodialysis
RFB	Redox Flow Batteries
RO	Reverse Osmosis
SEM	Scanning Electron Microscopy
SGE	Salinity Gradient Energy
SGP	Salinity Gradient Power
UF	Ultrafiltration
VPDU	Vapor Pressure Difference Utilization
WWTP	Wastewater Treatment Plant

LIST OF FIGURES

LIST OF TABLES

ABSTRACT

Investigation of Energy Generation Potential of Reverse Electrodialysis Fed with Synthetic and Real Solutions

Ali ZOUNGRANA

Department of Environmental Engineering

Doctor of Philosophy Thesis

Advisor: Prof. Dr. Mehmet ÇAKMAKCI

In addition to being quantitatively limited, fossil fuel is negative to the earth by inducing climate change. The energy transition is inevitable, and many alternatives and renewable energy sources are being considered to replace fossil fuels. Hydropower, wind and solar energy are leaders in the renewable energy world, but huge and accessible other energy sources such as salinity gradient power (SGP) exist and need to be collected to contribute to the energy demand. SGP is mainly extracted with reverse electrodialysis (RED) and pressure retarded osmosis (PRO) systems.

A lab-scale RED module was constructed and used to monitor the energy generation potential of different water bodies and the parameters associated with the performance of the process. The optimal feed solutions concentration, flow rate and their importance in improving the power density in RED were investigated and the experimental results showed that increasing the flow rate is beneficial by augmenting the power output of RED, but too high, it harms the process performance. The results demonstrated that the voltage and the stack resistance increased with increasing number of cell-pairs but the increasing trend of the voltage decreased from the linear trend due to the stack resistance.

Lastly, the RED power output performance with treated different municipal wastewaters was investigated together with natural seawater and synthetic solutions. The synthetic solutions resulted in the highest power density. Among the wastewaters, ultrafiltration (UF) effluent was more attractive for RED compared to membrane bioreactor (MBR) and advanced biological treatment (ABT) effluents. The SEM-EDX analysis showed that Mg^{2+} and Ca^{2+} were present in natural solutions and may have contributed to reducing the power output. Although treated municipal wastewaters discharged into seawater are important sources of RED-SGP, feed solutions quality together with improved, highly selective and cost-effective ion exchange membranes (IEMs) are necessary to optimize the power output.

Keywords: Ion exchange membrane, municipal wastewater, renewable energy, reverse electrodialysis, salinity gradient power.

ÖZET

Sentetik ve Gerçek Çözeltilerle Beslenen Ters Elektrodiyalizin Enerji Üretim Potansiyelinin Araştırılması

Ali ZOUNGRANA

Çevre Mühendisliği Bölümü

Doktora Tezi

Danışman: Prof. Dr. Mehmet ÇAKMAKCI

Fosil yakıtlar, niceliksel olarak sınırlı olmasının yanı sıra, iklim değişikliğine yol açarak yeryüzünü olumsuz etkilemektedir. Enerji geçişi kaçınılmazdır ve birçok alternatif ve yenilenebilir enerji kaynağının fosil yakıtın yerini alacağı düşünülmektedir. Yenilenebilir enerji dünyasında rüzgar ve güneş enerjisi liderdir, ancak tuzluluk gradyan gücü (SGP) gibi devasa ve erişilebilir diğer enerji kaynakları da mevcuttur ve enerji ihtiyacına katkıda bulunmak için toplanmaları gerekmektedir. SGP, esas olarak ters elektrodiyaliz (RED) ve basınç geciktirilmiş ozmoz (PRO) sistemleri ile elde edilir.

Laboratuvar ölçeğinde bir RED modülü inşa edildi ve farklı su kütlelerinin enerji üretim potansiyelini ve proses performansı ile ilişkili parametreleri izlemek için kullanıldı. Optimal besleme çözeltileri konsantrasyonu, akış hızı ve RED güç yoğunluğu geliştirmek önemleri incelendi ve sonuçlar, besleme çözeltilerinin akış hızındaki artışın güç çıkışını artırarak RED için faydalı olduğunu, ancak çok yüksek akış hızının işlem performansına zarar verdiğini gösterdi. Sonuçlar ayrıca, voltaj ve

yığın direncinin artan çift hücre sayısı ile arttığını, ancak voltajın artan eğiliminin, yığın direnci nedeniyle doğrusal eğilimden düştüğünü gösterdi.

Son olarak, arıtılmış farklı belediye atık suları, gerçek deniz suyu ve sentetik solüsyonlarla birlikte RED güç performansı incelenmiştir. En yüksek güç yoğunluğu sentetik çözeltilerden elde edildi. Atıksular arasında, ultrafiltrasyon (UF) permeatı, membran biyoreaktör (MBR) ve ileri biyolojik arıtma (ABT) permeatlarına kıyasla RED için daha cazipti. SEM-EDX analizi, Mg^{2+} ve Ca^{2+}'nın doğal çözeltilerde bulunduğunu ve güç çıkışını azaltmaya katkıda bulunmuş olabileceğini gösterdi. Her ne kadar deniz suyuna deşarj edilen arıtılmış belediye atık suları RED ile önemli enerji kaynakları olsa da, güç çıkışını artırmak ve optimize etmek için iyileştirilmiş, oldukça seçici ve uygun maliyetli iyon değişim membranlarla (IEM) birlikte yüksek çözelti kalitesi gereklidir.

Anahtar Kelimeler: İyon değişim membranı, evsel atıksu, yenilenebilir enerji, ters elektrodiyaliz, tuzluluk gradyan gücü.

1
INTRODUCTION

1.1 Literature Review

The quest for energy pushed human beings into investigating different possibilities to maximize energy production. This high interest in energy resulted in uncontrolled use of energy resources which is negatively impacting the world we live in. For years fossil fuel-based energy has been used through combustion where large energy is released and used for the world energy demand. Today, fossil fuel energy is proven obsolete; it is depleting and is a source of climate change and environmental disasters. Many concerns have been risen by international organizations as well as national policymakers about the impact of human activities on the environment and many actions have been taken to limit such impacts. A sustainable development together with sustainable use of our energy is required in the present context of industrialization and urbanization, which will continue to require an increasing energy demand.

To achieve the goals of sustainable development, alternative, environmentally friendly and renewable source of energy is required to meet the growing energy demand and to mitigate the consumption of fossil fuel-based energy. These are clean and renewable energies, with insignificant effects on the environment and the climate. Although the renewable market is large, solar and wind energy play an important role in the energy market as renewable sources but need to be optimized to increase the energy generation efficiency and consequently reduce the energy cost. Many energy sources are in connection with the oceans and a recently discovered is the SGP which is the energy generated by the mixing of water bodies with different salinity.

SGP is energy produced due to the chemical potential difference between water bodies when two solutions with different salt concentrations are mixed, and is known to have a high worldwide energy potential. RED is a membrane-based

process used to harvest the SGP when high and low saline water streams flow into the RED stack that controls the mixing process and converts the chemical energy into electricity. The RED process involves exploring the chemical potential difference between volumes of water different in their salt content and separated by IEMs which will induce the movement of the ions from the concentrated solution to the diluted solution, creating chemical energy that will be converted into electrical energy using appropriate electrodes. This is a new developing technology highly suitable for coastal countries with high energy generation potential. The process is however facing challenging parameters including the cost of the membranes and their availability and suitability, the electrodes, and other parameters related to the feed solutions.

1.2 Objectives

In a context of technological development and increasing demand for electrical energy together with a need for sustainable development, the energy transition from non-renewable to renewable, the factors piloting the transition, and the integration of a sustainable energy source in the large sphere of the world's energy by salinity gradient are of great interest. The salinity gradient energy can contribute with clean energy in meeting the world's energy demand, and the present Ph.D. research focuses on the RED process in harvesting electrical energy from various feed solutions and address the challenges faced by the RED process which hinders its marketing as well as the perspectives to mitigate the negative factors. The main objectives of the study are as follows:

- To investigate the optimal salt concentrations of seawaters and rivers and the influence of concentrated and diluted solutions concentration ratio on the RED performance. The influences of the concentration and flow rate of feed solutions on electrical energy production were studied to determine the optimal flow rates and feed concentrations.
- To fully understand the resistance effects induced by the membranes and the spacers, by assessing the power losses with the increasing number of cell-pairs in the RED stack using different types and structures of spacers.

- To investigate the RED-SGP potential of seawater (Marmara Sea) and different treated municipal wastewater effluents (advanced biological treatment, UF–treated effluent, MBR-treated effluent) used as a diluted solution. The influence of the quality of the wastewater in the process performance will be assessed and the importance of wastewater in RED energy generation will be investigated to highlight an opportunity for zero waste management and enlarge the scope of SGP by RED.
- Using Ataköy and Ambarlı WWTP as models, for being among the biggest WWTP of the city of Istanbul, investigate the RED energy generation potential with municipal wastewaters treated by advanced biological treatment, MBR and UF processes together with the Marmara Sea and simulation with optimal conditions will help to determine the net RED energy output in these WWTPs.

1.3 Hypothesis

When two solutions of different salinity get into contact, the exchange of ions between the two solutions creates chemical energy that can be converted into electrical energy by appropriate electrochemical methods using electrodes. Advanced treated municipal wastewaters are clean solutions with conductivity around 1000 $\mu S.cm^{-1}$ like river water. They flow similar patterns since after treatment they are either reclaimed (watering, cooling system…) or directly discharged into a water body. When these wastewaters are discharged into the sea, due to their low salinity, chemical energy can be generated and can lead to the generation of salinity gradient energy which could cover the energy demand for the wastewater treatment plant.

2
LITERATURE REVIEW

2.1 The World Energy Context

Energy has been over the years the root of the development and progress of human civilization. In its continuous struggle to raise living standards, human beings rely on enormous quantities of electrical power to sustain their evolution. Energy is the key to power; it is the pillar of the future and its evolution. The world's energy use has profound implications for the socio-economic-political sphere of humanity, and it has been a determining factor in international issues and will still play a decisive role in capturing space, which is the next race of world powers. The global total primary energy consumption from the year 1800 to 2018 presented in Figure 2.1 indicates the consumption of 5,652.78 terawatt-hours (TWh) in the year 1800 essentially based on traditional biofuel for the large part and a little percentage of coal. By the year 2018, the global primary energy consumption reached 157,063.77 TWh, led by crude oil followed by coal and natural gas [1]–[3]. The primary energy consumed by the planet in 2018 was over 27 times more than the world consumed in 1800 [4], and this exponential growth will continue. Most of this energy is extracted by burning fossil fuels which are non-renewable and rapidly depleting.

The quest for energy pushed human beings into investigating all kinds of possibilities to maximize energy production. The drawbacks associated with this quest were however not investigated. Recently, due to the dirty print on the environment and long-term effects on the climate [5] of the so-called fossil fuels, considered to be the main and most widely used energy source of human being, together with the knowledge of a limited quantity of this energy source, the scientific community turned into searching for a cleaner and long-term not depleting energy source. If the pattern of fossil energy consumption does not change, the environmental impact and generated greenhouse gasses (GHG) will cause the planet earth to be unviable in the decades to come. The so-called sustainable development

concept was developed to prevent this from happening, but can not be achieved without sustainable harvesting of energy resources. The United States (USA) Environmental Protection Agency (EPA) reported that the USA emitted 28% greenhouse gas from electricity production, 29% from transportation, and 22% from industrial production [6]. It is worth mentioning that up to 10 % of the industrial production cost of goods is consumed by energy, [7]. In the year 2011, the energy production has been responsible for up to 80% of GHG production in the 28 member states of the European Union [7]. This resulted in a growing need for renewable energy (RE) sources to cover the growing worldwide demand for energy, and progressively mitigate the dependency on the unreliable and polluting fossil energy sources. Researchers predict an increase in global power consumption by up to 50% in 2040 [8]. The uncountable disadvantages of fossil fuel; difficult to extract, toxic residual effects, source of climate change [9], just to mention a few, associated with the need for a diversified energy source, renewable energy is nowadays considered as an alternative source.

Renewable energy, in contrast to fossil fuel, is the energy that is renewed in a short cycle. It is a naturally readily accessible and abundant source of energy that does not produce any pollutants that may be harmful to the environment. Therefore it is a sustainable energy source that provides great economic and social benefits. It is worth mentioning that RE is still expensive to produce compared to fossil fuel-based energy, however, the growth of interest in the last decade contributed to decreasing its cost and RE is expected to be cost-effective in a near future. Renewable energy includes solar, biomass, wind, geothermal, tidal, hydropower energy, and others, less known. Today, solar and wind power represent the well-known and attractive RE sources, however, focusing on the salinity gradient at the contact of two water streams with different salinity, plentiful energy is released due to the chemical potential difference between the two water streams in contact [10]. SGP does not release any compound that may harm the climate or the environment, making it a sustainable source of energy.

Water represents two-third of the global world surface, making water one of the highest contributors anywhere it plays a role. Energy is not an exception, from non-

renewable energy sources where a great amount of petrol is extracted underneath waters to renewable energies where hydraulic power or tidal energy take their source from water. The importance of water in power generation is unlimited such a point that developing this concept may require larger investigation, not to count the undiscovered and unknown energy production routes from water. In 1974, R. Norman proposed the concept of SGP, quoting that: "Since energy is required to extract fresh water from seawater in any desalination process, in theory, the reversal of such a process should produce energy" [11], however, Pattle already proposed a technique in the year 1954 to harvest SGP [12]. Since then, this principle has been the motor for a new and reliable renewable source of energy that could be generated at the contact point of rivers and seawaters. Based on the aforementioned principle, when a river stream (freshwater) flows toward the sea, the ocean, or a high salinity lake, and discharge into it, energy is generated when the two different salt concentration solutions irreversibly mix one to another [9], [13], [14]. This source of energy named SGP or salinity gradient energy (SGE), also known as blue energy has a large worldwide potential of approximately 2.8 terawatts (TW) [15] but is lost in nature and could be an important source of RE to respond to the unsatisfied energy demand worldwide. It is a gigantesque source of clean and RE [15], [16], with a worldwide potential approximative to the current globally consumed electrical energy [15]. SGP is a clean, no polluting, and no carbon-emitting energy with no negative effect on the environment. It is directly related to the earth's dynamic water cycle and depends on the energy that dissipates when two solutions different from their salt content interact [10]. The potential energy of combining 1 m^3 of river water with a high quantity of seawater depends on the salt concentration of these waters being mixed [17] and is an average of 2.5 MJ, which is equal to the energy produced when water flows over 250 m high dam [18]. Different processes, mainly the reversal of formerly developed desalination techniques, have been proposed to convert this power into electricity. These processes include the Vapor Pressure Difference Utilization (VPDU), The mechanochemical turbine (MT), The reversal of the capacitive deionization (RCD), PRO, and RED. However, PRO and RED

technologies have remained the most commonly investigated techniques to harvest the SGP [9].

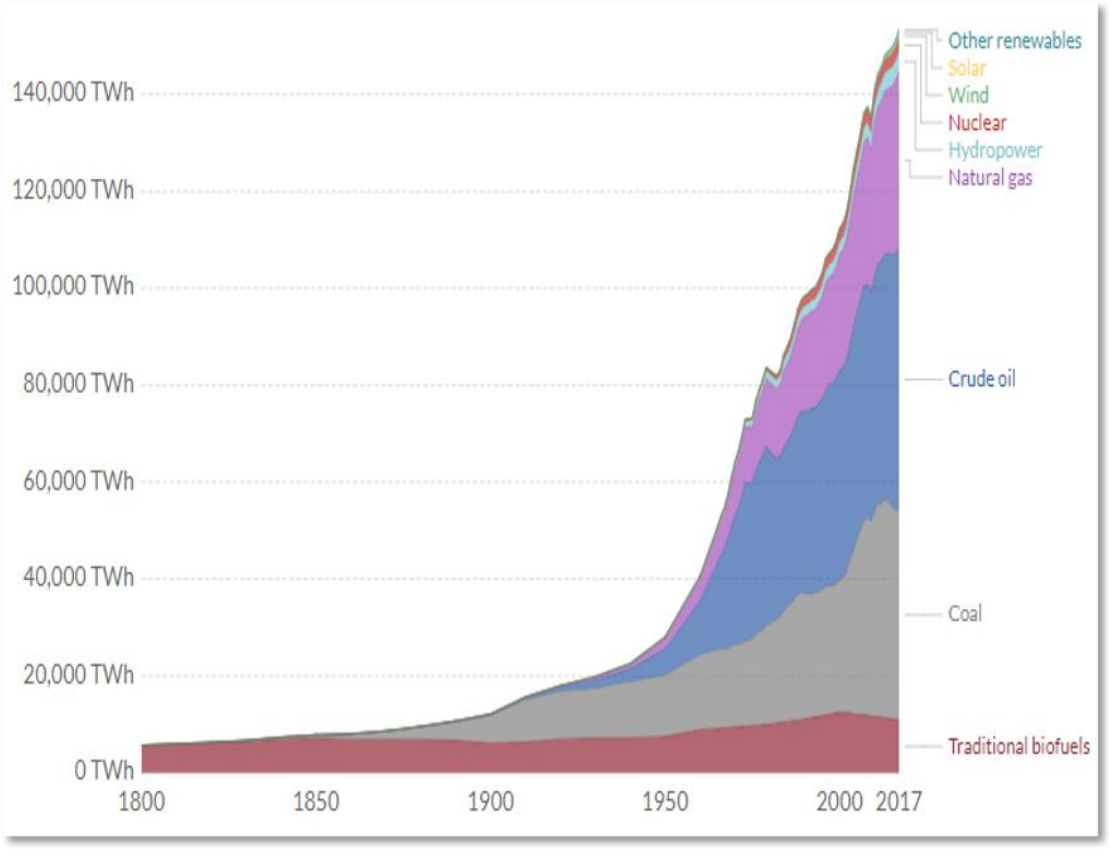

Figure 2.1 Global primary energy consumption from 1800 to 2018 (TWh) [3], [4] 'Other renewables' applies to renewable energies that do not include solar, wind, hydro and conventional biofuels

2.2 Energy, Sources and Prospective

2.2.1 Global Energy Outlook

Energy can occur in many different forms (chemical, electrical, thermal…) and can be converted from one form to another following the first law of thermodynamics, but it cannot be produced or destroyed. Considering the source of production, energy can be subdivided into non-renewable and renewable. Because they take hundreds of millions of years to develop and are exhausted much faster than new supplies can be produced, fossil fuel-based energies are called non-renewable

energy. Fossil fuel-based energies represent the largest non-renewable energy source available at present [1] and are expected to remain for many years the world's most important energy source [19]. Energy demand for diverse reasons including powering our appliances is increasing and is bounded to the economic development of the countries. Global electricity consumption has increased from 7,323 TWh in 1980 to 22,347 TWh in 2017 [20], see Figure 2.2.A. All fossil fuels contain hydrogen and carbon, giving them the nomination of hydrocarbons. They can be solids, liquids or gases, including coal, oil, shale oil, tar sands, and gas [21]. Besides being dense reserves of energy, hydrocarbons from fossil fuels can be used to fabricate other products of much greater value in our modern life, including drugs, paint, plastics, rubber, cloth and lubricants. The high energy state that is released by combustion is the reason hydrocarbons are useful as fuels. Fossil fuels are produced by a very long period of exposition to heat and pressure of the remains of dead plants and animals in the crust of the earth. During combustion, the chemical energy 'stored' in these fuels is released to produce electricity. Today, more than 85% of energy demand is based on fossil fuels (36.8% petroleum, 26.6% coal, and 22.9% natural gas) [22]. High capitals are invested every year in oil, coal, and gas exploration, mining, and transportation, reaching an average of around $1 trillion yearly over the last few years and are expected to cumulatively exceed $20 trillion from 2017 to 2040 under the New Policies Scenario of the IEA (International Energy Agency) [23], [24]. Besides being the fuel for climate change, they take hundreds of millions of years to develop and are exhausted much faster than new supplies can be produced. Further attention has been paid to the importance of renewable energy in recent years. RE is generally defined as energy from resources that are constantly replenished naturally on a human scale [25], such as sunlight, wind, ocean, tides, waves and geothermal heat [26]. The production of energy from these sources does not emit carbon and has a neglectable threat to the environment. Fossil fuels, with more than ten thousand million tons of oil, have been the energy that fueled the industrialized world and its economic growth since the industrial revolution, with about 80% of all primary energy today. Although they represent a negligible share in the energy market, nuclear, hydroelectric power and biomass and waste energy

are the most important non-fossil energy source in the global energy system. A small percentage of the world's primary energy comes from renewable and alternative sources [27]. The importance of RE is tremendous as the world's energy demand will continue to increase. Projected global energy demand from 1990 to 2040 is provided in Figure 2.2B. by energy source. In recent years, the global energy use has increased dramatically, and the increase is expected to sharpen in the coming years. The share of total RE increased from 35 metric tons of oil in 1990 to 571 metric tons of oil in 2017 and is expected to reach 2,748 metric tons of oil by 2040 [19].

Today, China is the world's largest user of energy and the country has built the most renewable energy capacity since 2018 [19]. China and India are expected to tremendously influence the global energy demand by the year 2040, while the Middle East and Africa will still keep the smallest share as shown in Figure 2.3. Considering the energy consumption by region, for the year 2016, China was the highest electrical energy-consuming country with 5,320 TWh, followed by the USA with 3,886 TWh and the European Union (EU) 2,857, while Africa is at the bottom with 655 TWh for the whole continent. By the year 2040, China is expected to create a big gap between the other countries with 9,230 TWh electrical energy consumption forecasted, followed by the USA 4,570 TWh and India taking the 3rd rang with 3,606 TWh and the EU with the 4th position with 3,178 TWh. Even though electrical energy is expected to grow in Africa, the continent will still hold the last position with 1,707 TWh behind the middle East and South East Asia with 1,798 and 1,997 TWh, respectively [24]. However, it is worth mentioning that, big countries such as China or India can present a global high energy consumption rate due to their large surface area and crowded population, but regarding the consumption per capita, the results are quite different. As reported by Statista, China, the USA, and India were the world's most primary energy users in 2017, but on a per capita basis, in 2015, Qatar, Bahrain, and Kuwait were among the countries with the highest energy consumption per capita [19]. Countries like China and India, due to their large population consume a large amount of energy in a country-based (generally for their industries), however, it does not mean the real energy consumed by inhabitants is huge.

The global primary energy demand continues growing in the year 2018, led by natural gas and renewable energies, while the share of coal has continued to decline. This growth was 1.2% in 2016, increased to 2.2% in 2017, and reached 2.9% in 2018, which is the fastest since 2010 and very high compared with the 10-year annual average [3], [28]. With the growing industrialization and urbanization, the global primary energy demand will continue to increase. Oil was the dominant consumed fuel in Africa, Asia, and America in 2017, while the Commonwealth of Independent States (CIS) and the Middle East were dominated by natural gas. A similar trend was observed in 2018. The consumption of coal-based energy by North America, Europe, CIS, and Africa dropped to its lowest level in the same year [3], [28]. But the rapid growth of the installation of solar photovoltaics (PV), with China and India being the leaders, forecasts solar energy to become the largest source of RE by 2040, with an expected share of all renewables in total power generation reaching 40%. On the other hand, the consumption of coal is expected to fall dramatically by the year 2040 [24].

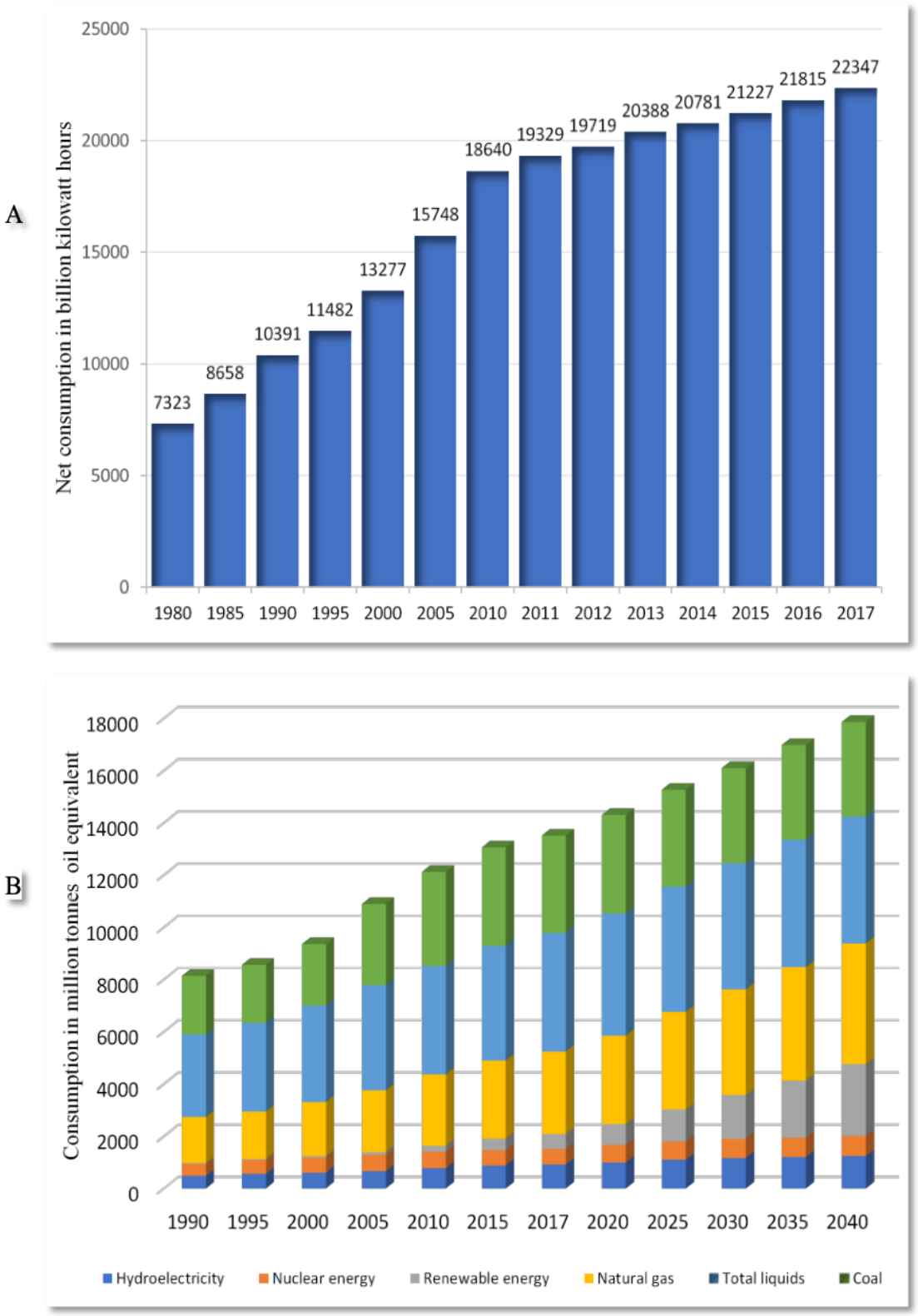

Figure 2.2 Worldwide energy demand: A) 1980-2017 electricity consumption (billion-KWh) [20], B) 1990-2040 projected energy consumption (million metric tons of oil equivalent) by source [19]

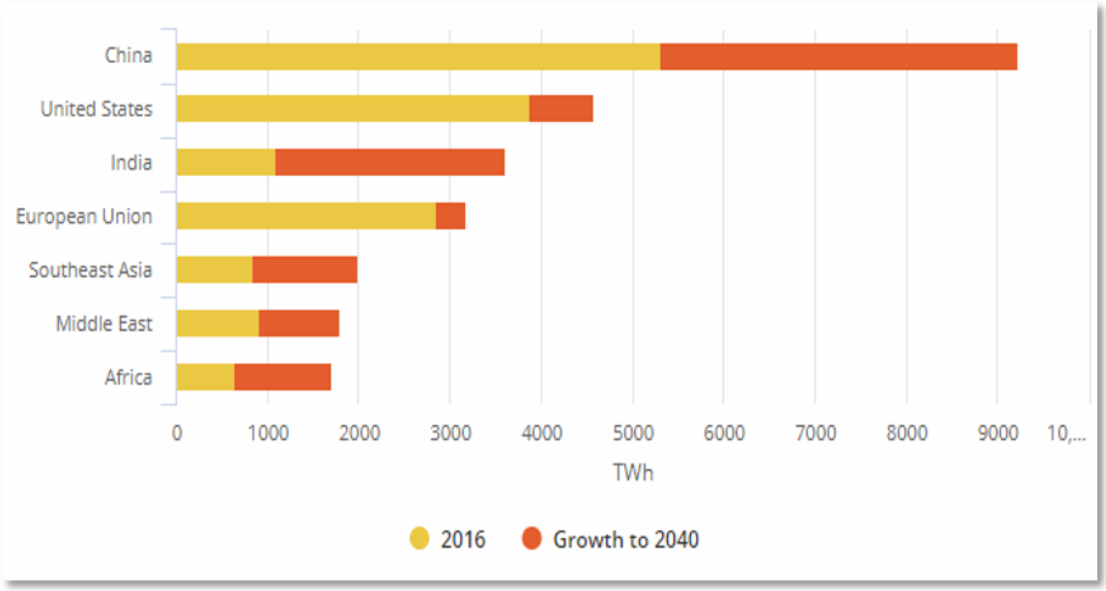

Figure 2.3 Energy demand by region for the year 2016 and projected year 2040 (in TWh) [24]

2.2.2 Energy Transition: From Fossil Fuel-based Energy to Renewable Energy

Since the industrial revolution, the consumption rate of electrical energy continues to grow and energy is today an essential good for economic and technological development. Goldemberg et al. (1985) stated that ''the increase of energy consumption is the foundation of economic and social development and the increase of the per capita energy use is a prerequisite for any developmental program aiming to reduce poverty'' [29]. A recent study reported that energy has significantly and positively impacted the growth of South Asia's economy, with a stronger impact induced by RE [30]. Since the discovery of fossil fuel, the global primary energy consumption entered a new era, led today by crude oil followed by coal and natural gas [1], [19]. The energy demand grows faster since 1970, mainly satisfied by fossil fuels and centralized power generation. But, RE is expected to share a larger contribution to the total global energy soon [32]. The combustion of fossil fuel is the most important anthropogenic GHG emission source, causing the release of over 30 billion tons of carbon dioxide (CO_2) yearly [33]. Reducing the use of fossil fuel-based energy is, therefore, the top priority of climate policy. Different countries and agreements are seeking a new energy agenda for decades by encouraging energy

efficiency, low-carbon technology, carbon pricing, and other steps to reduce the use of fossil fuels as energy sources [34].

With the uncountable drawbacks associated with fossil fuel, today's power systems are very likely to be subjected to change and mitigate to renewable energy sources [35] mainly due to the necessity to comply with climate change targets [36], [37] and market trends. The 2016 Paris climate agreement intended at reducing global warming and making the effort to limit it to 1.5 degrees Celsius [36]. Fossil fuels emit GHGs during their combustions, which is accelerating climate change such as global warming. Most countries that attended to Paris 2015 United Nations Climate Change Conference agreed to contribute to reducing global climate change [36], [37]. The Energy Return on Investment (EROI), defined as the ratio of the total energy output by the energy input [38], or more simply the amount of energy spent to produce a certain amount of energy, is in decline in fossil energy while increasing in renewable energy sector [39]. With increasing fossil fuel consumption rates, there is a tendency for an increase in fuel costs as a result of the scarcity of resources. More investment is needed to extract fossil fuel than before, as a consequence fossil fuel is getting expensive over time while RE extraction is being improved and costs being reduced over time. Recently, Brockway et al. (2019) reported that fossil fuels may remain the dominant energy source for many years, but the EROI ratios of fossil fuel may be much closer to RE than expected, soon, resulting in a sharp decline in fossil energy consumption giving rise to renewable energy [39]. The fossil fuels EROI of total gross production for the years 1995 and 2011 reported in Figure 2.4 were around 45:1 and 30:1 respectively. These ratios are much lower considering the final energy stages [39]. The EROI of fossil fuel (oil and gas) continue to decline and is below 20 today [40], [41]. To extract energy from fossil fuel, the energy invested may seem neglectable when considering the total gross primary energy production but a high energy investment is required for the total final energy ready for consumption. Considering the decreasing trend of the EROI of fossil fuel electricity production over years [39], [40], [41], fossil fuel-based energy will be very expensive to extract in the future, resulting in an expensive cost in the market. However, there is no

straigh relation between net energy and the EROI, which can largely vary from study to study, consequently be misinterpretted [40].

The aforementioned reasons led many countries to support a series of energy transition plans aiming to expand clean energy production and more efficient energy use. The uncountable disadvantages of fossil fuel; limited amount, difficult to extract, toxic residual effects, source of climate change [9], just to mention a few, associated with the need for a diversified energy source constrained the scientific community to devote the best of their attention into renewable energy sources. Therefore, in recent years, renewable energy has attracted much attention as alternative energy to mitigate fossil fuel climate change effects. The primary energy consumption between the years 2005 to 2015 presented in the chart in Figure 2.5 and showing a decreasing trend of fossil fuel-based energy at the expense of renewable energy, is a witness to the ongoing energy transition [42]. This trend is supported by the 2019 BP Statistical Review of World Energy which reported that RE occupied the third position in net increase in power generation, followed by coal (31%) and natural gas (25%). The share of RE jumped from 8.4% the previous year to 9.3% in 2018 [3]. Renewable energy refers to the energy that can be recycled in nature and has the advantages of being inexhaustible (renewable), and clean (green, low carbon), making it beneficial for the protection of the environment [43]. Solar and wind power are well known and most attractive RE sources to date. RE has many benefits which include Energy Security, Energy Access, Social and Economic Growth, Mitigation of Climate Change, environmental and health negative effect reduction [43].

Despite being attractive, RE faces many challenges, including market failures, the limitation of information, difficult access to raw materials to be used as a future renewable resource [43] and the most important is being more expensive compared to fossil fuel-based energies. As the supply of fossil fuel depletes the resources it relies on, the scarcity of the resources is increasing the fossil fuel-based energy costs, making the future market not economic and difficult to develop [44]. The recent increase in fossil fuel cost together with the reduction of the cost of RE and the acquisition of experience in the sector resulted in low-cost RE, replacing fossil

fuels in some areas. Kaberger et al. (2018) recently reported that the unit RE is now cheaper than oil, and its cost is almost similar to fossil methane, but, remains more expensive than coal [44]. Many reports from the year 2016 are showing a continuous and fast cost decrease in RE prices worldwide. On-shore wind prices decreased to one of the lowest, 30 USD/MWh in early 2016 in Morocco [45]. It was recorded 70 EUR/MWh in July 2016 [46], 60 EUR/MWh in September [47] and less than 50 EUR/MWh in November 2016 [48], in northern Europe. Solar Photovoltaic (PV) dropped to 50 USD/MWh in Latin America in 2016 [49], [50], followed by prices in Dubai, Chile and Abu Dhabi at about 30 USD/MWh [51]. In 2017, prices in Mexico and Chile continuously decreased down to 20 USD USD/MWh [52], [53], while Saudi Arabia and Mexico surpassed record offers of solar electricity at 17.9 USD/MWh, October 2017, and 17.7 USD/MWh, November [54], [55], respectively.

Today, RE is cheaper than thermal electricity [44]. It will sustain the mitigation of climate change and accelerate the achievement of sustainable future generations' energy demand. It is expected that the total RE consumption will reach about 2,748 metric tons of oil by the year 2040, compared to 35.02 metric tons recorded in 1990 [19]. Even though the transition from fossil fuel to RE seems slow, it is certain. It will not take long for attractive RE sources to reach an EROI much lower than currently used traditional energy sources. Also, the need for a clean planet at all costs may force humanity sooner than expected to a faster transition. Untile more reliable and sustainable energy sources are discovered, renewable energy will certainly be the energy of the future, and may remain so because no energy source, no renewable if it is, cannot overthrow the unlimited, both in time and quantity, of humans energy need.

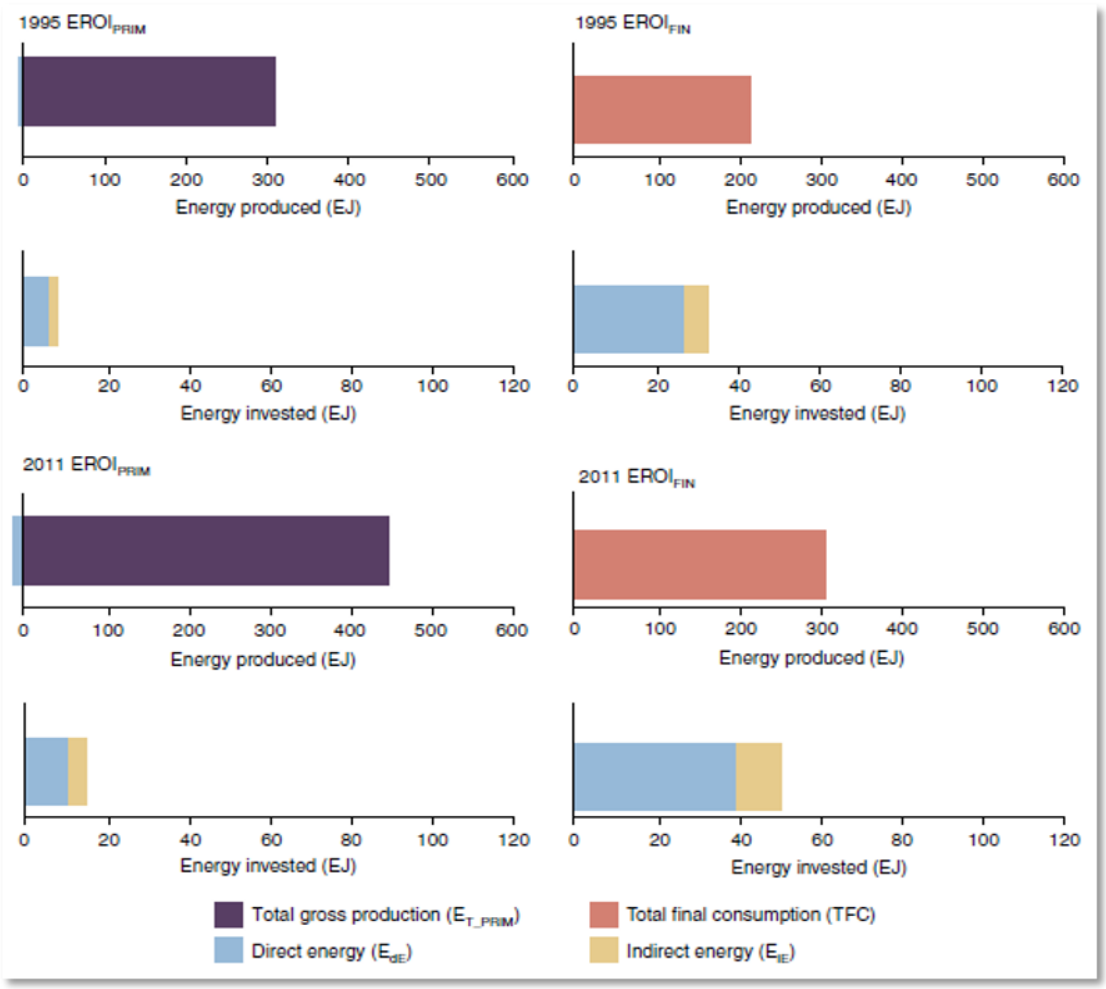

Figure 2.4 The evolution of the fossil fuel EROI for primary and final energy stages for the year 1995 and 2011 [39]

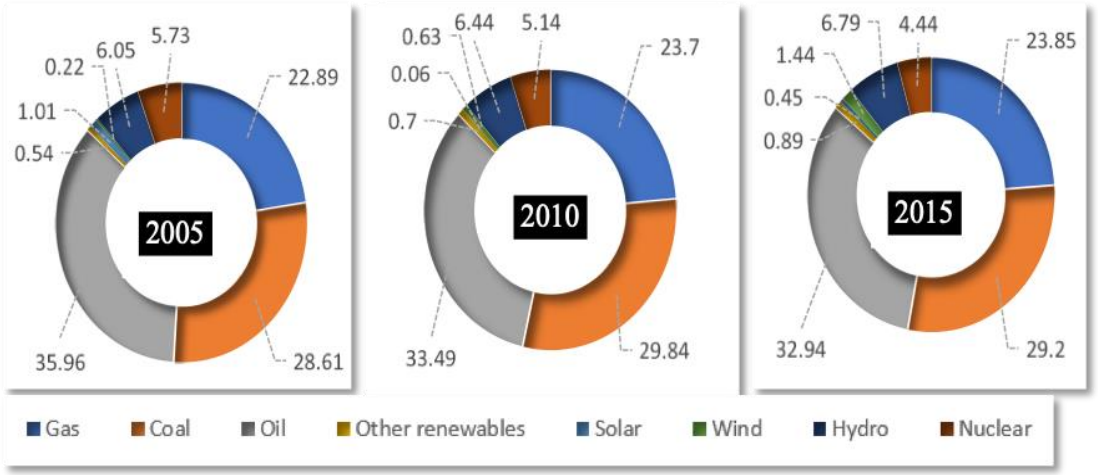

Figure 2.5 Comparative primary energy consumption for the years 2005, 2010 and 2015 [42]

2.3 Salinity Gradient Power

2.3.1 Salinity Gradient Power Harvested by RED and PRO

The increasing energy demand worldwide, the dependency on the economic stability in developed countries and the need for developing countries to faster their economy make energy the lungs of the present world. The advantage of renewable energy is not only being clean but being inexhaustible makes it reliable. Among the many renewable energy available nowadays, SGP although unfamiliar is a type of energy best suited for coastal countries. It is clean energy generated due to the chemical energy produced when two solutions with different salt content are in contact. In 1954, Pattle introduced the first idea of SGP extraction. He proposed a technique known as a hydroelectric pile (almost similar to the current RED process) that could be used to extract electric power from mixing fresh and saltwater [12]. He stated in his publication that irreversibly mixing a given volume V of pure solvent with a much larger volume of a solution of osmotic pressure P (for seawater ~20 atms), energy equal to PV is released. When river water runs to the sea and is mixed with the seawater, the freshwater becomes saline and generates energy equivalent to the energy released from a 680-foot waterfall [12]. The concept of harvesting energy by reverse desalination was proposed in 1974 by R. Norman [11]. However, the growth of this source of energy was not fast enough like well-known other RE sources such as wind and solar energy mainly due to the complexity of the process which requires skilled and multidisciplinary scientists who master engineering, electrochemistry, physiques, and electricity to optimize the process energy efficiency and power density. In 1977, Wick and Schmitt calculated and estimated the global potential power from SGP to be around 2.6 TW [56], close to today's estimated 2.8 TW [15]. Since the worldwide potential is estimated, scientists got attracted to the topic, resulting in many investigations published in recent years mostly in lab-scales. Very few pilot-scale results exist up to now. SGP is the energy generated by the mixing of two water bodies with different salinity resulting in a salinity difference; for instance, when river and seawater irreversibly mix one to another, energy is released [9], [13], [14]. Due to large oceans around the world, and

the uncountable rivers running into the sea, SGP appears to be a gigantesque source of clean RE [15], [16], with a worldwide potential able to cover the global electric power consumption by the year 2010 [15]. Taking profit of high salinity, Emdadi et al. (2016) assessed the power potential of RED-SGE between Urmia Lake and ZarrinehRud River (Iran) and reported based on thermodynamic calculations, literature, and field data a theoretical energy potential ranging from 400 to 1000 MW. They also reported a technical potential of about 20 to 30 percent of the above-mentioned values [57]. This shows the variety of potential feed solutions that can be used in an RED unit. Salt lakes, underground mines, desalination concentrates and industrial wastewaters are also adequate feed solutions since they can create a potential difference with other water bodies [58], [59]. Due to many factors, mainly the feed solution and membrane characteristics, the energy obtainable can be very different from the theoretically available energy, and optimization is required to minimize energy loss during harvesting. As warned by Emdadi et al., (2016) the membrane cost and characteristics, achieved power density, and the harvested electrical energy price will be the determining factors in the implantation of any SGP plant [57]. The techniques used to harvest the SGE [60] are mainly the reversal of desalination techniques among which PRO and RED are the most commonly studied membrane-based technologies [9], Figure 2.6. PRO has some advantages of lower membrane cost and possible higher power densities and efficiencies compared to RED, whereas RED is less sensitive to membrane fouling and has the advantage of direct conversion of the SGP to electricity [61].

PRO is the reversal process of RO [15]. In the PRO system, two different salinity solutions (river water and seawater for instance) are separated by a semi-permeable membrane, allowing only water to pass through the membrane while dissolved salts (ions like Na^+ and Cl^-) are rejected [15], [17]. As schematically depicted in Figure 2.6A, during the process, water is transported through the semipermeable membrane from the diluted solution to the concentrated solution [63] because of the concentration difference of chemicals between the two solutions [17], [18]. Water transport through the membrane engenders an increase in the pressure in the concentrated solution. This creates a pressure difference that

generates a turbine, which can be used to produce electrical energy [17], [18]. In other words, the PRO system is operated by creating a hydraulic pressure of the freshwater (river water) lower than the osmotic pressure of the saline water (seawater). Due to low hydraulic pressure, the water will flow through the membrane against the hydraulic pressure gradient [63], resulting in the production of energy [15], [16]. The membranes are the key component of PRO and effective membranes are fundamental for improving its performance. Nagy et al. (2016) reported that the membrane selectivity and structural parameters are essential and need to be investigated to improve the PRO process efficiency [64]. Besides the membranes, the solute concentrations in the feed solutions and the PRO module play a key role in its performance [63], [65], [66]. With the PRO process, depending on the membrane characteristic and the hydraulic pressure, the power densities have been reported to be between 2.2 and 5.8 W/m^2 [65]. However, a power density of 5 W/m^2 at least has been recommended for PRO to be economically feasible.

In contrary to PRO where water is transported through a semipermeable membrane, the extraction of SGP by RED occurs during the mixing of two solutions of different salinity which induces the transport of ions through IEMs [18], [67]. In the RED system, alternating CEMs and AEMs form a stack between an electrode system [63], where the transport of dissolved salt generates an electrical potential that can produce electricity [15], [16]. RED is a renewable, pollution-free technology that generates energy by combining solutions with different salinities [9], [10], [13]–[16]. The operating principle of the RED process is schematically illustrated in Figure 2.6B.

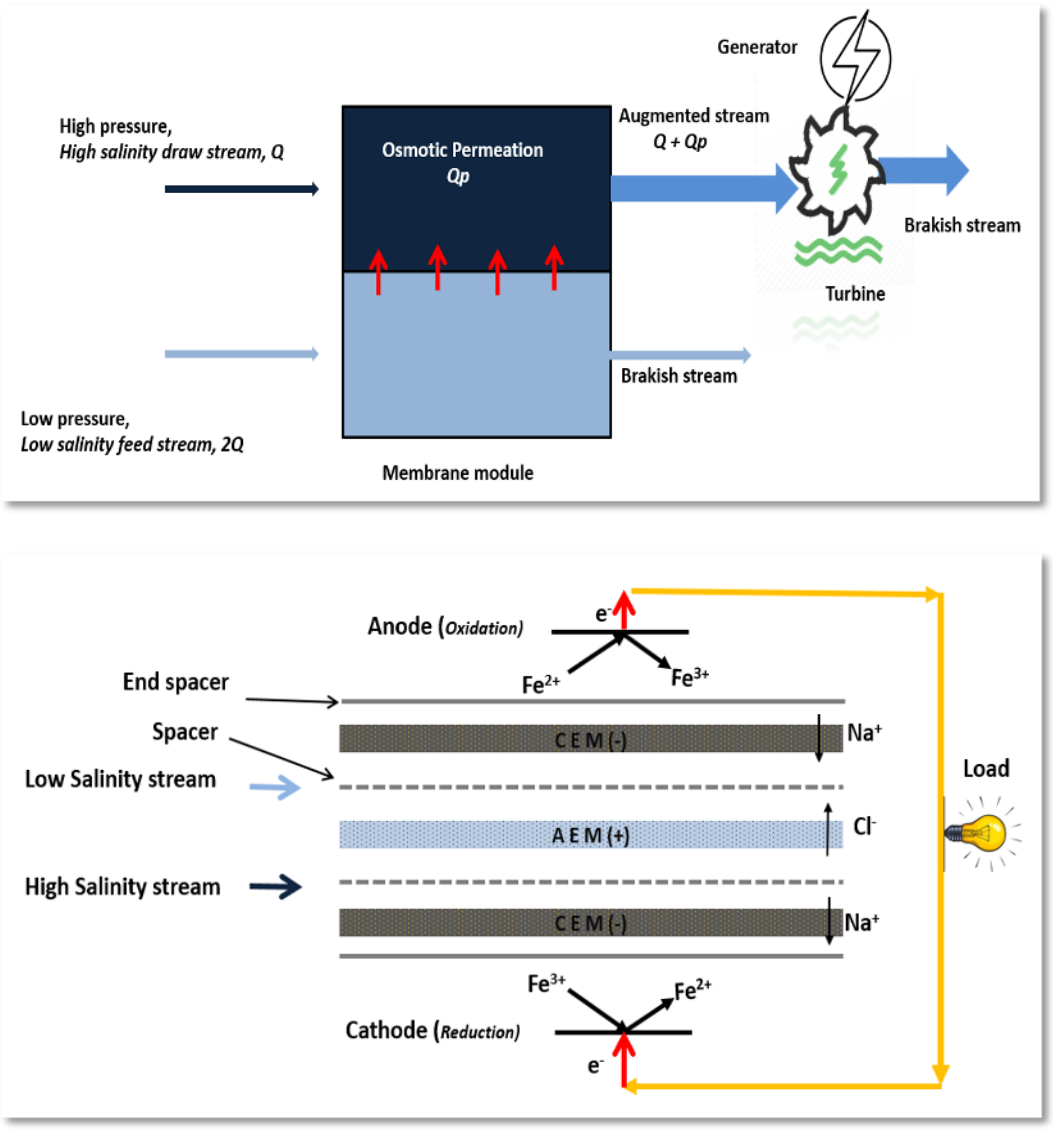

Figure 2.6 Schematic illustration of the most frequently studied membrane-based technologies for SGP harvesting: A) PRO process, B) RED Process

2.3.2 Comparison of Salinity Gradient Power and Other Renewable Energy Sources

SGE is RE which has advantages similar to all renewable energy processes of no emission of GHGs, main responsible for climate change. Its most accurate disadvantage is its availability mainly for coastal countries. Another disadvantage may be the impact that the infrastructure construction might have on the landscape, ecological system, hydraulic systems. But compared with other renewable energies such as wind energy, implementing an SGP plant requires less land usage and

produces fewer negative impacts to produce the same amount of energy [68]. Even though the amount of energy produced from SGE can be affected by seasonal changes due to the variation of water flow in different seasons of a year, precipitation, or melting snows, it is less sensitive to seasonal variations compared to wind and solar powers. The energy conversion efficiency of SGP is on average similar to the other renewable energies. It also has the advantage of being continuous, 24h/7 days, and 365 days/year. As water is continuously flowing, the yearly expected amount of energy is easily and accurately predicted compared to wind and solar energy. Table 2.1 below presents a detailed comparison of salinity gradient-based energy and other energy conversion system [68], [11], [68], [69]–[71], [60], [72], [73]. Since SGP technology is still in the lab researches and a few pilot scales, the energy pricing and the determination of the EROI for real plants are impossible and not available. The estimated SGP EROI and price as depicted in Table 2.1 are based on theoretical values made upon academic research. Based on these theoretical values, SGP by PRO and RED would be as cheap as close to well-known other renewable energies, but this is still based on the assumption of very high-power densities and low membrane cost which is yet to achieve. Jalili et al. (2019) reported prices between 0.23 USD and 0. 31 USD per kWh for RED and PRO with the possibility of lower prices with membranes cheaper than 2.9 and 3 USD.m^{-2} for RED and PRO, respectively [72]. Improving the power density and the energy conversion efficiency of osmotic energy remains the key challenge to overcome. Considering the water transport through the IEMs which induces losses caused by concentration polarization or osmotic losses, the energy conversion efficiency can be weak. Various RED efficiency among which the most promising 35.7% [74], 40% [72] has been reported in the literature and still needs to be improved with new membrane properties and controlled nanofluidics. It is worth mentioning that RED is among the energy conversion systems with the highest conversion efficiency and SGP by RED and PRO are responsible for an insignificant production of GHGs compared to available other RE processes. Nanofluidic osmotic energy conversion seems to be promising with single nanopores able to theoretically reach a power density up to 10^3 to 10^6 W.m^{-2}, however, this breakthrough remains a theoretical estimation and

translating such estimated high value into real power creates a giant gap which needs to be resolved since real obtainable practical energy is still below 4 $W.m^{-2}$ [75]. The future of SGP can rely in the improvement and the resolution of such big gap between theoretical and real nanofluidic osmotic energy conversion technique which hugely enhance the energy conversion efficiency and the power density. Although current SGP seems to be an expensive RE to produce, it has a low EROI and is expected to be cheaper when appropriate membranes for RED and PRO are marketed and all the required materials for plant installation are readily available.

Table 2.1 Comparison of salinity gradient based energy and other energy conversion systems [11], [60], [68], [69]–[71], [72], [73]

Energy Conversion Systems	GHGs (g CO_2-e/kWh)	Electricity Price USD/kWh	EROI	Energy Conversation Efficiency (%)
Photovoltaic	90	0.24	1.6-6.8	4-22
Wind	25	0.07	18	24-54
Hydro	41	0.05	>100	>90
Geothermal	170	0.07	na.	10-20
Coal	1004	0.042	80	32-45
Gas	543	0.048	10	45-53
RED	<10	0.10	7	34-40
PRO	<10	0.065-0.13 with Subsidies 0.05-0.06	6.7	44

EROI: Energy Return on Investment *na.: Non-available*

2.4 Reverse Electrodialysis

2.4.1 Composition of an RED Unit

An RED unit is composed of a module, the feed solutions tanks, the feed solutions flow facilitating materials and a multimeter for the measurement of the electricity

data. The module consists of IEMs, spacers, and the electrode system. The spacers are placed between alternating CEMs and AEMs to create stark compartments. Essentially three tanks are used, containing respectively the concentrated solution in the high compartment (HC), the diluted solution in the low compartment (LC), and the electrode rinse solution (ERS) circulated through the RED stack with a pump.

2.4.2 Reverse Electrodialysis Principle and Operation

The global potential of SGP reported to be around 2.8 TW [15] is a theoretical value estimated based on the rivers and seas worldwide and their flow rates. In real applications, many of these rivers will not be suitable or beneficial for the installation of an SGP harvesting unit, and the energy efficiency far from being 100% will reduce the global power to values lower than the estimated potential power. Nonetheless, the SGP remains huge and can contribute enormously to the energy demand worldwide. In recent years, many researchers got involved with studies and publications from lab-scale investigations, mostly on RED and PRO processes to fewer pilot scales. The RED process is still under development and fewer pilot-scale results exist up to now, with no installation of any real plant yet up to date.

RED is the inverse process of ED [66], both in their processing techniques as well as their principles. It involves the exploitation of the potential chemical difference between volumes of water with a difference in concentration separated by IEMs to generate electrical energy. The difference in salinity, sea and river water, for instance, known as the salinity gradient is the driving force responsible for energy generation in an RED process. Although both ED and RED are membrane-based technologies [63], ED is used for desalination for decades, while RED is under improving new technology used to harvest the energy of mixing saline and freshwaters. Both technologies operate by transporting ions through IEMs, either induced by an external voltage (ED) or influenced by the concentration difference between the two water bodies (RED) [76]. In practice, electrical current is used in the ED process to migrate the ions against the chemical potential resulting in a distilled solution as the final product, while RED aims to produce electrical energy

as a final product by diffusion of ions in the opposite direction through the IEMs. In other words, ED is an IEM process that uses energy to convert saltwater into freshwater and RED is an IEM process that uses saltwater and freshwater to generate electrical energy. The main differences between ED and RED are summarized by the Figure 2.7.

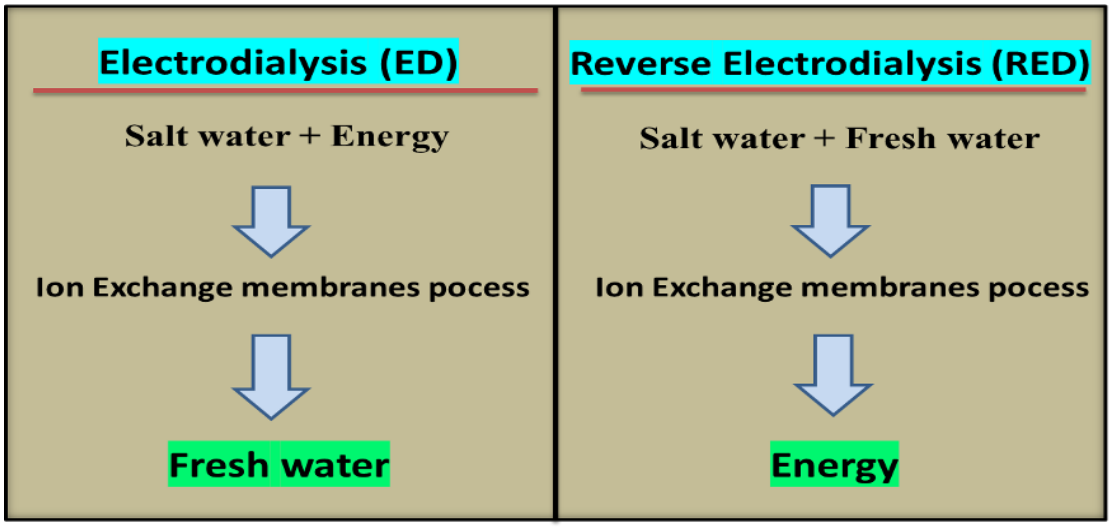

Figure 2.7 Difference between ED and RED processes

The gradient of salinity that induces the chemical potential and consequently the difference of Gibbs free energy is the driving force for the production of energy in an RED process. When two solutions of different NaCl concentration are mixed under control of alternating series of AEMs and CEMs stacked between two electrodes, the movement of ions to opposite directions create a chemical potential that can eventually be turned into electricity. RED is a membrane-based technology that generates renewable, non-polluting power by combining solutions with different salinity [15], [63], [77].

As shown in Figure 2.8, the RED module consists of alternative IEMs (CEMs and AEMs), thin spacers between alternating IEMs (not shown by Figure 2.8) and the electrode system case containing the anode and the cathode, where the oxidation and reduction reactions take place, respectively. The ions in the HC solution, Na^+ and Cl^-, migrate through the IEMs toward the LC solution; Na^+ crosses the CEMs toward the cathode while Cl^- crosses the AEMs toward the anode. There is a migration of the

counter-ions through the IEMs from the HC solution to the LC solution while theoretically, the co-ions and water are not transported. There will be an opposite migration of cations and anions in the HC toward CEMs and AEMs, respectively [10], [15]. The opposite ion flow will create a chemical potential. SGE is converted into electrical energy, utilizing an appropriate redox couple using electrodes [10], [13]. The concentration difference of ions across the membrane creates a difference in voltage across each membrane. If several CEMs and AEMs are lined, with alternately two solutions different in salt concentration supplied in the compartments between the IEMs, there is an accumulation of the membranes voltages, resulting in higher voltages. The stack's total voltage is proportional to the number of cell units in the RED module. A single cell unit includes a CEM, HC, AEM, and LC. By applying an electrical load to the electrodes, the opposite migration of the ions produces an ionic current at the electrodes which is converted into an electrical current [63], [66], [78].

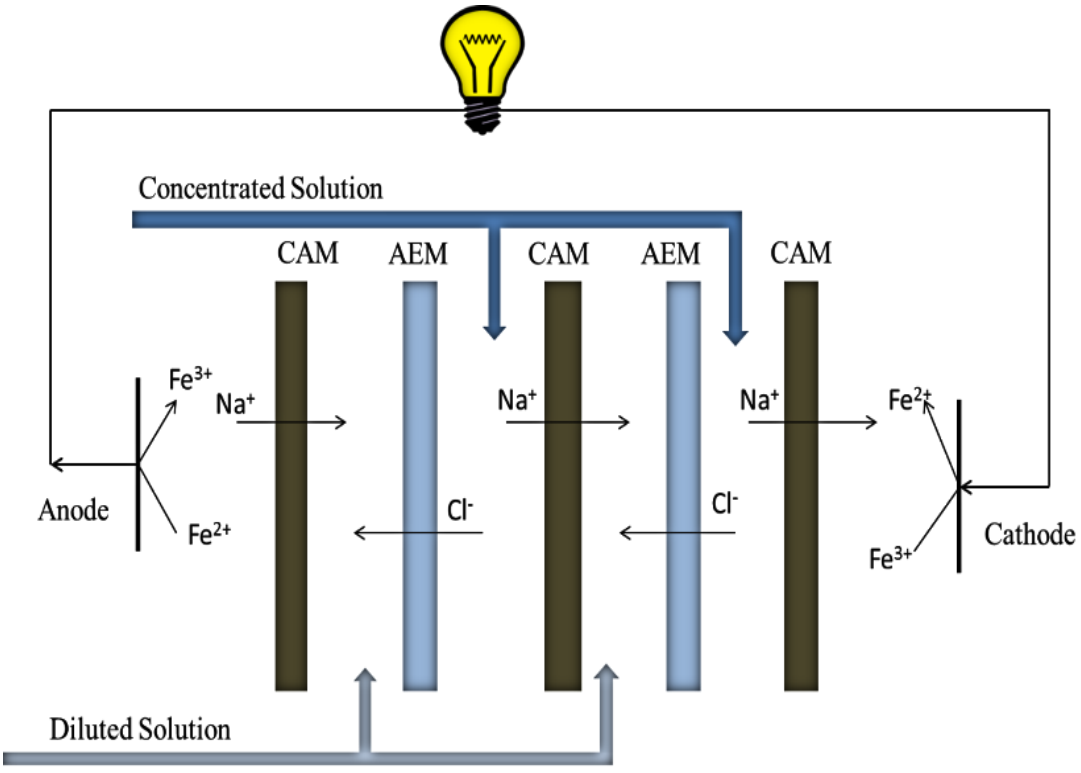

Figure 2.8 Schematic representation of the RED principle

2.4.3 Energy Efficiency, Energy Costs, and Performance of RED

During the RED operation, the ions migrate from the HC solution to the LC solution until the mixed solution becomes neutral. The energy of mixing saline and freshwater can be defined through the Gibbs free energy. In Figure 2.9 the behavior of the ions toward the mixing state is shown. Considering a continuous process in a close environment, the movement of the ions will continue until the equilibrium, where the ions concentration in the diluted solution is equal to the concentrated solution. The energy produced from salinity gradient (ΔG_{mix}) when 1 m^3 of the diluted solution is mixed to 1 m^3 or more concentrated solution can be determined by the difference between the Gibbs free energies of the resulting mixed solution (Gb) minus the sum of the Gibbs free energies of the original system (Gc and Gd) as shown in the following Equation 2.1 [57].

$$\Delta G_{mix}\,(E) = Gb - (Gc + Gd) \tag{2.1}$$

where c refers to the concentrated NaCl solution, d to the diluted NaCl solution, b to the brackish NaCl solution after the mixing.

The Gibbs free energy for an ideal solution is the summation of the chemical potentials of the individual substances as illustrated by Equation 2.2.

$$G = \sum_i \mu_i n_i \tag{2.2}$$

The chemical potential (μ) or molar free energy of component i, (μ_i) for an ideal solution, may be calculated following Equation 2.3.

$$\mu_i = \mu_i^{\,o} + \vec{V}_i \Delta P + RT \ln x_i + |z_i| F \Delta_\varphi \tag{2.3}$$

where μ^0 is the molar free energy under standard conditions in J/mol, $\vec{V}$ the partial molar volume, ΔP the pressure change compared to atmospheric conditions in Pa, R the gas constant (8.314 J/mol K), T the absolute temperature inK, z the valence of an ion in equiv./mol, F the Faraday constant (96,485 C/equiv.), and Δ_φ is the electrical potential difference (V).

The theoretical amount of free energy generable from mixing two solutions of different salinity can be computed by using Equation 2.3. Considering no pressure change or charge transport, the difference in Gibbs free energy generated by the

mixing of the concentrated NaCl solution and the diluted NaCl solution (ΔGmix) may be computed from the chemical potential difference before mixing subtracted by the chemical potential after mixing as illustrated by Equation 2.4.

$$\Delta\text{Gmix} = \sum_i [G_{i,b} - (G_{i,c} + G_{i,d})]$$

$$\Delta\text{Gmix} = \sum_i [\{(n_{i,c} + n_{i,d})RT\ln x_{i,b}\} - (n_{i,c}RT\ln x_{i,c} + n_{i,d}RT\ln x_{i,d})] \quad (2.4)$$

By substituting the molar ratio (n) by (CV), Equation 2.4 can be rewritten and is illustrated by Equation 2.5,

$$\Delta\text{Gmix} = \sum_i [C_{i,c}\, V_c\, RT\, \ln(x_{i,c}) + C_{i,d}\, V_d\, RT\, \ln(x_{i,d}) - C_{i,b}\, V_d\, RT\, \ln(x_{i,b})] \quad (2.5)$$

where ΔGmix (E) is the free energy (J) and V the volume (m^3), c refers to the concentrated salt solution, d to the diluted salt solution, b to the brackish salt solution which remains after mixing [17], [57].

Although SGE harvesting is rare or nonexistent in the field, it is a significant and sustainable resource of clean energy. When 1 m^3 of river water (0.01 mol/l NaCl) is mixed with a larger amount of seawater (0.5 mol/l NaCl), a theoretical average of 2.5 MJ energy is available [77], which is equal to the energy generated by water flowing over a 250 m high dam [18]. This theoretical energy depends on the chemical potential (NaCl concentration difference) between the concentrated and the diluted solutions [17], [79]. More energy is extracted from the system when the difference is higher. By comparison, mixing 1m^3 of 0.5 mol/L NaCl seawater and 1m^3 of 0.01 mol/L NaCl river water (both 293K temperature) theoretically generates 1.5 MJ, while mixing 1m^3 of 5 mol/L NaCl brine and 1m^3 0.01 mol/L NaCl river water at 293K results in energy higher than 16.9 MJ [17]. However, good knowledge of the process and careful assessment of the operating conditions is required to optimize the RED efficiency and make it competitive in the energy market.

A

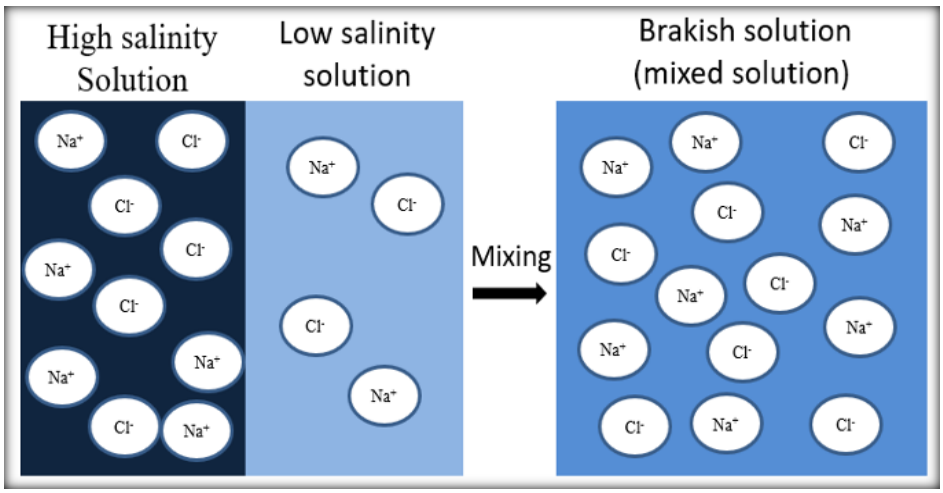

B

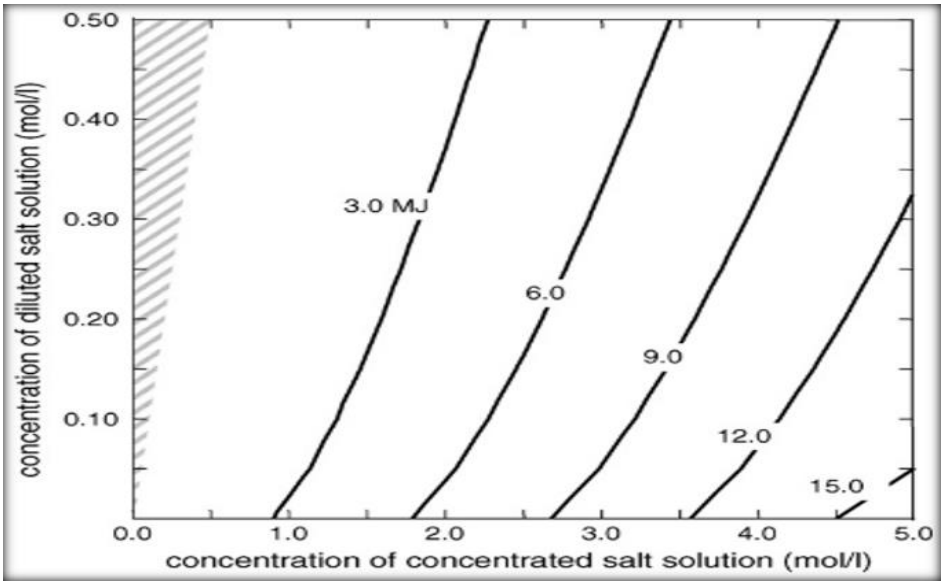

Figure 2.9 A) Brackish solution from the mixing of concentrated and diluted solutions, B) Theoretically available energy (MJ) from mixing 1m^3 of diluted and concentrated NaCl solution (T= 293 K), Shaded area: was not considered, because the NaCl concentration of the HC solution was lower than LC solution [17]

Up to now, accurate data about the full-scale PRO and RED systems does not exist, however, based on knowledge from lab-scale and pilot-scale studies and some assumptions, cost projections can be made. The membrane cost, pretreatment, and pumping are key elements that influence the capital, operating and maintenance costs of SGP. When it comes to the membranes, they consume up to 80% of the investment costs [80]. The high energy cost for pretreatment and feed solution pumping contributes to the process cost. The capital cost was estimated at around

EUR 7.33 million for the installation of a 50 kW capacity pilot-scale RED plant at the Afsluitdijk site (North Netherlands) [81]. The construction of another SGP plant at the Afsluitdijk Dam, covering a land surface area up to 2 soccer pitches and capable of producing 200 MW energy was estimated to reach a capital cost of 600 million USD. The retail cost of this plant was estimated to be around USD 90/MWh [80]. The capital cost is expected to decrease together with a drop of the SGP energy cost. The 2020 cost estimates using the years 2005-2007 ranged between EUR 0.09/kWh and EUR 0.27/kWh, EUR 0.11/kWh and EUR 0.28/kWh, respectively. Recently, the estimations range from EUR 0.08/kWh to EUR 0.15/kWh. In general, the cost of hybrid system installations seems to be lower and is estimated at EUR 0.11/kWh [80], [82]. The membranes contribute a lot to the process performance and cost. A membrane with characteristics respecting the RED requirement and with affordable cost is needed for a real plant RED implantation. Besides, measures should be taken to limits membrane fouling, concentration polarization and other parameters that could reduce the membrane life or performance [56], [78]. The drop in SGP cost will encourage the marketing of such energy. However, even though many research funds are available and some big SGP projects such as the Blue energy project in the Netherland, still now RED process (SGP in general) has not yet made its way to the energy market.

2.4.4 Ion Exchange Membranes Characteristics and Fabrication

The membrane separation process is an important filtration process present in living bodies and transferred into industries where it is applied with varied goals. In industrial use and water treatment, it is called membrane a thin semi-permeable layer of shit able to separate two solutions of different concentrations. But a membrane can generally be defined as a selective barrier that separates and/or contacts two adjacent phases and allows or promotes the exchange of matter, between the phases [83]. The importance of the membrane technology resulted in the development of innumerable membranes with varied properties according to their requirements, and they are used in reverse osmosis (RO), nanofiltration (NF), ultrafiltration (UF), microfiltration (MF), membrane distillation (MD),

pervaporation separation, ED and for medical use such as artificial kidney [84], [85]. IEMs are known to be one of the most advanced separation membranes among available membranes [84], [86]. IEMs are generally applied in the separation of ionic materials and transport technologies. They contain negatively or positively charged groups, which are attached to the membrane backbone and discriminate between cations and anions. CEMs allow cations (referred as counter-ions) and exclude anions (referred as co-ions) and AEMs allow anions (counter-ions) and exclude cations (co-ions) [16]. Basically, they separate cations and anions from each other in a solution. In principle, only counter-ions (charge different to the one of the fixed charges in the polymer matrix) can permeate the IEMs, while co-ions (charge similar to the ones of the fixed charges in the polymer matrix) are excluded by the fixed charges, see Figure 2.10.

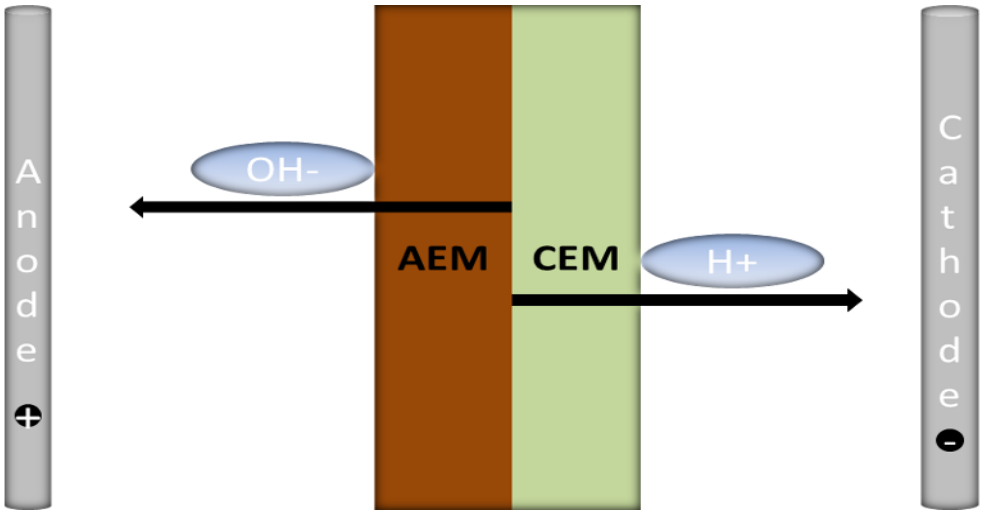

Figure 2.10 Migration of ions through the ion exchange membranes toward the electrodes

2.4.4.1 Classification of IEMs

The IEMs process is based on the Donnan membrane equilibrium principle and is mainly used for the recovery and enrichment of valuable ions, and the removal of undesirable ions (toxic metal ions) from wastewater [85]. From the desalination of sea and brackish water to the treatment of industrial effluents, they became efficient tools for the concentration or separation of food and pharmaceutical products containing ionic species as well as the manufacture of basic chemical products [87].

Based on the functions of ion-exchange groups fixed in the membrane, CEMs contain negatively charged groups fixed to the polymer matrix and AEMs contain positively charged groups fixed to the polymer matrix are dominant [83], as shown in Figure 2.10. IEMs membranes are classified according to the species and charge of the ion-exchange groups fixed in the membranes and their distribution in the membrane into various groups that determine the IEMs functions as follows;

- CEMs: contain cation exchange groups (negatively charged) allowing the cations to selectively permeate through the membranes,
- AEMs, contain anion exchange groups (positively charged) allowing the anions to selectively permeate through the membranes,
- Amphoteric IEMs, in which both cation and anion exchange groups are fixed randomly throughout the membranes,
- Bipolar IEMs which are bilayer membranes in which a CEM layer and AEM layer are joined,
- Mosaic IEMs, which have domains with cation exchange groups over cross-sections of the membranes and domains of anion-exchange groups. An insulator may exist around the respective domains [86], [88], [89], [90].

However, most commercial IEMs can be divided, according to their microstructure and preparation procedure, into 2 major categories; homogeneous and heterogeneous membranes [84], [85], [86], [88], [89], [90], [91]. As the main difference, the functional groups are chemically bonded with the membrane polymer chains in homogenous membranes, but it is not in heterogeneous membranes. This results in homogenous membranes having good electrochemical properties but in general, being poor in mechanical strengths and highly costive compared to heterogeneous membranes [91].

Based on the materials constituting the membrane, IEMs are also divided into hydrocarbon membranes, perfluorocarbon membranes, inorganic membranes and composite membranes of inorganic ion exchangers and organic polymers [86], [88], [90]. According to their functional groups, they are classified into strongly acidic (typically sulfonic acid groups), weakly acids (mostly carboxylic acid groups),

strongly basic (typically quaternary amino groups), and weakly basic (mostly primary, secondary, or tertiary amino groups) [88].

2.4.4.2 Application of IEMs

IEMs are generally applied in the separation of ionic materials and transport technologies. They are used in various industrial fields; however, they are mainly used for the recovery and enrichment of valuable ions, and the removal of undesirable ions (toxic metal ions) from wastewater [85]. They are used in the solutions containing multi-components, such as the electrodialytic concentration of seawater to produce sodium chloride, demineralization of saline water, desalination of cheese whey solutions, demineralization of sugarcane juice, a separator for electrolysis of sodium chloride to produce chlorine gas, sodium hydroxide and hydrogen gas, recovery of acids and alkalis from waste acids and alkalis by diffusion dialysis, etc. [84], [90]. They are the indispensable components in some traditional processes, such as diffusion dialysis (DD), ED, and bipolar membrane electrodialysis (BMED). More recently, IEMs have been extended to novel applications associated with energy conversion and production, including RED, fuel cells (FC), and redox flow batteries (RFB) [89]. The application of IEMs for renewable energy generation with the RED process is becoming important for clean no carbon print energy production. The membranes for this process should, however, present adequate properties of counter ion selectivity and resistance to salt degradation as well as high conductivity. Adequate membranes for this process are missing in the membrane market and researches in improving both the membrane quality and reducing its cost are one of the preoccupations of membrane scientists and engineers.

2.4.4.3 IEMs Characteristics and Preparation Routes

In principle, the concentration of the counter-ions is similar to that of the fixed charges in IEMs. However, the mobility of the ions in the membrane mainly depends on steric effects such as the hydration radius and the membrane chemistry (e.g. the crosslinking density of the membrane). Generally, the counter-ions with a higher

valence and a smaller hydrated radius have a higher permeability in an IEM than ions with lower valence and larger hydrated radius [1]. The durability of membrane materials and fine physicochemical characteristics are of great importance in many applications. Thermal and chemical stabilities are good indicators of the durability of the membranes. Transport-related properties defined below, such as the fixed-charge density swelling degree, permselectivity, ion exchange capacity (IEC), and ionic conductivity and resistance influence the electrochemical characteristics [10].

- Membrane area resistance
- Permselectivity: An IEM should be highly permeable to counter-ion but should be impermeable to co-ions.
- IEC
- Swelling degree
- Fixed-charge density

The membrane properties play an important role in electrodialytic processes such as RED, but a high membrane conductivity and selectivity, low resistance, and cheaply available are adequate IEMs generally desired in an RED process [86], [88]. Klaysom et al. [11] synthesized via controlled phase inversion procedures (dry and wet phase inversion or both combined) polymer membranes based on sulfonated polyethersulfone with various structures and pore sizes. Insisting on the importance of the IEMs properties, they investigated the properties of the membranes including their morphology, physical and electrochemical properties as well as their thermal and mechanical stabilities. They reported that the porosity of the membranes can be easily controlled by changing the drying period and casting film thickness; an increase in the drying period led to membranes with less porosity and denser structure [92]. Balster et al. (2005) analyzed the separation properties of various commercial CEMs and their permselectivity for monovalent ions. They focused on the effect of current density and calcium ion concentration in the feed stream on the membrane selectivity and reported that the conductivity and the charge density of the membranes determine the calcium transport efficiency through the membranes. They stated that calcium transport increases with increasing conductivity, however, it is lower for membranes with lower charge density [93].

An IEM requires three essential properties which are; to be a membrane, to be insoluble in solvents, and to have fixed charges in the membrane. Though IEMs have been used in many fields, most are used in electrochemical processes such as electrodialysis, separation of electrolysis, and solid polymer electrolytes for fuel cells. The required properties depend on the intended application of the IEM, but generally required properties are as reported in the previous section. Depending on the application, additional properties or modification may be necessary, for example, high selectivity and electrical conductivity are required for the application in the RED process [86]. Various IEMs have been proposed based on the ion exchange groups and their distribution in the membranes. Negatively charged groups are used for the preparation of CEMs while positively charged groups are used to prepare AEMs. As shown in Figure 2.10, AEMs allow the flow of the negatively charged ions while the CEMs allow the flow of positively charged ions. The most widely used ion-exchange groups and their apparent pK is presented in Table 2.2. IEMs used in industry are mainly CEMs having sulfonic acid and/or carboxylic acid groups, and AEMs with quaternary ammonium groups [86]. The membranes can be prepared from commercially available polymers. Commercially available polymer films such as polyethylene, poly(vinyl chloride), poly(vinylidene fluoride), etc., are directly reacted with reagents to introduce ion-exchange groups e.g. with concentrated sulfuric acid; a mixture of SO_2 and Cl_2 gas to introduce sulfonyl chloride groups; chlorosulfonic acid; trimethylamine, etc.

The cation exchange groups introduced into a polymer to form CEMs are sulfonic acid, carboxylic acid, phosphonic acid, mono-sulfate ester groups, mono- and diphosphate ester groups, hydroxylic groups of phenol group, thiol groups, perfluoro tertiary alcohol group, sulfonamide groups, N-oxide groups, and other groups that provide a negative fixed charge in aqueous or mixed water and organic solvent solutions [86]. Kristensen et al. synthesized a sulfonated poly (arylene thioether sulfone) based on CEM and investigated its electrochemical characterization. Their research resulted in a membrane with high selectivity and researchers reported a successful preparation of the membrane and its applications within electrochemical processes [61].

In AEMs, transport of anions is allowed while all cations are more or less excluded since the fixed charges are positive (such as ammonium, phosphonium, guanidinium ions) in the polymer matrix. AEMs are most widely used in electrodialysis, electro-membrane reactor, diffusion dialysis as well as Chlor-alkali process as they allow the transportation of anions via electrostatic interaction and oppose the transportation of cations. However, the permselectivity of the membranes is an important endowment to evaluate their efficiency in electro-membrane-based separation processes. Thus, highly conductive, selective, chemical, thermal, and oxidative stable AEMs are urgently required for the practical applications in the aforementioned membrane-based separation processes [94]. Garcia-Vasquez et al. (2013) investigated the evolution of physicochemical, structural, and mechanical properties of an AEM in a full-scale electrodialysis stack and they pointed out the dramatic performance drop of the process when the membrane deterioration occurs [95]. Anion exchange groups are positively charged groups: primary, secondary, and tertiary amino groups, quaternary ammonium groups, tertiary sulfonium groups, quaternary phosphonium groups: cobalticinium groups and other groups that provide a positive fixed charge in aqueous or mixed water and organic solvent solutions such as complexes of crown ethers with alkali metals [86].

Many different kinds of polymers have been used in AEM fabrication, for instance, polystyrene, polysulfone, polyetherimide [16], [96], poly(arylene ether), poly(phthalazinone ether ketone) (PPEK), and poly(phthalazinone ether sulfone ketone) (PPESK) [16] and many others. The conventional process to prepare AEMs requires several steps such as polymerization-choloromethylation-amination. To provide the membranes with desired properties, such as mechanical stability and controlled swelling, a post-processing so-called crosslinking stage, may be required [83]. However, the process requires extensive safety and health precautions and this causes the fabrication of AEMs more complicated compared to CEMs. In addition, optimizing the membrane properties is another challenge; for instance, AEMs have a lower permselectivity due to their higher swelling degree compared to CEMs [83], [96]. Most commercially available anion exchange membranes have quaternary ammonium groups as ion-exchange groups. These membranes may be prepared, for

example, by the reaction of trimethylamine with a copolymer membrane prepared from chloromethylstyrene and divinylbenzene or by alkylation with the alkyl halide of a copolymer membrane prepared from vinylpyridine and divinylbenzene [83], [86]. AEMs having weakly basic anion exchange groups, such as primary, secondary, and tertiary amino groups can be prepared by the reaction of a copolymer membrane having chloromethyl groups with ammonia, a primary amine or a secondary amine, respectively. Membranous polymers having chloromethyl groups are generally prepared by copolymerization of chloromethylstyrene with other vinyl or/and divinyl monomers. Chloromethyl groups, though, can be introduced into polymers having aromatic groups by the reaction of chloromethylmethyl ether in the presence of a Lewis acid such as stannic chloride anhydride, or by other methods. Khan et al prepared an AEM from brominated poly (2, 6-dimethyl- 1, 4-phenylene oxide) and dimethylethanolamine for electrodialysis. They claimed that the prepared membrane possesses a high ion exchange capacity, an excellent thermal and alkaline stability and showed high desalination performance by ED; all the analysis results showed a better performance than the commercial membranes [97].

Güler investigated the design, characterization, and application of tailor-made AEMs in an RED system to generate electricity. He used the active polymer polyepichlorohydrin (PECH), the inert polymer polyacrylonitrile (PAN) and the amine component 1,4-diazabicyclo[2.2.2]octane (DABCO), also used for crosslinking, to prepare the membranes by solution casting on a glass plate. The prepared membrane was characterized and used in an RED system with success to generate electricity [83]. Liu et al (2018) prepared an in situ self-crosslinked AEM and applied it in ED. They reported high properties of the membrane and very good performance of the ED with the synthesized membrane [96]. Maiti et al. synthesized an imidazolium functionalized poly(vinyl chloride-co-vinyl acetate)-based AEM, where the chlorine atom of poly(vinyl chloride-co-vinyl acetate) is replaced by a nitrogen atom at the 3 positions of 1,2-dimethylimidazole via nucleophilic substitution reaction. The authors claimed the technique to be simple and low-cost, and they stated that the analyses of the chemical structure proved that it is was an

adequately chemically stable membrane [98]. Similarly, Yang et al. prepared imidazolium-type AEMs by functionalization of bromomethylated poly(2,6-dimethyl-1,4-phenyleneoxide) with six kinds of imidazole compounds (containing rigid phenyl or a different length of flexible saturated alkyl groups) to investigate the influence of the structure of imidazolium functional groups on the physicochemical properties of the generated polymer membranes. They reported that the different structures of the imidazolium influenced almost all the properties of the synthesized membrane [99]. Lin et al. prepared and investigated the properties of a series of AEMs based on 1, 2-dimethyl-3-(4-vinylbenzyl) imidazolium chloride ([DMVIm][Cl]. The authors reported that the synthesized membrane showed excellent thermal stability, sufficient mechanical strength, and high conductivity; the membrane demonstrated great potential for alkaline anion exchange membrane fuel cell applications [100]. To enhance the properties of the membranes, some scientists choose to modify an existing membrane as reported by Zhao et al. [101]. They investigated the development of an AEM through poly (sodium 4-styrene sulfonate) (PSS) and hydroxypropyltrimethyl ammonium chloride chitosan (HACC) alternate electro-deposition to enhance the monovalent ions selectivity. The authors reported that this modification by membrane coating led to remarkable monovalent anion selectivities in the electrodialysis process.

Table 2.2 Apparent pK of usable ion-exchange groups for IEMs [86]

Cation Exchange Groups	Apparent pK	Anion Exchange Groups	Apparent pK
$-CF_2SO_3H$	-6	$N(CH_3)_3OH$	>13
$-SO_3H$	0-1	$N(CH_2OH)(CH_3)_2OH$	>13
$-CF_2COOH$	2	$S(CH_3)_2OH$	>13
-COOH	4-6	$P(CH_3)_3OH$	>13
$-PO_3H_2$ pK_1	2-3	NH_2	7-9
pK_2	7-8	NH	7-9
-Phenolic OH	9-10	Aniline (NH_2)	5-6
$-C(CF_3)_3OH$	5-6		
CF_2SO_2NHR	0-1		

2.5 RED Components and Performance Influencing Parameters

The performance of RED regarding energy efficiency and power density [102] is relevant for the implementation of a real RED plant. In the first RED researches, the power densities were very low, 0.05 W/m^2 [12], but were improved over time up to 6.7 W/m^2 [103] and are expected to reach very high values with the improvement of the process and the RED components. Using hypersaline concentrated solutions such as brines, power densities up to 12 W/m^2 can be produced [104]. Many limits need to be overcome for the RED process to be viable and the cost of the membrane must be reduced to make it cost-effective. The limits in the application of RED are connected to the lack of specific membranes made for RED. The high cost of IEMs and their inability to produce high power densities resulted in high installation and gross energy production costs [105]. Many parameters, dominated by the membrane cost and properties, the geometry and structure of the spacer, the feed solution ions content and concentration, the system resistance and the characteristics of the electrode can affect the performance of the RED process [106]. Tong et al. (2016) summarized that low energy efficiency and power density as well as IEMs fouling are major elements that hinder the marketing of RED [102].

2.5.1 Ion Exchanges Membranes

The membrane's properties play a major role in electrodialytic processes (ED, RED), diffusion dialysis (DD), membrane capacitive deionization (MCDI), and Donnan dialysis. The existing commercial IEMs are mainly developed for electrodialysis applications but do not specifically meet the requirements for RED. For instance, currently available membranes usually contain a reinforcing material to provide mechanical stability and they are usually relatively thick. Therefore, current IEMs are overdesigned for the RED applications. However, the performance of the membranes has an important effect on the overall performance of an RED system [83]. For the wide applications in electrodialytic processes, especially RED, the most desirable properties for successful IEMs are;

- Low electric resistance (3 $\Omega \cdot cm^2$ maximum area resistance), with low electrical resistance the potential drop is reduced during electro-membrane processes,
- High permselectivity (over 95%) for specific ions with the same charge,
- High transport number of counter-ions,
- Low diffusion coefficient of salt,
- Low osmotic water and low electro-osmotic water,
- Anti-organic properties,
- High mechanical strength and form stability, should have a low degree of swelling or shrinking in transition from dilute to concentrated ionic solutions,
- Dimensional stability,
- High chemical stability and durability, should be stable over a pH-range from 1 to 14 and in the presence of oxidizing agents,
- Low cost, as cheap as 2 Eur/m^2 [1,3,4,8,10] [16], [83], [84], [86], [88].

Relevant commercial IEMs properties were reviewed and discussed by Nagarale et al. [84]. Since they directly affect the electrochemical properties, attention should be given to the mass transport-related properties of IEMs used in RED [16]. Balster et al. (2005) reported that the IEMs' conductivity and charge density define the transportation of calcium. The transport rate of calcium raises with increasing

conductivity and falls with a lower charge density of the IEM [93]. Such property is important in RED because the power generation efficiency is connected to the transport rate and the selectivity of ions in the solution. The properties of the IEMs can be controlled during the preparation phase. For instance, Klaysom et al. (2011) demonstrated that IEMs porosities may be controlled by adjusting the time of drying and casting film thickness; an increase in drying time results in IEMs with low porosity and dense structure [92]. Due to the similarity between ED and RED, most of the membranes used for RED process investigations, are commercial membranes specifically developed for ED processes. These membranes do not reflect exactly the exigence of RED [61], [107]. Membrane electrical resistance, IEC, and permselectivity are the key parameters controlling the performance of RED. The ideal RED IEMs should present a very low resistance, high permselectivity and high IEC. The membranes should be highly selective for monovalent ions, as divalent ions affect the power output of RED. With such membranes, the ohmic losses are reduced and the SGP output is enhanced [108]. Membrane permselectivity describes the degree of co-ions exclusion by the IEM [109]. A perfect IEM has a permselectivity of one and does not transport any co-ion, contrarily to an IEM with no ionic selectivity which permselectivity is zero, and transports co-ions at the same rate as the solution [110]. This is the Donnan exclusion which is the ability of the IEM to discriminate between ions of opposite charge [111]. IEMs in an RED system must exhibit a high permselectivity (above 95%). The permselectivity and the resistance of an IEM are strongly influenced by its charge density. There is no direct relationship between these properties, but generally, IEMs with a lower fixed charge density have a lower selectivity and a higher resistance, and vice versa [111]. CEMs generally show a higher charge density, therefore a higher permselectivity than AEMs, however, local-scale heterogeneity also may seriously influence the permselectivity [109]. Geise et al. (2013) reported that the transport or exclusion of an ion depends on the chemical nature and the water content of the polymer IEM. The increase in the water content induces a drop in permselectivity [109]. It has also been reported that the permselectivity rises with the increase of the concentration difference between the two solutions [112]. Veerman et al. studied the thermodynamic efficiency of

different IEMs and reported various power densities from 0.5 to 1.2 W/m^2 [113], suggesting the importance of the membrane structure and characteristics in the RED power output efficiency, while Avci et al. recommended special monovalent-selective IEMs to reduce the transport of divalent ions through the membranes [114]. As reported by Hong et al., a novel and cost-competitive technique for the fabrication of IEMs with high IEC and low resistance is the typical expectation to improve the power output in an RED unit [115]. Traditional membranes are sensitive to high saline feed solutions, making them unsuitable for RED applications with high saline solutions which are ideal to some extent for high power production. Avci et al. prepared CEMs using sulfonated polyethersulfone and reported better results when used in an RED process of hypersaline feed solution compared to commercial membranes. They believe that membranes produced with polyethersulfone present better characteristics for RED and is cheaper due to the low cost of the hydrocarbon polymer RED [61]. The anti-fouling property of a membrane is also a requirement in membrane processes, IEMs included, to maintain the membrane's longevity. The effect of membrane fouling on RED especially with natural feed solutions, induced by organics, multivalent ions, and biomaterials contributes to postponing the commercial application of the RED process [116]. Fouling resisting membranes will encourage the usage of wastewaters as feed solutions in RED processes. Highly concentrated solutions such as concentrates from RO and other desalination units could readily become ideal candidates in a high potential salinity energy production by RED. Tong et al. (2016) prepared a fouling resistant nanocomposite CEM with high hydrophilicity and charge density for the RED application and reported a better power output compared to commercial membranes [102]. Simple membrane surface modification such as reported by Gao et al. can increase the IEM monovalent anion selectivity and anti-organic fouling potential compared to the original commercial membrane [117] which is necessary to hinder the negative effect induced by the presence of multivalent ions and natural organic matter (NOM) that lower the open-circuit voltage (OCV) and the RED power output. Besides the anti-fouling property and high affinity for the ions of interest required by the membrane, a spacer with good geometry and thickness can help

enhance the efficiency of the RED process. In fact, the membranes and the spacers can significantly contribute to the resistance, however, power loss due to the system resistance can contribute to lower the energy output. Recently, profiled membranes have been proposed to remediate the need of spacers and the negative spacers effect in the RED stack [118], [119], see Figure 2.11. The effects of the spacer shadow in the RED unit is attributed to the ohmic losses caused by the resistance [118] from the spacer material, leading to a high drop in efficiency by up to 60% [108]. Such amount of energy lost contribute to step back the RED attraction and hinder the possibility for large scale installation. Many attempts, from proposing different spacer materials to suggesting different spacer geometry and thickness and even spacer-less RED unit have been investigated as an attempt to solve the energy lost due to spacer effects. Building an RED unit without a spacer would solve both the spacer resistance problem but at the same time would simplify the RED module. The installation of the spacers in the module is a simple task but can be confusing for novices in the topic. Vermaas et al. introduced profiles in the form of ridges (230–245 μm) on one side of IEM by hot pressing [120]. The profiles open a path to the feed solutions to circulate in the stack and separate them from mixing, similarly they also create a distance between the stacked membranes. They reported that the ohmic resistance of the profiled IEM stack was significantly lower compared to an RED stack with regular spacers. With low resistance, voltage and intensity increase, resulting in higher power density with the profiled IEM compared to a similar stack with regular spacers. Even though profiled membranes are not well mastered yet, it could be an ideal alternative to simplify the RED module in near future and improve the process performance. However, the engineering of such membranes need to be assimilated and investigated to widespread in the IEM industry for the profit of membrane electrochemical processes such as ED and RED.

(I)

(II)

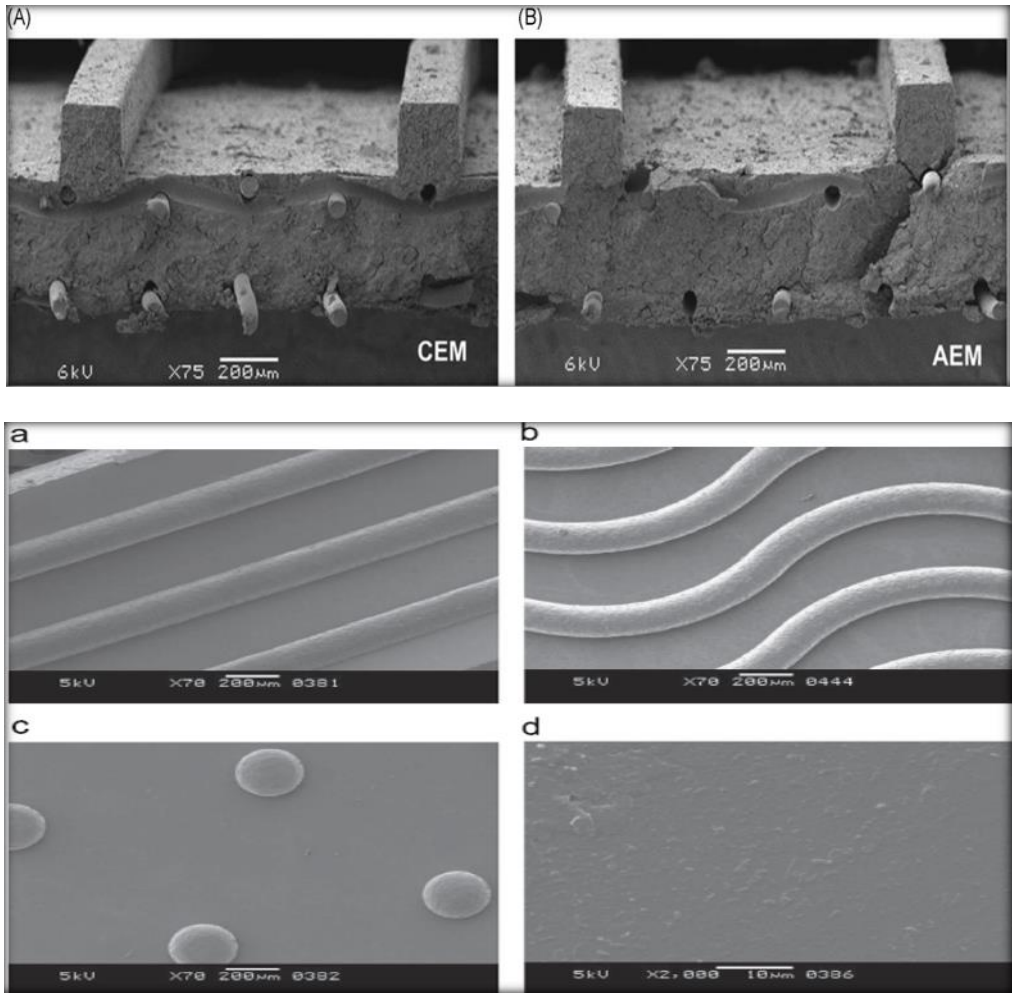

Figure 2.11 Image of scanning electron microscope (SEM): (I) cross-section of profiled (A) CEM and (B) AEM [120], (II) tailor-made IEMs: (a) ridges (b) waves (c) pillars and (d) flat membrane

2.5.2 Electrodes

RED operates through the movement of ions toward the CEMs and the AEMs. The opposite flow of the ions generates chemical energy that is converted at the electrodes into electricity by appropriate redox reactions. The electrode materials are of tremendous importance in the enhancement of the power output of the SGP-RED. The electrode systems consist of the electrodes and the electrolytes which are filled in the electrode compartments, and they play a major role in the RED unit by converting the current from ionic to electrical by redox reactions [121]. The electrode systems generally used are subdivided into 2 categories; systems without

opposite electrode reactions (involving the formation of gas such as Cl_2, H_2, O_2), and systems with opposite electrode reactions [121], [122], [123]. The second system is preferred in RED. They are used to improve the power output and for safety reasons (there are no net chemical reactions). Whereas electrode systems without opposite reactions are typically associated with losses of voltage for gas production and extra equipment is needed to collect the toxic (Cl_2) and/or explosive (H_2) gases [121].

The systems with opposite electrode reactions are subdivided into; reactive electrodes such as Cu-$CuSO_4$ [12] and Zn-$ZnSO_4$ system [123] and the ones with homogeneous redox couples such as $FeCl_3/FeCl_2$, $[Fe(CN)_6]^{3-}/[Fe(CN)_6]^{4-}$ and Fe(III)-EDTA/Fe(II)-EDTA) [124] with inert electrodes (such as Ti mesh coated by Ru-Ir metal oxide, graphite electrodes) [124], [125]. The major disadvantage associated with the reactive electrodes is the necessity to periodically change the feed solution inlets and inverse the electrical current [121], [124], to keep the balance with the electrodes which are affected by the redox reactions of the electrochemical process. On the other hand, there is a preferential choice of the inert electrodes with homogeneous redox couples, especially in the application of RED [121], [124], [125], because they are not affected by the redox reactions, therefore no need of any inversion of current and feed solutions entrance. Because they are cost-effective, improved and highly competitive, low-cost carbon electrodes may replace conventional electrodes made of noble metal oxide [125] in the future. It is worth mentioning that iron-based redox couples such as $[Fe(CN)_6]^{3-}/[Fe(CN)_6]^{4-}$ may poison the outer IEMs or cause iron precipitation [121], thus affecting the process performance and maintenance.

The ideal electrode system in an RED unit should demonstrate some characteristics among which but not limited to physical stability, chemical and electrochemical stability, low toxicity and strong redox species solubility. With the idea that electrodes are one of the key components to incorporate RED on a commercial basis, Veerman et al. performed a comparison study of electrode systems for RED, focusing on the technical feasibility, safety and environmental impact, and economic aspect of the electrode systems. They reported that the inert DSA-type (Dimensionally stable anode) electrodes systems together with a NaCl–HCl supporting electrolyte

using reversible Fe^{2+}/Fe^{3+} redox couple or the $[Fe(CN)6]^{4-}/Fe(CN)6]^{3-}$ couple was among the best in consideration with the study aspects aforementioned. They distinguished 3 types of systems; the systems with an obligatory, the systems with a facultative, and those with a forbidden interchangeable feed solutions inlet. Fe^{2+}/Fe^{3+} pair in a NaCl–HCl supporting electrolyte with Ti-Ru-Ir electrodes occupied the best position ranking for all the 3 systems [121]. The electrodes system must be considered with care to optimize the RED energy output. Although the dissipation of energy on the electrodes could not be avoided, it can be minimized by using an important number of cell-pairs (over 50) in the RED unit or by electrode segmentation which has been reported by Simoes et al. to be beneficial in terms of power and energy efficiency [126].

2.5.3 Spacers

To keep the CEMs and AEMs separated and allow the feed solutions to circulate in the RED stack without mixing one to another, spacers are used. The spacers arranged between the IEMs are designed to preserve their intermediate distance [127] and enhance the mass transfer by facilitating turbulence in the system [108]. They are usually made of woven materials (non-conductive) and using such materials in a RED stack causes a massive drop in energy production efficiency. The spacers highly contribute to the RED stack resistance by a phenomenon called the spacer shadow effect which can cause up to 60% efficiency drop of the RED process [118]. The spacers only can be a source of resistance and could result in a huge decline of the RED efficiency by up to 60%, causing an important decrease in the produced energy efficiency, as reported through theoretical projections [108] and experimental works [118]. Moreover, the spacers contribute to hindering the feed solution circulation over time due to pressure drop. The spacer geometry and thickness are the main parameters that control the spacer resistance effect. Spacers used in RED are generally designed for ED purposes and are thicker, less appropriate in an RED unit due to the high resistance that they induce. Thin spacers usually induce less resistance, but they create very narrow channels where the feed solutions circulate, leading to fouling and pressure drop with natural feed solutions.

To prevent or limit the pressure drop and maintain the power output high, the spacers must have an adequate geometry and thickness [128]. Mehdizadeh et al. investigated the spacer resistance and shadow effects on IEMs with 16 different spacers with various geometries, and porosity between 56 % and 84 %, thickness 0.100 and 0.564 mm, and reported that the spacer geometry influences the spacer shadow effect [118]. Some researchers proposed different spacer materials such as conductive spacers or spacers made of IEMs, others tried to improve the spacer geometry and thickness, and recently spacer-less RED units have been investigated. Conductive spacers are supposed to reduce the spacer resistance effect, therefore decrease the energy lost in the RED stack. Ion conductive spacers and spacer-less RED stack are under development to offset the negative effects induced by the spacer effect. As discussed in section 2.5.1, the spacer-less membrane would simplify the RED stack, reduce the system resistance, and eliminate the extra cost of buying spacers. Vermaas et al. proposed a spacer-less RED stack by introducing profiles in the form of ridges (230–245 μm) on one side of the IEMs by hot pressing [120]. The study improved the power density of the RED unit by significantly reducing the ohmic resistance in the profiled membrane stack. However, profiled membranes require engineering skills to produce and operate successfully. Further studies emphasizing large scale applications will enlighten our understanding and the behavior of such membranes in long-term large processes.

2.5.4 Feed Solutions Flow Rate and Pumping Energy

The feed solution flow rate is an important parameter in an RED process since it affects both the energy efficiency and the pumping energy demand, and directly impacts the EROI of the process. When the flow rate increases, the power density increases as well due to a better salinity difference between the diluted and the concentrated solution. However, a very high flow rate gives less time to the ions in the solution to adequately move toward the IEMs, causing a drop in the chemical energy and of course the electrical energy, resulting in a lower voltage and power density. Kang et al. reported that at the very high flow rate, the pressure inside the module increases causing augmentation of the RED stack resistance that will

eventually contribute to lower the power density [129]. At a low flow rate the movement of the ions will decrease the salinity difference between the diluted and concentrated solutions, resulting in a lower potential difference, consequently lower chemical energy and a decrease in the production of electricity with the drop of the voltage, consequently the power density [127], [130].

In terms of economic feasibility, operating an RED system at a low flow rate contributes to reducing the operating cost by reducing the energy need for pumping the feed solutions [131], [132]. Zhu et al. investigated the behavior of different flow rates with the RED system, and they reported that 20 mL/min was the optimum flow for both LC and HC to reduce the energy needed for pumping [131]. The energy consumption in the RED process is entirely based on the pumping of the feed solutions. Energy use for pumping is estimated to reach 25% of the total energy generated by the RED system [130], and it affects both the net energy recovery and the operational costs of the process. Besides, high flow rates may negatively affect the membrane by increasing its fouling or reducing its life. An optimal flow rate is important both in reducing the useless flow rate increase and protecting the membrane by increasing its life and resulting in a more economically effective RED process.

2.5.5 Feed Solutions Concentration, Composition, Velocity and Temperature

Among the many factors that can affect the performance of a RED process, membrane characteristics and the feed solution concentration and characterization are key factors. The feed solutions flow velocity, temperature, concentration, and composition are important parameters that contribute to affecting the performance of the RED power output. Optimizing and monitoring these parameters will contribute to increasing the power output. Tedesco et al. reported that increasing the flow velocity may augment the gross power output to some degree, but a velocity over 2-3 cm/s can result in lower power output. They also outlined that with feed solutions of NaCl content between 0.1 and 5 M and temperature up to 40 ^{o}C, the power output and energy efficiency reached the highest values reported up to now in an RED process, up to 12 $W/m^2_{cell\text{-}pair}$ [104]. This result outlines the positive

catalytic effect of temperature and the high salinity gradient in the RED power output.

The feed solutions NaCl concentration directly affects the driving force of the RED process, by affecting the salinity gradient. With high NaCl concentrations (hypersaline brine) of the HC and low NaCl concentrations of the LC, the high difference in salt content between the two water bodies which is the salinity gradient induces a high driving force of the RED process and eventually causes an increase of the power output [104], [131]. Recently, Daniilidis et al. investigated the RED performance with a stack fed with solutions of various salinity ranging from 0.01 M to 5 M. The effect of the feed solution concentrations and concentration differences on the RED performance in terms of membrane permselectivity, energy efficiency, power density, and electrical resistance was the element of interest. They observed a drop in both permselectivity and energy efficiency when the RED unit was operated with solutions with higher salt content and higher salinity gradients, contrarily to the power density which increases with higher gradients [103]. Even though energy efficiency is a determining factor in the energy sector, in an RED process using a naturally abundant and continuously following water stream, the power density is of major importance compared to the energy efficiency. The natural waterbodies salts content cannot be controlled but suitable mapping can be operated to determine the optimal concentration for RED applications. Concentrates from seawater desalination plants are also a source of high NaCl waterbodies which can result in a high chemical potential difference with river water. For these last feed solutions, because there are limited, optimizing the energy efficiency is required to retrieve the highest possible energy from a given solution. One way of achieving high energy efficiency is by decreasing the flow velocity, at the expense of the power density which decreases with decreasing velocity. Generally, the power density and energy efficiency of RED operate in opposite interest, so that the factors that are beneficial to one are harmful to the other.

The synthetic solutions generally used for RED processes contain only Na^+ and Cl^- ions. Operating an RED unit with real feed streams has proven that multivalent ions [114] and NOMs [133] which are usually present in natural waters are harmful to

the RED performance. Widely known divalent ions in natural water streams are K^+, Mg^{2+}, $Ca^{2+,}$ and SO_4^{2-}, among which magnesium (Mg^{2+}) with a concentration of around 1200 mg/L, is the most abundant in seawaters [76]. Vermaas et al. studied multivalent ions effects on IEMs and reported that Mg^{2+} and SO_4^{2-} were responsible for the decrease of the power density between 29% and 50% [134]. Similar results were observed by many other studies in the field, resulting in discomfort about the applicability of RED in a real environment. Using both synthetic and real solutions in a pilot-scale RED module, Tedesco et al. reported a power output up to 1.6 W/m^2 of cell-pair with natural solutions, but with artificial NaCl solutions at the same conditions, an increase of 60% was observed. They attributed the decline of the process performance with real feed stream to a high concentration of non-NaCl salts, especially Mg^{2+} in these solutions [76]. Moreover, as reported by Post et al., the uphill movement of $Mg^{2+}$and SO_4^{2-} against their concentration gradient causes the decline of the OCV of the RED process [135]. Recently Guo et al. reported that the presence of K^+, Mg^{2+}, $Ca^{2+,}$ and SO_4^{2-} in the feed solutions is the result of low OCV, high internal resistance, and low maximum power density. The negative influence order as they reported is led by Ca^{2+} for the ions coexisting with NaCl and is Ca^{2+} > Mg^{2+}>SO_4^{2-}> K^+ [136]. Based on the aforementioned results, considering the abundance of Mg^{2+} and Ca^{2+} in seawaters, dealing with divalent ions is an obligation if RED processes are to be optimized. One of the best alternative today is the development of highly monovalent selective IEMs rather than the application of feed solution pretreatment techniques, which would be expensive and less effective. Avci et al. claimed that the presence of Mg^{2+}, even at low concentrations, significantly reduces the performance of the RED energy production performance. They reported that a solution with 10% molar $MgCl_2$ caused a reduction of up to 20% of the OCV and 60% of the power density in their study, and suggested the development of new generation monovalent-selective IEMs to reduce the transport of divalent ions [114]. The pretreatment of the feed solutions, especially when wastewaters or high saline solutions are used, as part of recent investigations, will be of great importance to prevent membrane scaling and organic fouling. With microfilters 10 to 100 μm pore size, most of fouling agents can be removed from natural solutions. This will

increase the process cost but relatively low compared to the energy improvement rate that will be observed.

The high flow velocity of the feed solutions positively influences the hydrodynamic mixing, consequently the mass transfer in the RED channel, resulting in a high potential difference across the membranes, thus an increase of the power density [108]. Zhu et al. investigated the behavior of various flow velocities in the RED system and reported that 20 mL/min was the optimum flow for both LC and HC to minimize the energy consumptions of the pumps [77]. Tedesco et al. reported that an increase of the feed flow velocity can improve the power output to a certain limit, after which can result in a decrease in the power [104]. Even though there might be an increase in the power density with high flow rates, the energy needed for pumping increases as well, resulting in a decrease in the net power output and process cost. Also, Kang et al. claimed that at the very high flow rate, the pressure inside the module raises causing the augmentation of the RED stack resistance that will eventually contribute to lower the power output [129]. Besides, increasing the flow velocity does not give enough time to the ions to perform an efficient movement in the RED stack, which results in lower energy efficiency at high flow velocity. Operating the RED unit at optimal conditions including the flow rate is crucial in optimizing the power output. Up to now, most of the flow velocities proposed in the literature are very variables due to many parameters connected with the RED stack used.

Among the important parameters affecting the RED process, the temperature of the feed solutions has not been considered with more attention, probably since most seawater and river have an average temperature and very high temperature in a natural condition is not expected to be available to be used in an RED stack, but temperature exerts a strong influence on the RED performance [137]. In chemistry, temperature faster molecular reactions and high temperatures result in high solution conductivity, which, in an RED process would decrease the solution resistance and increase the power density [128]. In a cause-effect base, when temperature increases, the solution conductivity increases as well, and ionic mobilities are facilitated, ohmic losses are reduced resulting in higher power output

[108]. Stack resistance being well known as a key parameter in an RED unit, it is obvious that temperature may influence the RED performance by influencing the resistance of the feed solution [127]. Guo et al reported that with the rising temperature, the OCV increases and the internal resistance reduces, as a result, higher power density is generated [136]. In a recent study, Mehdizadeh et al. pointed out how hugely the net power output was affected by temperature [127]. They claimed that by increasing the temperature, the solution compartment and membrane resistance will reduce, driving with it an increase of the OCV, consequently the power output of the RED stack. All the physicochemical properties available in the RED stack are temperature dependent, thus a variation in temperature affects the electrical conductance by affecting the physicochemical properties [138]. Daniilidis et al. however reported that, although increasing temperature negatively affected the energy efficiency and permselectivity, the power density increased exponentially and almost double with feed temperature from 25 ^{o}C to 60 ^{o}C [103]. Benneker et al. analyzed the temperature of the feed solutions in both ED and RED systems and claimed that there is a decrease of the stack resistance when the temperatures are high, which induces higher voltage and power density. They achieved up to 25 % increase in the power density by doubling the feed temperature which was initially 20 ^{o}C [139]. However, the increase of the temperature should take into consideration the withstanding temperature of the membrane; too high temperatures would damage the membranes and affect the entire process. Oceans temperatures are generally below 30 ^{o}C, may not exceed 20 ^{o}C in most cases, consequently, cannot be a source of high-temperature feed solutions for an RED process. But tropical countries with warmer oceans and rivers will tend to have a slight increase in their RED energy output compared to countries of the West with identic ionic strength feed solutions.

2.6 Electrical Resistance in RED

The RED stack resistance is theoretically the summation of the resistances of each component resistance in series, which are the resistances of the AEM and CEM, diluted solution compartment and concentrated solution compartment [130], and

the resistance of the spacers. Electrical resistance needs to be considered carefully in RED-SGP processes since it affects the efficiency of the energy output and it is an important parameter in other electro-separation processes [140]. Among the LC and the HC, the resistance exerted by the LC has a dominant influence on the RED performance [137]. The resistance of an RED stack should be minimal to maximize the energy output. Membrane resistance as an example should be as low as possible in the RED stack. The feed solution concentration [141] and composition (Mg^{2+}, Ca^{2+}, SO_4^{2-}) affects membrane resistance [142]. Długołecki reported that the resistance of IEMs is highly connected to the solution concentration. The resistance effect is stronger with low salinity solutions, especially when operating at low concentrations with NaCl below 0.1 M, the membrane resistance becomes significant [141]. The resistance is also affected by the feed stream temperature. It decreases when the temperature increases [111]. Also, Długołecki et al. reported that the charge density of IEMs strongly impacts the permselectivity and membrane resistance. By comparison, CEMs have a higher charge density than AEM, resulting in higher permselectivity of CEMs. Compared to homogeneous IEMs, heterogeneous ones have a generally low charge density. Homogeneous IEMs have higher resistance compared to heterogeneous ones due to the IEM structure and the separation of charged domains in a polymer matrix (not charged), [111]. Thinner IEMs operated in an RED stack fed with feed solutions characterized by high salinity and temperature would reduce the membrane resistance but improving the IEMs fabrication technology and polymer matrix would be a better alternative in reducing the resistance.

Spacers are used in the RED system with two main goals; providing mechanical support to the IEMs and forming the flow channels for the feed solutions by keeping them separated in the module. Because the meshes used as spacer materials are made of non-conducting elements, they contribute to additional stack resistance; the spacer shadow effect [108], [118]. The resistance of the flow channel is proportional to the thickness of the spacer and inversely proportional to the conductivity of the solution [143]. Veerman et al. [130] and Danidilis et al. [103] reported in different experiments, 45%, and 66% respectively, as the contributions

of the resistances of the spacer-filled dilute channel to the resistances of the cell pair. It is worth mentioning that thicker spacers impact enormously the resistance of the cell pair when operating with very low NaCl concentrations of a dilute solution, and using thinner spacers can significantly reduce the influence of the resistance of the dilute channel [130]. A similar observation was reported for the IEMs. The resistance contributes to tremendously affecting the efficiency of RED by up to 60% energy reduction [108]. The fabrication and application of the so-called spacer-less profiled IEMS for RED and described in section 4.4.1 above, can eliminate the need for spacers and similarly get rid of the major resistance induced by the spacers in the channels of the RED stack.

2.7 Application of RED with Real and Alternative Feed Solutions

Due to the complex nature of natural waters, rich in divalent ions, dissolved matters and suspended solids, most of the researches of SGP extraction by RED are lab-scale studies using synthetic solutions, with only a few investigations using natural sea and river waters. When natural feed streams such as river and sea waters or supersaline lake are used in an RED system without adequate pretreatments, a mixture of fouling particles mainly composed of scaling minerals and organic foulants can accumulate on the membrane's surface [144] over time and affects the RED performance and life. Membrane fouling with natural waters is a big challenge, especially fouling of AEMs by organic matters identified as the main cause of performance loss in RED with natural waters [116], [145]. Taking advantage of the high salinity gradient between urine and urine flushing water, Volpin et al. extracted SGP with RED and reported performance loss caused by organic fouling and the presence of multivalents ions in the solution [146]. Avci et al. investigated the effectiveness of natural feed streams SGP harvesting by RED. They compared the result to synthetic equivalent ionic strength. They reported that the highest power density obtained for real and synthetic feeds at 60 ^{o}C feed solution temperature was 0.46 and 1.41 W·m^{-2}, respectively. The authors stated that the low performance with natural feeds solutions was the result of high membrane resistance, low OCV and the transport of Ca^{2+}, $Mg^{2+,}$ and SO_4^{2-} through the membrane [147]. Results from

natural solution RED researches reported that up to 50% of the power output is lost in the first hours of operation [144], [148], [149]. Electrochemical impedance spectroscopy revealed that the efficiency of the RED system decreases mainly because of the resistance of the CEMs. Similar to all membrane processes, fouling and concentration polarization are the major problems with natural streams; the quality of the feed solution is an important and determining parameter in the RED power density [150]. Especially in long period operation with natural waters, pressure drops in the RED unit and fouling are major challenges [151]. Some alternatives such as the improvement of the IEMs properties making them resistant to fouling through membrane modifications [152] and profiled membranes [144] can contribute to reducing the fouling effects in RED processes. Besides, antifouling strategies have recently been proposed among which, periodic inversion of the feedwater and air sparging [148] or by using CO_2 saturated feed water as two-phase flow cleaning to reduce membrane fouling [149]. As reported by Vermaas et al., inter-changing seawater and river water in the RED module feed inlet channels recover the initial power density for a period of operating time, probably due to removal by the reversed electrical current of the multivalent ions and organic foulants in the RED stack [148]. Recent studies on antifouling techniques also include the use of finer prefiltration and the increase of the intermembrane distance, with a major influence of the pretreatment technique used [153], [154]. Even though the integration of a pretreatment process might prevent these problems as well, it will require an extra cost that affects the net power density and result in less cost-effective energy production by RED.

2.8 Pilot Scale RED

The lab-scale RED performance has considerably improved over the last years. However, typically small scale performed RED plant with an active membrane area of some tens to hundreds of square centimeters cannot give reliable information about the practical real implementation of the RED process. Nijmeijer et al. claimed that this upscaling and practical implementation is beyond the academic expertise, and the need for collaboration with industry is a necessity [18]. There are a few

numbers of RED pilot plant investigations in the literature. More pilot-scale investigations are required to motivate the scaling up and draw a full understanding and monitoring of the RED technology [58]. In fact, without pilot-scale researches, much unclear or misunderstood information related to RED will remain, and these pilot-scale plants should as well be investigated with real feed solutions to project a real feasibility plant under natural conditions. Verman et al. studied a pilot-scale RED process with 50 cells and a total membrane area of 18.75 m^2 to follow the performance of a scaled-up RED stack. They compared the results to a small-scale stack and reported that the hydrodynamic design of the stack is one of the determining parameters of RED performance. They also reported that increased hydrodynamic losses negatively affected the large stack due to the longer flow path followed by the feed solutions which induces a longer residence time of the fluids in the stack [155]. When a real scale RED plant is built, challenges among which the membrane stabilization in the stack and the water residence time will be encountered. A longer flow route in large-scale RED will increase the residence time of the feed solution which will result in a lower salinity gradient in the stack, and a direct consequence will be the decrease of the power density. Increasing the flow rate may solve part of the problem but simultaneously it will increase energy consumption. The best stack arrangement would be with multiple feed solution entrances, which will reduce the path of the flow. To well understand the RED process in a field application, Tedesco et al. claimed to have tested the first RED pilot plant operated with both natural and synthetic solutions. They reported a power output up to 1.6 W/m^2 of cell-pair with natural solutions, and 60% higher with synthetic NaCl solutions at the same operating conditions. The performance reduction with natural streams was likely caused by non-NaCl ions, especially Mg^{2+}, in relatively large concentrations, which adversely affected both the electromotive force and stack resistance. No membrane fouling, scaling, or aging occurred during 5 months of operation, consequently no performance losses [76]. Nam et al. investigated a pilot-scale RED of 1000 cell-pairs, 250 m^2 fed with municipal wastewater has LC solution and seawater as HC solutions and reported 95.8 W of power, 0.38 W/m^2 power density [156]. Tedesco et al. Conducted a 400 m^2 active

membrane pilot-scale RED process and reached around 700 W of power capacity with synthetic brine and brackish solution. They observed up to 50% power output decline when they operated the system with real solutions at similar conditions [157], enlightening the negative effects of real solutions in RED power performance as reported by former authors. D'Angelo et al. evaluated the possibility of using a pilot-scale RED process (500 cell-pairs with 44 × 44 cm^2) fed with natural solutions, brackish water as the diluted solution and concentrated brine from the saltworks as the concentrated solution, for simultaneous energy production and the wastewater treatment. Their results confirmed the ability of the system to operate for months without a noticeable decrease in the power output [158] as reported by Tedesco et al. [76]. Only a small decrease in RED performance was observed after 4 months of operation in a real environment with the same redox solution [158]. Unlike other membrane processes, the IEMs used in RED have the advantage of resisting fouling and deterioration. Regardless of the power hindering parameters, RED can be operated for a long period with the same membrane without any loss of power caused by the membrane structural modification. Mehdizadeh et al. studied the impacts of the feed solutions temperatures on RED performance in terms of energy output. With a pilot-scale RED stack of 200 cell-pairs (40 m^2 active membrane area), they claimed a huge influence of the net power output as a result of temperature effects [127]. The temperature is known to facilitate chemical reactions and ions movements, consequently high temperature helps increase the power density. The results from the different pilot-scale studies point out many difficulties, especially when natural feed solutions are used, and the non-NaCl ions as well as foulants in real streams are main hinderers of the RED performance. Nonetheless, these challenges are not limiting factors that would condemn the applicability of the process, mostly if appropriate IEMs for RED is made available.

2.9 Hybrid RED System

The RED system can effectively be combined with existing desalination processes and water treatment technologies to form a hybrid system. RO, ED, forward osmosis (FO), ED and MD are well-known desalination processes used in seawater. These

processes produce clean water and generate a concentrate that needs to be handled because it affects the ecology of the surroundings due to the very high salt content of the concentrate. A hybrid system composed of an RED stack and one of the desalination processes mentioned above can be effective [159] in such a way that the concentrated brines from these systems are transferred into the RED to be used as feed solution, as depicted by Figure 2.12. While seawater salt concentration is around 0.6 mol/L, membrane-based desalination such as RO brine and FO brine can contain NaCl with a concentration over 1.2 mol/L and 2.4 mol/L, respectively [160]. This results in an upper-saline solution with a high potential of SGE when used in HC together with river waters. Kwon et al. intended to increase the power density with brine as concentrate solution, and discovered that the power density using the concentrate from RO (1.48 W/m^2) and FO (1.86 W/m^2) as a concentrated solution, raised 1.5-fold and 2-fold, respectively, compared with the power density of an RED using seawater as a concentrated solution [160]. Ashu et al. operated an integrated direct contact membrane distillation (DCMD)-RED process for simultaneous seawater desalination and electrical energy production with a target of low energy and Near-Zero Liquid Discharge (ZLD) in seawater desalination. Their results pointed out an OCV in between 1.5 and 2.3 V and a gross power density ranging from 0.9 to 2.4 $W/m^2_{MP\ (membrane\ pair)}$ from the integrated DCMD-RED process [161]. The concentrates of desalination processes are very high saline solutions resulting in a high salinity gradient in the RED process and are a source of high voltages and power densities. Another advantage attached to this hybrid system is solving at the same time brine management problems [161] as this brine concentrated from the desalination process can feed the RED unit and results in a diluted brackish solution (Figure 2.12), and this contributes to stabilizing the marine ecosystem. Such an integrated system will simultaneously produce clean water and energy [162], open a gate to the implementation of ZLD and low-energy desalination plants [163]. Also, operating RED with warm feed solutions can dramatically influence the power output [137], with increasing temperature increasing the net power density [127]. Concentrates from MD being warm (40 to 75 ^oC), when used in a RED process, the power output is increased due to two factors; high salinity and high temperature.

Long et al. reported that the heated brine solution from MD yielded relatively better electrical efficiency in the RED system. Using the hot concentrate solutions from the MD system as a feed solution in the RED process, they claimed that the efficiency of electrical energy generation of the proposed hybrid system can reach 1.15% when operating with solutions of temperature ranging from 20 °C to 60 °C in the MD and 5 mol/kg NaCl concentration [164].

As illustrated in Figure 2.12, the combination of the hybrid system with RED can be a mutualist relationship, each of the processes taking advantage of the other. In this case, diluted effluent from the RED process is used in the desalination plant. Desalination technologies are high energy-consuming processes, for the process operations and feed solution pumping and circulation. MD, for instance, requires high energy for heating and cooling the different feed solutions while reverse osmosis requires high energy to ensure the high pressure needed in the process. When combined with the RED process, low-cost energy can be conceivable. Moreover, when the diluted effluent from RED is used, the need for desalination and membrane fouling is lower compared to direct seawater which contains more salt. Li et al. investigated a hybrid desalination system by combining an RED and an RO process. The mixed effluent from the RED process resulting in a solution with low salt concentration was used to feed the RO unit while the concentrated RO brine is used to feed the RED unit. They reported that the RED–RO combined processes could effectively decrease the energy consumption in RO and provide a better and alternative solution to handle the concentrated brine [165]. Effluents from advanced biological wastewater treatment plants [150] can also be used as a diluted solution in the RED unit. This effluent is generally discharged in the sea and hybrid systems combining an RED stack and a municipal wastewater treatment plant can contribute and generate energy to cover the energy demand of the plant. Wastewater treatment plants with integrated UF or MBR units are ideals due to the quality of the effluent solutions which do not require any additional pretreatment and can be used directly in an RED unit as a diluted solution [150].

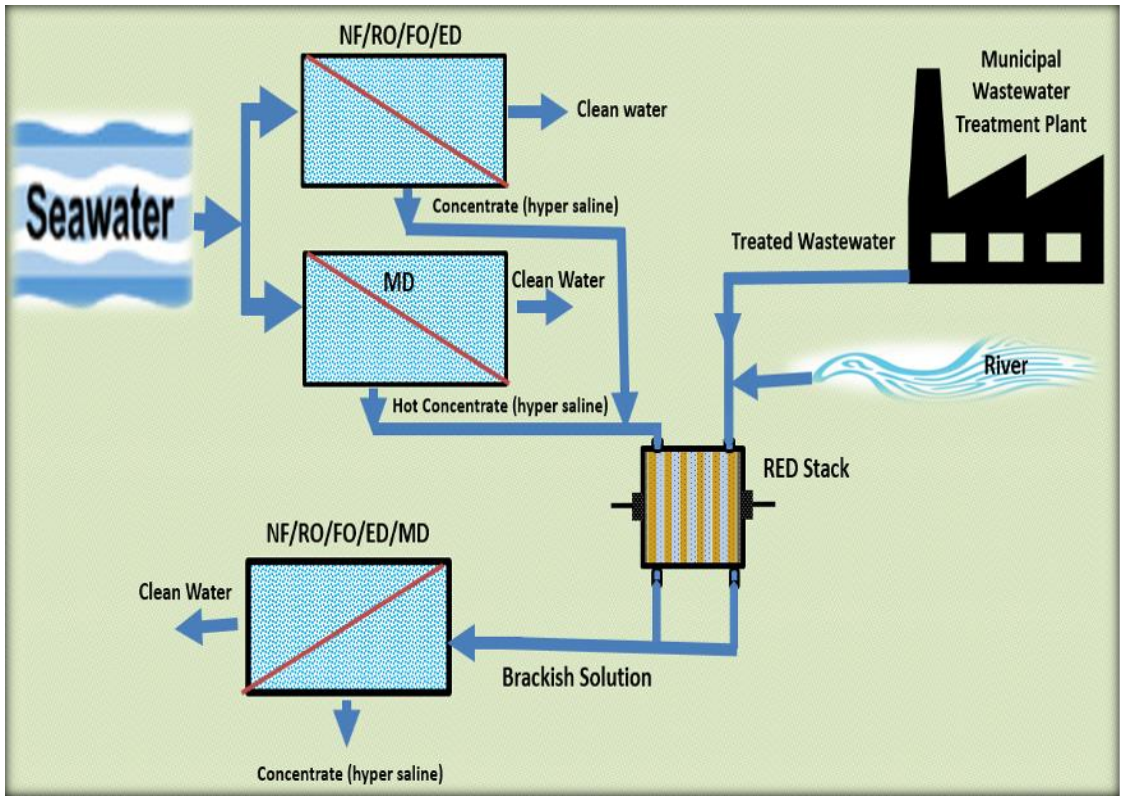

Figure 2.12 Schematic illustration of a possible combination of RED with other desalination and water treatment processes

2.10 Challenges and Future Perspectives

The extraction of SGP by the RED process is new, under-developing with many challenges among which the most relevant ones are the acquisition of suitable and cost-effective IEMs, spacers and electrodes for the energy generated to be efficient and cheap. Experiments using real feed solutions, seawater, salt lakes, river streams, brines, desalination concentrates, wastewaters are being investigated to understand the real challenge in RED processes with natural feed streams in comparison to widely investigated synthetic feed solutions. Pilot-scale studies are being performed recently to enlighten the limits of labs scale RED processes and project for the feasibility of real plant installations. As a common knowledge in RED SGP extraction and claimed by Daniilidis et al., membrane price, performance, and many other parameters are important factors influencing the installation of real scale RED plant [166]. Therefore, new researches should focus on the realization of

commercial RED applications by reducing membrane cost and fabrication IEMs adapted to such a process.

Most of the challenges faced by RED processes are based on the IEMs properties and cots, and changes are expected with new researches and probable marketing of specific membranes for RED. Natural sea and river waters remain the ideal solutions for RED application but due to the presence of divalent ions in these solutions, IEMs resistance is increased, hindering the RED performance. Many ongoing investigations in producing better IEMs are expected to increase the RED power efficiency and performance. For instance, novel and tailor-made IEMs are being investigated [167] to mitigate the negative effects of divalent ions in the RED process with natural feed streams. The electrochemical properties of IEMs such as permselectivity and resistance are important in RED; while the first one should be high the second must be very low. Many researchers are investigating the improvement of such properties among which organic-inorganic nanocomposite membranes [168], halogenated polyethers [169], sulfonated polyethersulfone (sPES) CEM [61] can be mentioned. Recently, the development of membranes with two different faces, chemically treated on one side by inducing modification, the so-called Janus membrane has shown good results in membrane application and is expected to be a solution in harvesting the osmotic energy, affected by the ion polarization phenomenon and low ionic conductance [74]. Zhu et al. built a high-performance Janus membrane-based generator to prevent the ion polarization phenomenon in a single-layer membrane by integrating a nonlinear current into the energy conversion system, and similarly, they improved the conductance by chemically tuning the porosity and surface charge density. The diode-type membrane in their study was able to block any current that flows back into the membrane [74]. They achieved excellent power densities which suggest that the diode current–type Janus membranes could exhibit great potential in collecting SGP. Understanding nanofluidics and nanoconfinement will enlengthen the ionic transport in a confined nano-environment which will open a new gate in IEMs design SGP extraction by RED. Alessandro et al. fabricated a new class of nanofluidic devices to investigate the properties of fluid transport inside a single boron nitride

nanotube which allowed the investigation of fluidic transport through a single nanotube under diverse forces [170]. Constructing distinct and well-controlled nanochannels remains however a challenge that requires high engineering skill. Zhang et al. suggested the development of thinner, low-resistance membranes that promote their ion selectivity. They prepared ultrathin (approximately 500 nm thickness) and ion-selective Janus membranes (AEM), able to extract up to 2.04 W/m^2 by mixing natural seawater and river water [171]. By engineering an ultrathin membrane with nanoscale pore size allowed a low fluidic resistance and rapid mass transport which improved the conversion of the osmotic energy. However, even though this IEM can solve major performance-related issues of the RED system, such a thin membrane requires high engineering in stack installation and the membrane may be sensible to long term operation. In addition, surface modification of the Janus membrane is required to allow it to operate in the neutral pH that is relevant for natural waters. As investigated by Güler et al. by coating a standard commercial AEM by copolymerization [152], the properties of IEMs can be improved through modifications. The production of thin IEMs which are low resistance and spacer-less membranes which eliminate the need for spacers in the RED stack responsible for spacer shadow and extra stack resistance [119], [120] are part of the future of high-performance RED processes. The spacer shadow effect and resistance are of high limits in RED, giving importance to profiled membranes that make the use of non-woven spacers obsolete. Under real feed solutions, membrane fouling effect is less sensitive when profiled membranes are used compared to traditional membrane-spacer [144]. The current state of RED results in high Levelized Cost Of Energy (LCOE) compared to many other power production technologies, but with the decrease of membrane price (below €4/m^2), better power densities (above 2.7 W/m^2) expected in near future, RED can become more efficient and competitive compared to conventional and established renewable technologies, with an expected lower LCOE index of 0.16 €/kW h [166]. Cost-effective tailor-made IEMs with low resistance, high permselectivity, appropriate chemical and mechanical stability and environmentally friendly manufacturing paths are the future of a low-LCOE RED process that is competitive on the energy market. Recently, investigations

are giving interest in pilot-scale research, natural feed solutions (sea/river) and hybrid RED. Many papers have already been published with lab-scale RED fed with synthetic solutions, and researchers are giving more interest to the real streams and the behavior of the membranes to such streams. Membrane fouling and divalent ions contribution to membrane resistance are other challenges to overcome. The pilot-scale plant is limited up to now but is expected to grow if SGP is to be considered to enter the energy market. Hybrid RED processes are taking a stronger position, generally combined with desalination techniques (ED, FO, RO, MD), and the application of RED in wastewaters energy extractions. Concentrated brines from RO or MD can be used in RED as a concentrated solution [161], [163], [164], [165]. These solutions, although limited compared to seawater, have a higher potential and lower LCOE [166]. Being an alternative to the use of river/seawater, concentrated brines and brackish water results in enhanced power output (up to 12 $W/m^2_{cell\text{-}pair}$) of RED through the increase of the driving force and reduction of the internal stack resistance [104]. In addition, RED behaves like a technique for handling the concentrates from desalination plants, or as a pretreatment process when less concentrated RED mixed effluent solutions are used in a desalination plant. This mutualist symbiotic combination can be improved and contribute to reducing the desalination plant cost and the LCOE of RED.

3
MATERIALS AND METHODS

3.1 Laboratory Scale RED Stack

The experimental study of the present Ph.D. research was performed in the wastewater laboratory of the Department of Environmental Engineering of Yildiz Technical University, Istanbul.

A lab-scale RED apparatus essentially composed of an RED stack capable of holding 20 cell-pairs has been designed and constructed locally. The feed solution tanks have been constructed using plastic jerrycans. The external view of the RED systems was composed of the RED stack, the feed solution tanks, a peristaltic pump to circulate the feed solutions and the electrode rinse solution (ERS) into and out of the module, a multimeter used as the electrical measurement apparatus, the pipes to circulate the different feed solutions and an LED in a closed circuit and connected to the electrodes of the RED system to testify a visual electricity generation of the system, as shown in the picture of Figure 3.1. The RED stack consisted of IEMs, purchased and home-made spacers, and the electrode system. The spacers are placed between alternating IEMs to create stark compartments. Three tanks with 2 L volume were used as solution reservoir. One of the tanks was filled with the high concentrated saline solution (Seawater, synthetic high saline solutions) representing the high compartment (HC), the second tank with the low concentrated saline solution (river water, synthetic low saline solution) representing the low compartment (LC), while the third tank carried the ERS. A peristaltic pump was used to circulate the feed solutions from the tanks through the RED module. The schematic representation of the RED diagram is presented in Figure 3.2.

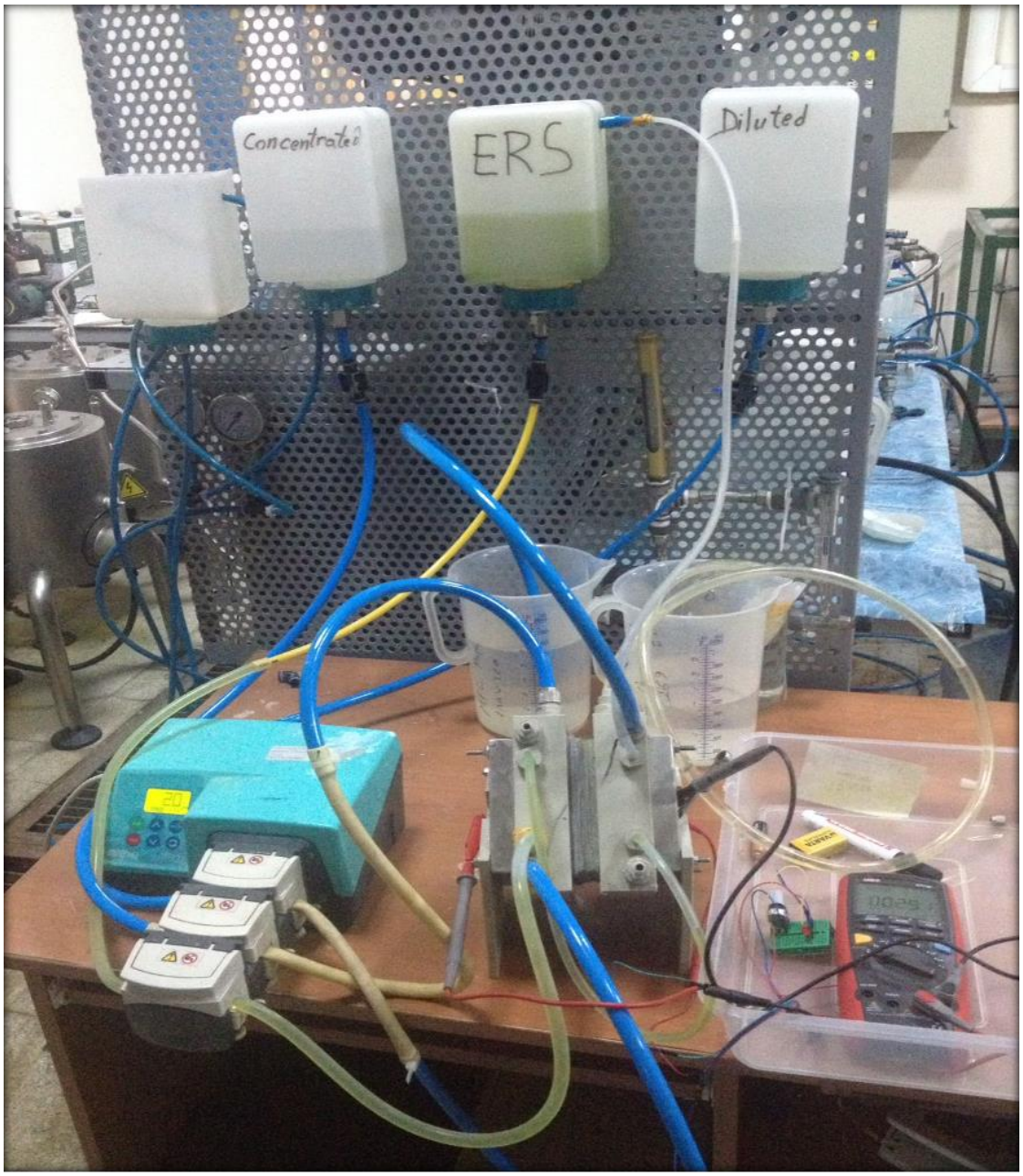

Figure 3.1 Picture of the lab-scale RED system

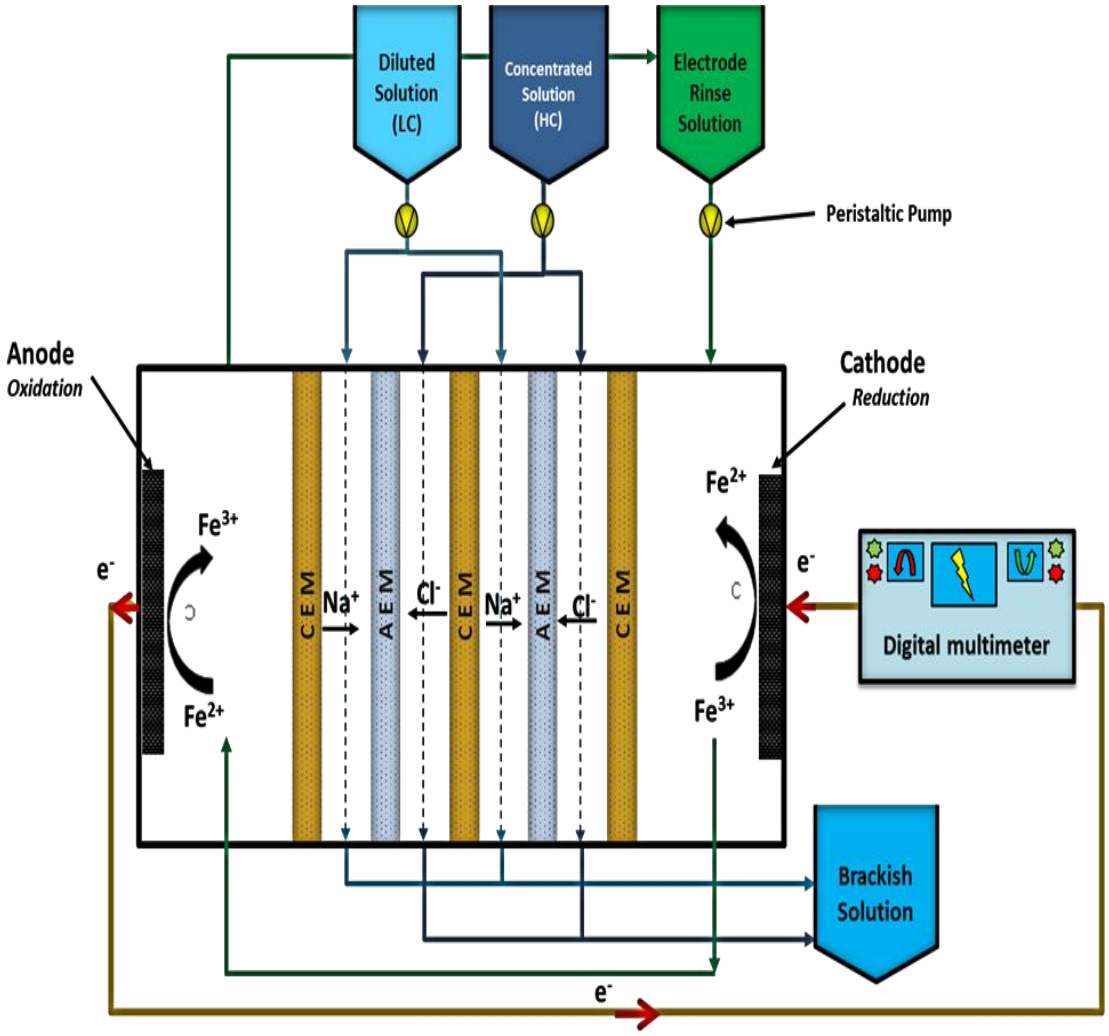

Figure 3.2 Schematic design of the lab-scale RED system

3.2 The Components of the RED Stack

The module consists of alternative IEMs (CEMs and AEMs), thin spacers between alternating IEMs and the electrode system in the electrode case (anode where the oxidation reaction takes place and a cathode where the reduction reaction takes place). The pictures of the closed module are shown in Figure 3.3 and the internal configuration of the RED stack is depicted in Figure 3.4. The following sections will discuss and give detailed information about each component present in the RED stack.

Figure 3.3 Pictures of the closed RED module

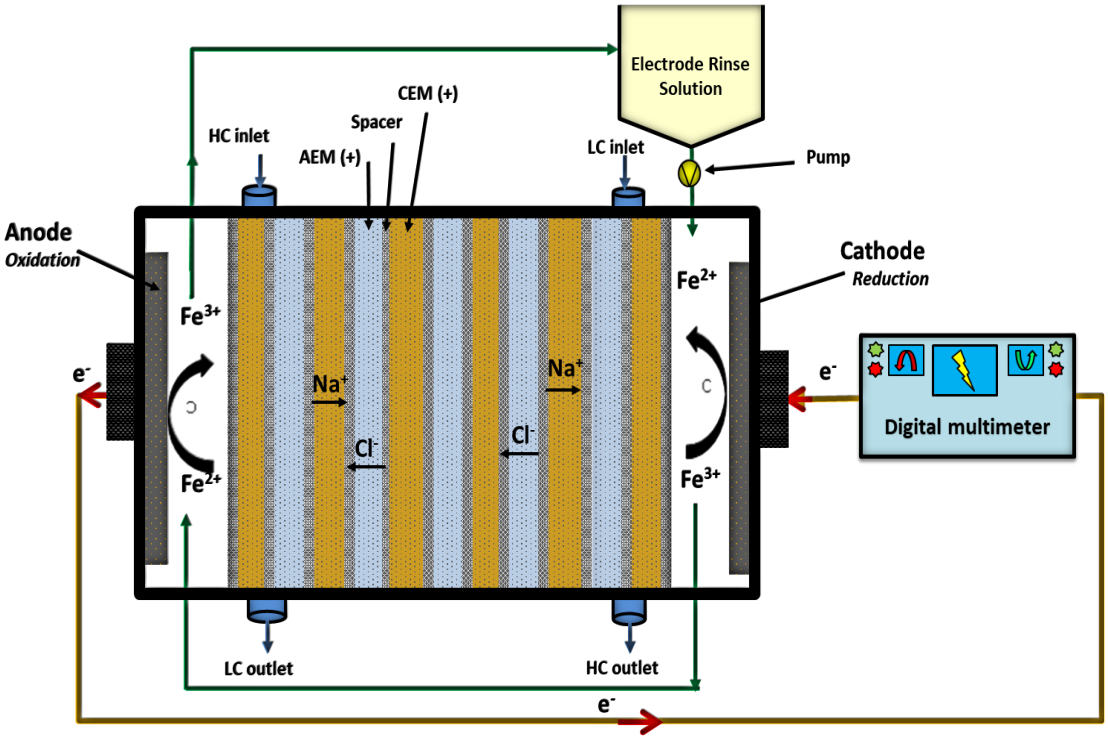

Figure 3.4 Schematic design of the internal configuration of a RED Stack

3.2.1 Ion Exchange Membranes

Both CEMs and AEMs used in the study were purchased from Iontech, China. The images of the membranes can be seen in Figure 3.5 and their characteristics are presented in Table 3.1.

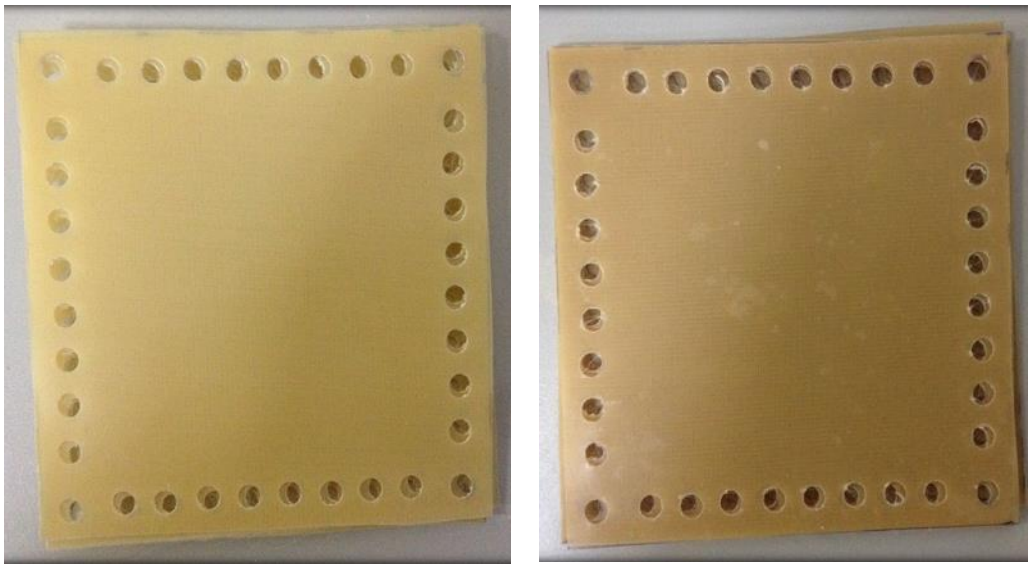

Anion Exchange Membrane Cation Exchange Membrane

Figure 3.5 Pictures of the ion exchange membranes

Table 3.1 Characteristics of the ion exchange membranes

Characteristics	CEM	AEM
Ion Exchange Group	Sulphon ($R\text{-}SO_3^-$)	Quaternary ammonium ($R\text{-}(CH_3)_3N^+$)
Ionic Form	Sodium (Na^+)	Chloride (Cl-)
Thickness of Dry Membrane	0.33 ± 0.02 mm	0.33 ± 0.02 mm
Exchange Capacity	>2 mol/kg	>2 mol/kg
Water Content	<50%	<30%
Diffusion Coefficient	$<6 *10^{-3}$ mmol NaCl/(cm^2*h*mol/l)	$<6 *10^{-3}$ mmol NaCl/(cm^2*h*mol/l)
Permselectivity	>90 0.1/0.2 M KCl	>90 0.1/0.2 M KCl
Surface Electric Resistance	5-8 0.1 M NaCl	6-8 0.1 M NaCl
pH range	1-12	1-12
Temperature	5-50 ^oC	5-50 ^oC

3.2.2 The Electrodes

Both electrodes (anode and cathode) of dimensions 1x100x100 mm, purchased from China, were Titanium mesh coated with Rubidium and Iridium (Ti/Ru–Ir).

3.2.3 The Spacers

Four different spacers were used during the study. An ED woven spacer purchased from pccell, Germany (Spacer 1), a handmade woven spacer (Spacer 2), a handmade PVC spacer (polymerizing vinyl chloride) with less surface contact (Spacer 3) and a handmade PVC spacer with more opening (Spacer 4). The Spacer 2 was made by drying silicone on the borders of the woven which is cut as a prototype of the spacer applied on the top in other to open the water routes. The Spacer 3 and Spacer 4 were made by opening water routes on PVC plastic. The main difference between Spacer 3 and Spacer 4 is the contact area that they allow the IEMs to have with the feed solutions, which are 11.25 cm^2 and 48.375 cm^2, respectively. The thickness of Spacer 1, Spacer 2, Spacer 3 and Spacer 4 were, 380 μm, 410 μm, 180 μm and 180 μm, respectively. The images of the different spacers are presented in Figure 3.6.

Space 1, Thickness 380 µm

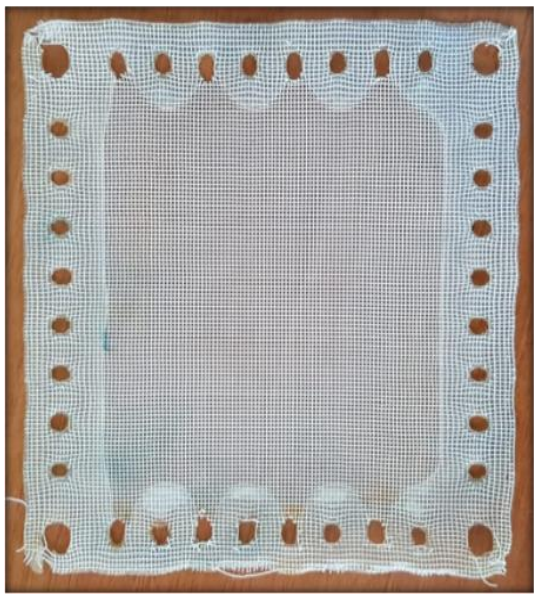

Spacer 2 Thickness 410 µm

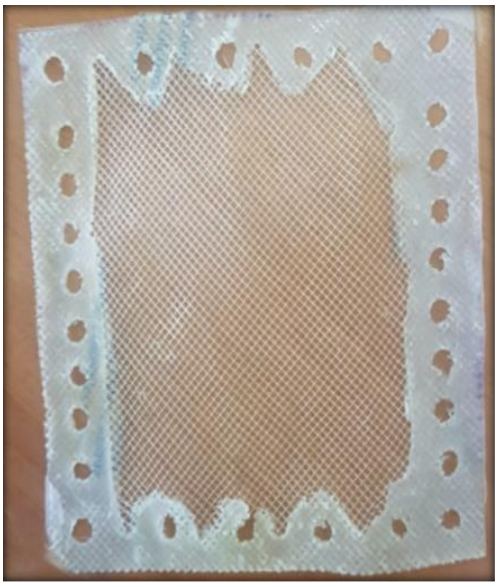

Spacer 3 Thickness 180 µm

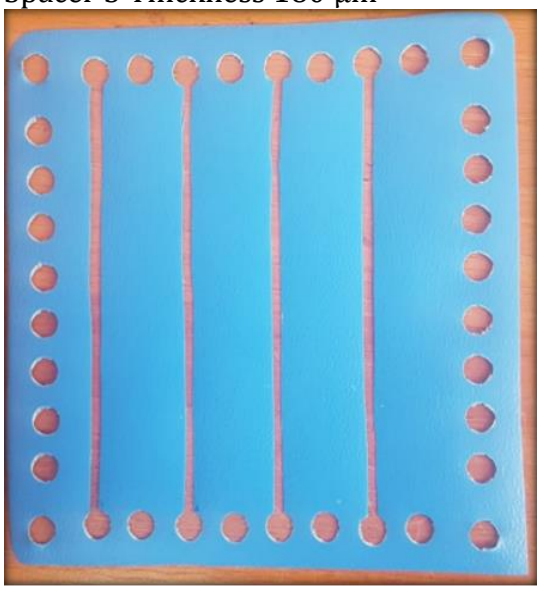

Spacer 4 Thickness 180 µm

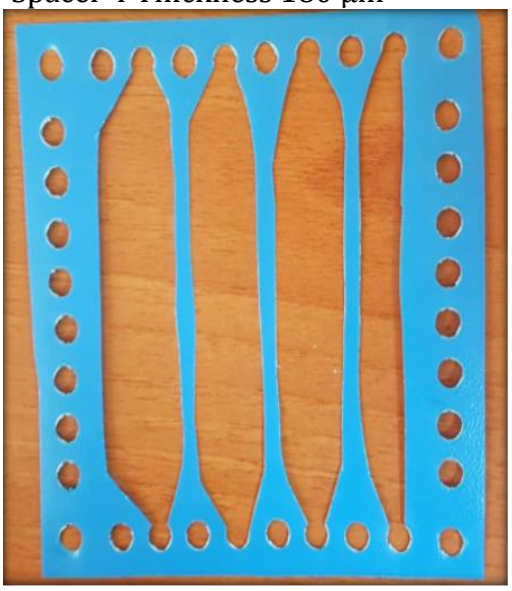

Figure 3.6 Images of the spacers used in the study

3.2.4 The Feed Solutions

The feed solution ion content and purity are important for RED. Divalent ions in the solution and pollutants in raw waters can limit the performance of the process and shorten membrane life. Pretreatment to remove the pollutants, and the use of suitable membranes and electrode system could reduce the effect of the feed solutions on the process.

Various synthetic solutions with different salt concentrations were used during this study. Table salt (NaCl) was used in tap water to increase the salinity consequently the conductivity to a set value in both diluted and concentrated solutions. Seven different HC concentrations, 171, 257, 342, 428, 513, 600 and 684 mM NaCl were prepared corresponding to HC1, HC2, HC3, HC4, HC5, HC6 and HC7, respectively. The LC solution concentration was fixed as 2, 4, 6, 8, 10, and 12 mM NaCl corresponding to LC1, LC2, LC3, LC4, LC5 and LC6, respectively.

The Marmara Sea and treated municipal wastewaters were collected from Istanbul. The Marmara Sea was collected from the vicinity of the plant where municipal wastewaters are discharged after treatment. Istanbul disposed of 89 municipal wastewater treatment plants (MWWTP) composed of 8 pretreatment plants and 81 advanced biological treatment plants resulting in a total capacity of 5,815,260 m^3/day, which receive around 3,927,030 m^3/day of wastewater [172]. Both located in the European side, Ataköy and Ambarlı are among the high capacity treatment plant of the city with a total capacity of 600,000 m^3/day and 400,000 m^3/day, respectively, and receives 411,250 m^3/day and 336,820 m^3/day, respectively. Ataköy WWTP includes an MBR treatment unit with a capacity of 30,000 m^3/day, and Ambarlı WWTP contains an UF unit with a capacity of 25,000 m^3/day expected to reach 50,000 m^3/day shortly [172]. Four wastewater samples were collected and used as diluted solutions in the RED stack. Two Ataköy WWTP samples were collected from advanced biological treatment effluent (AB1) and MBR unit effluent (MBR). And two Ambarlı WWTP samples, one was from advanced biological treatment (AB2) and the other was from the UF membrane treatment unit (UF). The characteristics of the feed solutions are presented in Table 3.2.

Table 3.2 Characteristics of the feed solutions

	AB1	MBR	AB2	UF	Marmara Sea
Conductivity, µS/cm	1280±3	1180±2	1270±3	1050±2	33,200±7
Total Hardness, mg $CaCO_3$/L	263±3	200±3	265±3	192±4	4570±5
Non-Carbonate Hardness, mg $CaCO_3$/L	54	50	54	12	4390
Alkalinity, mg $CaCO_3$/L	209±3	150±2	211±3	180±4	180±4
COD, mg/L	207±2	104±2	196.5±2	109±1	701.5±3
pH	6.6	6.5	6.7	6.5	7.4

3.2.5 Analysis Methods and Equipements

The different analysis methods and types of equipment used during this study are illustrated in Table 3.3. The temperature and pH of the feed solutions were measured according to the 2550 Standard and 4500 H Standard Method, respectively, by using a temperature and pH probe. The conductivity analysis was performed following the 2519 Standard Method. The conductivity probe Thermo-scientific brand Orion 5-Star Plus multi-parameter device (Figure 3.7) was used. Titrimetric Standard Method 2340 C. with ethylenediamine tetraacetic acid (EDTA) and Standard Methods 2320 was used for the analysis of hardness and alkalinity, respectively. COD content was determined by using a closed reflux colorimetric method according to the standard method 5220 D with a spectrometer (Figure 3.8). The samples were diluted 10 fold before analysis. With the help of an automatic pipette, 2.5 ml of each diluted sample and a distilled solution used as blank is taken and put into test tubes. Then 1.5 ml silver dichromate solution and 3.5 ml sulfuric acid solution were added to each tube. Chloride ions are commonly known to interfere with COD analysis. The dilution of the Seawater reduced the Chlorine concentration to below 2000 mg/L and mercuric sulfate was added to remove chloride interference. The samples were mixed in test tubes to homogeneity and

were heated at 150 °C for 2 hours. The tubes are then cooled and the absorbance of each sample is measured at 600 nm in a spectrophotometer. COD concentration in mg/L is finally calculated using the curve of calibrated standard COD solution that has a concentration between 100 and 1000 mg/l prepared with Potassium hydrogen phthalate (KHP). A True-RMS digital multimeter shown in Figure 3.9 was used to measure the intensity and voltage of the RED process.

Figure 3.7 Thermo-Scientific Orion 5-Star Plus multi-parameter device

Figure 3.8 Apparatus used for COD analysis; from left to right: VELP ECO 23 Thermoreactor, 6600 UV-VIS Spectrophotometer

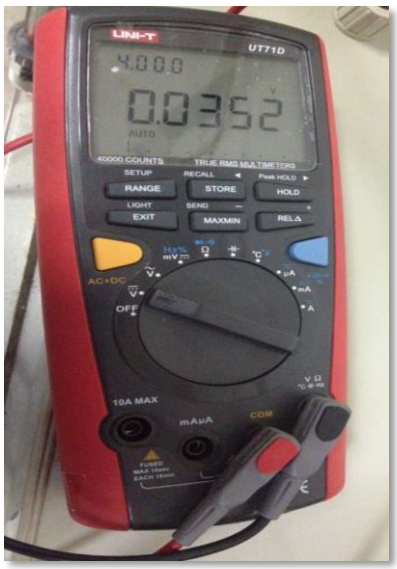

Figure 3.9 True-RMS digital multimeter device

Table 3.3 Analysis methods and equipment

Parameter	Analysis Method	Equipment
Conductivity, μS/cm	2519 Standard Method	Conductivity probe
COD, mg/L	5220 D Standard Method	Spectrophotometer
Hardness	2340 Standard Method	Titration
Alkalinity	2320 Standard Method	Titration
pH	4500 H Standard Method	pH probe
Temperature	2550 Standard Method	Temperature probe
Voltage, Intensity		True-RMS digital multimeter

3.3 The Feed Solutions Flow Rate (Flow Velocity)

LC and HC feed solutions were separately pumped into and out the stack in a single pass while the ERS was continuously circulated to the stack and back to the tank. The flow rates (q) of LC, HC, and ERS were 15, 30, 45, 60 and 75 ± 2 ml per min, and the equivalent velocity were 0.0108, 0.0216, 0.0325, 0.0433, 0.0541 $m^3.m^{-2}$ h^{-1}, respectively.

3.4 Power Density

Power density (PD) and energy efficiency (EE) are of key importance for the generation of power in an RED unit. Depending on the final unit, many definitions of PD are available among which, the generated power per unit of investment (W/Eur) or per cubic meter installation (W/m^3) are well known. Power density is defined in the RED process as the power generated per membrane area (W/m^2), while the energy efficiency is known as the fraction of the potentially available energy from the salinity difference that is converted into electrical energy (%) by an RED unit [58]. Early RED researchers obtained low PD and EE. A PD around 0.4 W/m^2 and below was achieved using a high concentrated NaCl solution (250 g/L) together with 1 g/L NaCl as a diluted solution [173]. In recent years, with the introduction of commercial, tailored IEMs and better stack design, significant power efficiency improvements have been achieved [113], [130]. The power density of an RED cell unit measured in Watt per square meter (W/m^2) is computed using the Equation below;

$$PD = \frac{V*I}{A} \tag{3.1}$$

Where PD is the power density, V is the voltage in volt, I is the current in ampere and A the total area of the CEM and AEM in square meter (m^2).

3.5 Energy Calculations

Power and energy are two important values used to understand the performance of the RED process, and the Equation below are used to determine their values. Power is calculated as follow:

$$P = I*V \tag{3.2}$$

Where P is power in watt (W), I is the intensity in Ampere (A) and V is the voltage (V).

The power consumed by a pump to circulate the feed solutions is calculated with the following Equation:

$$Pp = \frac{Q*\rho*g*h}{3.6*10^6*\eta} \tag{3.3}$$

Where P_p is the pump power (kW), Q is the volumetric flow of the fluid through the pump (m^3/h), ρ is the density of the fluid being pumped (1000 kg/m^3), g is the gravity (9.81 m/s^2), h is the head produced by the pump (m) and η is the efficiency (%).

The energy generated or consumed by a device is computed as follow:

$$E = P*t \tag{3.4}$$

Where E is energy kilowatt-hour (kWh), t is the time of operation in hour (h).

The total membrane area (At) required to operate a real plant fed by a limited river flow is calculated using the formula below,

$$At = \frac{Q}{q} \tag{3.5}$$

Where q is the flow rate of the feed solution and Q is the flow rate of the river.

Total Power (Pt) is determined as follow,

$$Pt=PD*At \tag{3.6}$$

Where PD is the power density, A is the total membrane area.

3.6 Data Collection and Membranes Analyses

The intensity (A) and the voltage (V) were measured with a multimeter connected to the electrodes. Scanning Electron Microscope (SEM), SEM-EDX and Fourier Transform Infrared Spectrophotometer (FTIR) (Agilent Technologies, Cary 630 FTIR Spectrometer) were used to analyze the membrane morphology and structure before and after the RED process. These analyses were conducted to monitor the behavior of the membrane and the influence of the feed solutions on the membrane's structures.

4
EXPERIMENTAL STUDY RESULTS

4.1 Optimization of Reverse Electrodialysis Power Output

The performance of RED in terms of energy efficiency and power density [102] is important for the implementation of a real RED plant. In the preliminary RED studies, the power densities were very low as 0.05 W/m^2 [12], but they increased up to 6.7 W/m^2 in later researches[103]. High values have been reached up to 12 W/m^2 with the improvement of the process and the RED components, and the use of brine and other high salinity solutions [104]. Besides, the efficiency of the generated power decreases rapidly when using natural feed water as feed solutions [134], unless the feed solutions follow some pretreatment standards [150]. Even though RED is among the highest energy efficiency techniques, it has a low EROI. Increasing the power density, reducing the internal resistance and lowering the membrane prices can contribute to reducing the capital cost of RED process and make it a marketable renewable energy technology. The high cost of membranes and their inability to produce high power densities have resulted in high installation and gross energy production costs [105]. The performance of an RED process is mainly affected by membrane characteristics, feed solution concentration and characterization. The feed solutions flow velocity, temperature, concentration, and composition are important parameters for power production by RED. Kang et al. (2017) showed the positive impact of increasing flow rates of feed solutions in the RED power output [129] and Tedesco et al. reported that an increase of the velocity could slightly augment the gross power density to a certain limit [104]. A higher flow rate of the feed solutions positively influences the hydrodynamic mixing and facilitates the mass transfer in the RED channel which augment the potential difference across the membranes, increasing the power density [108]. Even though some studies reported that the RED processes are more suitable to less concentrated saline water compared to PRO [16], it is worth mentioning that the

NaCl contents of the feed solutions control the driving force of the RED process by affecting the salinity gradient. The big difference in salt contents of two water bodies used in RED (salinity gradient) induces a high driving force which results in a high power output [104], [131]. However, the optimal salt concentrations of the feed solutions for optimal power output, the effect of the concentrations outside these ranges on the RED performance and the effect of the salinity rate of diluted and concentrated solutions were not investigated.

Good knowledge of the RED process and a careful assessment of the operating conditions is required to optimize the process efficiency. A lab-scale RED stack equipped with 6 cell pairs for a total active membrane area of 0.071 m^2 was used in this study to investigate the effect of various salinity and flow rate of feed solutions electrical energy production potential of RED.

4.1.1 The Effect of the Feed Solutions Flow Rate on RED Performance

The LC NaCL concentration was fixed at 4 mM, Figure 4.1A and 6 mM, Figure 4.1B. Three (3) different HC solutions of NaCl concentration 257, 342 and 428 mM were used and resulted in the power densities PD2, PD3, PD4, respectively. The system was operated with various feed solutions flow rate from 15 mL/min to 75 mL/min. The results depicted in Figure 4.1 underline the importance of the feed solution flow rate in the RED performance.

The experimental results indicate that the power density of the RED unit increases with the increasing flow rate. An important increase was observed from 15 mL/min to 45 mL/min and the stabilization started after. There was a very low or almost no increase of the power output at 60 and 75 mL/min flow rates, on the contrary, the power density decreased. The highest power density obtained was 0.54 W/m^2 and was observed at a low NaCl concentration of the LC solution and high NaCl concentration of the HC solution with 60 mL/min feed solutions flow rates. The increase of the power density with increasing flow rate up to 45 mL/min is mainly due to the faster renewal of the solution in the module by a new solution having high chemical energy potential. In fact, when the solutions enter the RED stack, the anions move toward the AEM when the cations move toward the CEM. There is a

drop in the salinity of the HC solution and an increase of the salinity in the LC solution in the RED stack within a given fraction of time, causing a decrease of the NaCl concentration difference between the two solutions. At this exact time, the movement of ions decreases between the membranes, resulting in a lower potential difference, consequently lower chemical energy, and a decrease in the production of electricity with the drop of the voltage, consequently the power density [127], [130].

When the flow rate increases over 45 ml/min, the solutions in the module exit very fast the membrane stack allowing a new solution to enter, and this continuous process allow the system to keep a high salinity difference between the two solutions inside the module. However, when the flow rate is too high, the solutions exit the stack too fast and do not give enough time to the ions to migrate effectively, causing a drop of the chemical energy and of course the electrical energy, resulting in a lower voltage and power density. Kang et al. (2017) supported the same idea by reporting that at the very high flow rate, the pressure inside the module increases causing augmentation of the RED stack resistance that will eventually contribute to lower the power density [129]. The optimal flow rate determined during the study was between 30 and 45 mL/min.

In terms of economic feasibility, operating an RED system with a low flow rate of the feed solutions contributes to reducing the operating cost by reducing the energy need for pumping the feed solutions [131], [132]. Zhu et al. (2015) investigated the behavior of different flow rates with the RED system, and they reported that 20 mL/min was the optimum flow for both LC and HC to reduce the energy needed for pumping [131]. Our results might be connected to the low feed solution concentration. As reported by Długołecki et al. (2010), the resistance is highly dependent on the solution concentration when working at low feed concentration below 0.1 M, the membrane resistance strongly increases with decreasing concentration and affects the process performance, with 0.017 M solution having over 10-fold resistance compared to a solution with 0.5 M NaCl concentration [129]. In this case, an increase in the process flow rate highly contributes to reducing the effect of the resistance and improve the process performance and efficiency. As a result, the optimal feed solution flow rate is also connected to the feed solution NaCl

concentration. The high flow rate may negatively affect the membrane by increasing the internal pressure which can lead to the membrane wetting, allowing water molecules to cross the membrane or reducing its life. An optimal flow rate is important both in reducing the useless flow rate increase and protecting the membrane by increasing its life and resulting in a more economically effective RED process.

A

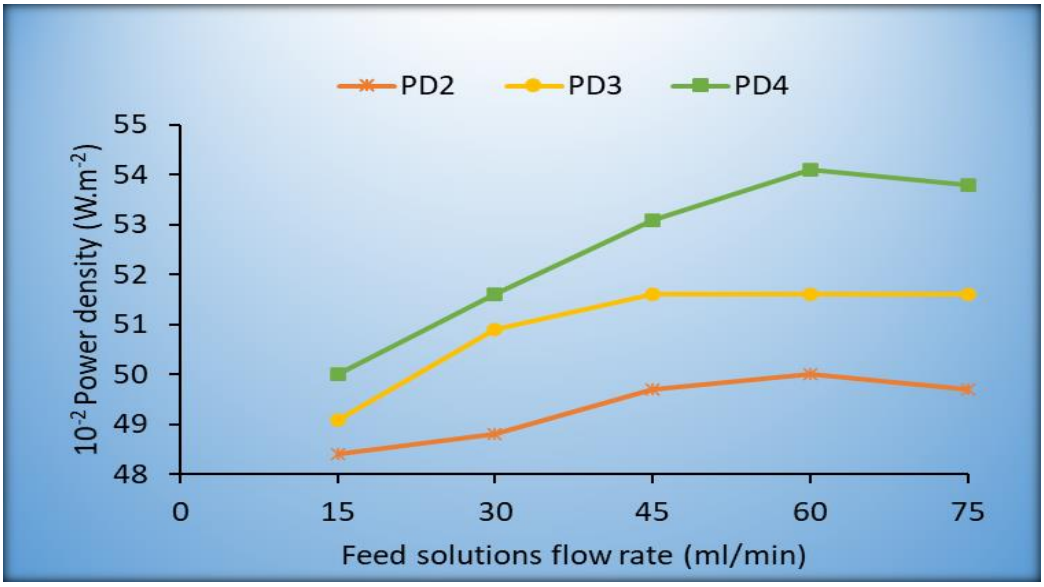

B

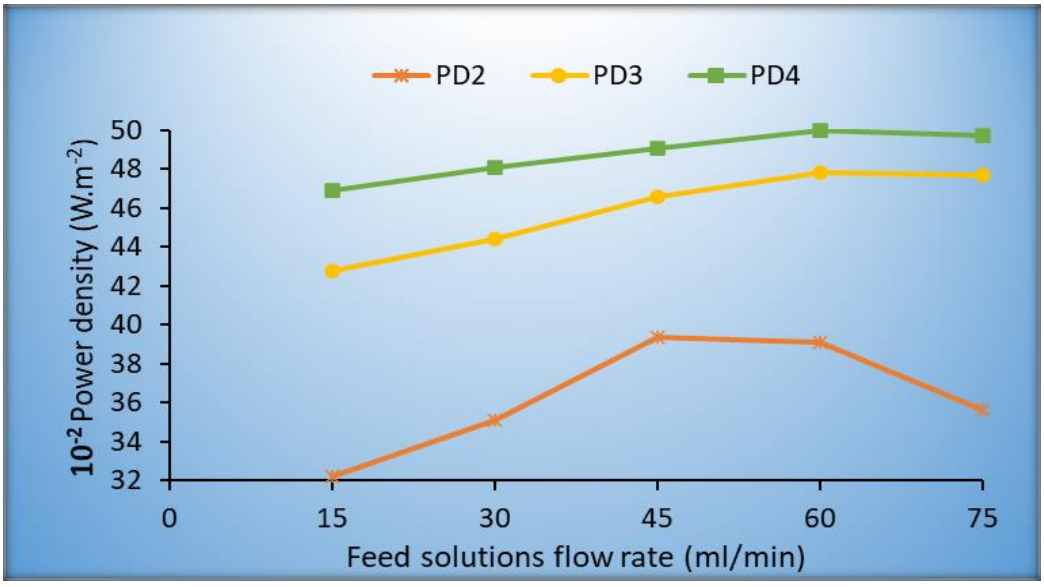

Figure 4.1 Power density over various feed solutions flow rates at various HC solution NaCl concentration (PD2 (257 mM), PD3 (342 mM), PD4 (428 mM)); A) LC salt concentration: 4 mM, B) LC salt concentration: 6 mM

4.1.2 The Effect of the Feed Solutions NaCl Content on RED Performance

4.1.2.1 The Effect of the HC Solution salt Concentration on RED Performance

The SGP is based on the chemical energy released due to the salinity gradient of the fresh and seawater in contact. At the high salt content of the HC, the salinity gradient increases and lead to higher power output [77], [104]. As presented in Figure 4.2A, the power density ($W.m^{-2}$) augmented with increasing HC solution salt content, regardless of all the other parameters (flow rate, LC solution salt content). The energy output in terms of power density increased almost linearly with the HC NaCl concentration due to the higher salinity ratios [127]. However, Daniilidis et al. (2014) reported that above 2.5 M of HC NaCl concentrations, this result crumbles down leading to a decrease in the energy generated [103]. With LC NaCl concentration fixed at 6 mM (750 µS/cm), the power density increased from 0.345 to 0.705 $W.m^{-2}$ when increasing the HC solution concentration from 171 to 684 mM. The increase of the HC NaCl concentration four-folds resulted in the power density values doubling. At higher salt content, the ions exchange rate in the RED stack increases due to the high salinity gradient, consequently causing an increase in the total power density. Similar results were reported by Daniilidis et al. (2014) [103]. The concentration difference of Na^+ and Cl^- ions is the driving force of the RED process which can explain the important role of salinity in power generation.

4.1.2.2 The Effect of the LC Solution Salt Concentration on RED Performance

Different LC salt concentrations have been used to understand the importance of LC concentration in the energy generation with RED. The lowest power density was achieved with an LC concentration of 2 mM, being the lowest concentration in this study. At high LC concentration, 12 mM, the power density decreased as well. The highest power densities were achieved with LC concentrations between 4 and 6 mM. Below or above these concentrations, the power output was negatively affected. A very high increase of the power density takes place when the diluted solution salt content is reduced from 8 mM to 4 mM (1000 µS/cm to 500 µS/cm) as depicted in the graphs of Figure 4.2B. At a low salt content of the diluted solution, the driving

force dramatically increases, ions movement from the concentrated solution exponentially increases resulting in higher chemical energy to be converted at the electrodes into electrical energy. The salinity ratio between HC and LC solutions should be over 25 for effective power production, at a lower ratio the power produced is negatively affected [77]. This explains the drop observed in the power output at high salinity in the LC solutions. It was also noticed that the changes in the salinity of the LC are more sensible in affecting the power generated compared to the salinity of the HC. The salinity of the LC solution is very important; too low NaCl content in the LC solution increases the stack resistance, while too high NaCl content reduces the salinity gradient which is the driving force of the process.

A

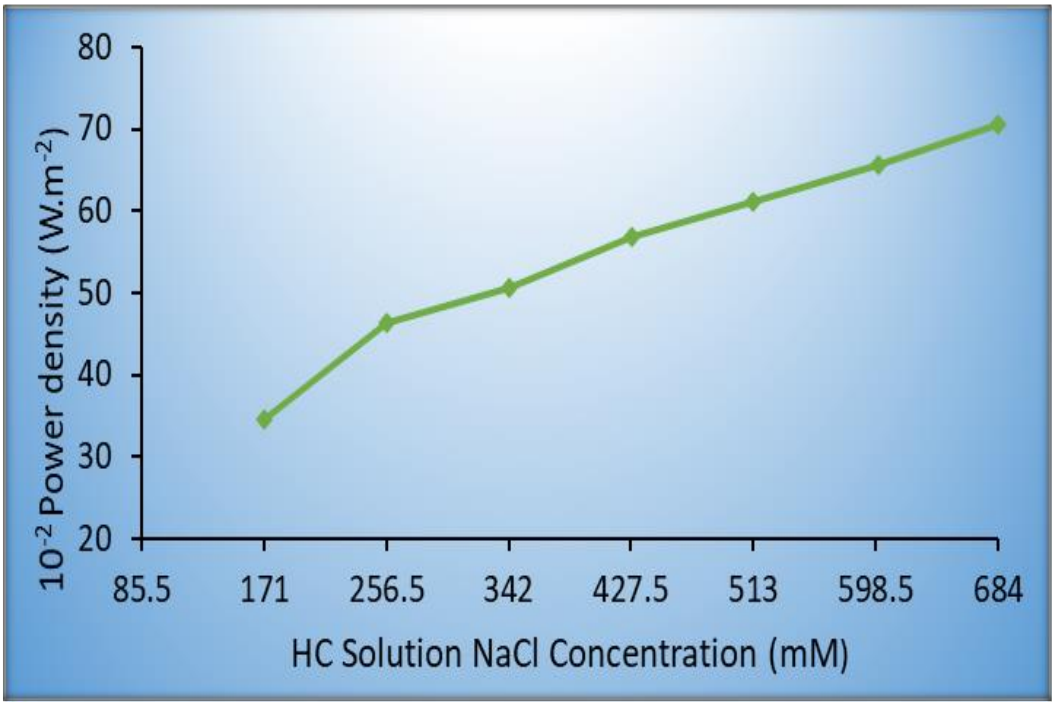

B

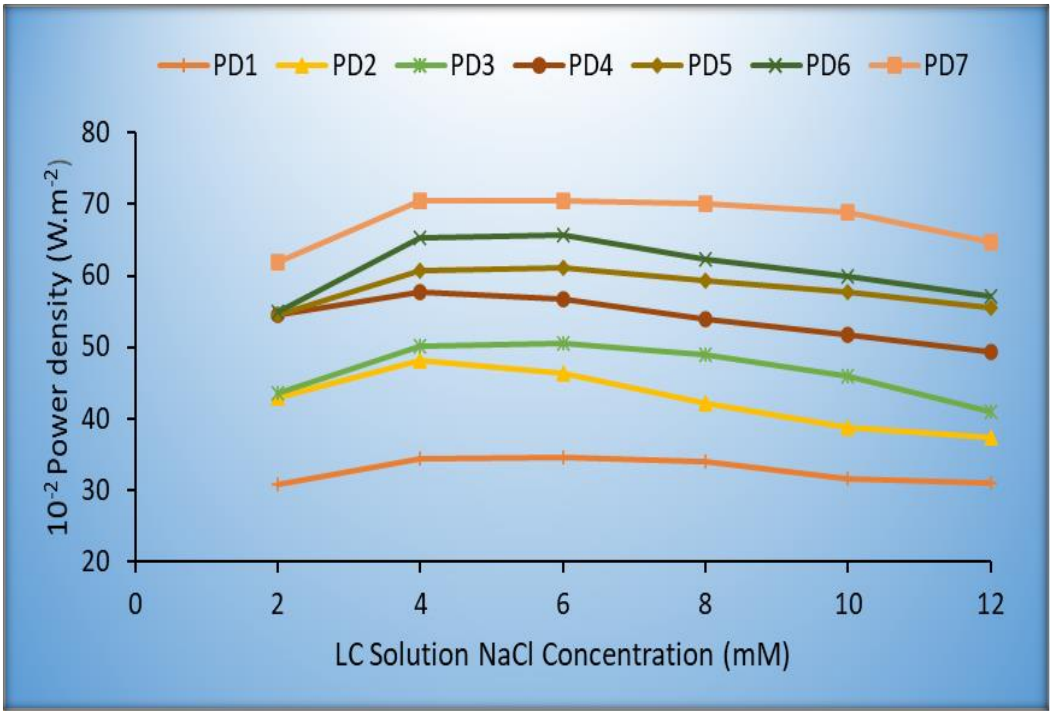

Figure 4.2 Influence of the feed solutions salinity on the Power density and RED power generation performance, HC solution NaCl concentration (PD1 (171 mM) PD2 (257 mM), PD3 (342 mM), PD4 (428 mM), PD5 (513 mM), PD6 (600 mM), PD7 (684 mM)).); A) Influence of HC salinity on RED energy generation, B) Influence of LC salinity on RED energy generation

4.1.2.3 Power Density Increase Percentage (%) with Increasing HC and Decreasing LC Solutions Salinity

The results in Table 4.1 show that the power density did not increase when the LC solution salinity is decreased from 4 mM to 2 mM, on the contrary, it decreased sharply, resulting in a negative increase in terms of percentage. At 2 mM, the LC solution is too poor in NaCl and this results in poor energy potential. There is also a sharp increase of the power generation when the salinity of the LC solution is decreased from 12 mM to 8 mM. 12 mM was high and reduced the salinity ratio between LC and HC solutions, as a result, the power output was low. Similar results were observed when the LC solution salinity was decreased from 8 mM to 6 mM. However, by decreasing the LC solution salinity from 6 mM to 4 mM, there is almost no change or increase of the power generation at different HC solutions. Between 4

and 6 mM, the LC solution presented the optimum salinity for the power generation with RED.

Table 4.2 illustrates the percentage of power density increase with increasing NaCl concentration of the HC. The highest increase percentage was observed with the lowest HC solution salinity, 171 mM, this shows that the process was not stable at this low salinity. When the salinity increased, the percentage still increased but the increase rate was lower. 513 mM to 600 mM concentrations presented the average lowest increase rate registered. At the concentration of 600 mM, the HC solution resulted in a power generation much more stable compared to the other solutions. Although this value represents the optimum HC solution salinity considering seawater salinities (except for the dead sea), increasing the HC solution salinity will still participate in an increase of the power density. These may be high saline lakes or concentrates from desalination plants such as reverse osmosis or membrane distillation.

The results of Table 4.1 and Table 4.2 indicate that the decrease of diluted solution salt content is beneficial compared to the increase of the concentrated solution salt content. A little change in the diluted solution NaCl concentration has a huge impact on the power generation performance and efficiency. Other researchers have also reported that the sensibility is much higher with a change of LC NaCl concentration than HC [132]. One should take advantage of this information and implant an RED system where LC respects the optimal values with care taken into matter compared to HC solutions. Because optimizing the power density is not only about increasing the concentrated solution salt content to get a high salinity ratio between LC and HC, however, the power density can be effectively improved by using an LC solution with salt content not too low enough to create a salinity gradient, but not very high to reduce the migration of Na^+ and Cl^- ions toward the IEMs.

Table 4.1 Increase rate (%) of the power generation with decreasing NaCl concentration of LC at different concentration of HC solution

LC Salinity	Power Density increase percentage				
mM	HC1	HC2	HC3	HC4	HC5
4 to 2	-10.47	-10.81	-13.15	-5.37	-10.05
6 to 4	-0.3	3.53	-0.79	1.56	-0.65
8 to 6	1.16	12.27	23.9	6.59	2.3
12 to 8	8.53	11.61	16.32	8.35	6.24

Table 4.2 Increase rate (%) of the power generation with increasing NaCl concentration of HC at different NaCl concentration of LC solution

HC Salinity	Power Density increase percentage					
mM	LC1	LC2	LC3	LC4	LC5	LC6
171 to 257	25.21	28.48	25.65	19.43	18.09	16.62
257 to 342	1.61	4.18	8.3	13.88	15.67	9.02
342 to 428	20	13	10.92	9.1	11.39	17
428 to 513	0.18	4.94	7.04	9.1	11.36	11.15
523 to 600	0.73	7	6.7	4.6	3.67	2.8
600 to 684	11	7.38	7	11.1	12.8	12

4.1.3 Recommended Estuaries for the Implantation of an RED System, and RED Power Generation Potential of some Estuaries in Turkey

The average general salinity of seawater is 600 mM, however, the salinity varies highly depending on the sea, the collecting point, and deepness. The average NaCl concentrations of seawaters around Turkey are as follows; the Black Sea around 308 mM, Marmara Sea 376 mM, Aegean Sea 667 mM, Mediterranean Sea 680 mM. The average NaCl concentration of the Red Sea is 700 mM, and the Dead Sea is much higher; 5800 mM. Besides, salt lakes in Turkey, Senegal, Ethiopia, Djibouti, Iran just to mention a few have a salinity reaching 6800 mM or over. Turkey benefits from three oceans and one internal sea as illustrated by Figure 4.3 [175], and many rivers

run into these seas (Table 4.3) [176]. Based on the information given in Table 4.3, in Turkey, the Aegean Sea and the Mediterranean Sea are more suitable for optimal power generation by RED with seawater as HC solution. The average salinity of the Ceyhan river is 3-12 mM [177], Seyhan river 6 mM [178], Göksu river 3-12 mM [179], and they are some suitable rivers to be considered as diluted solutions.

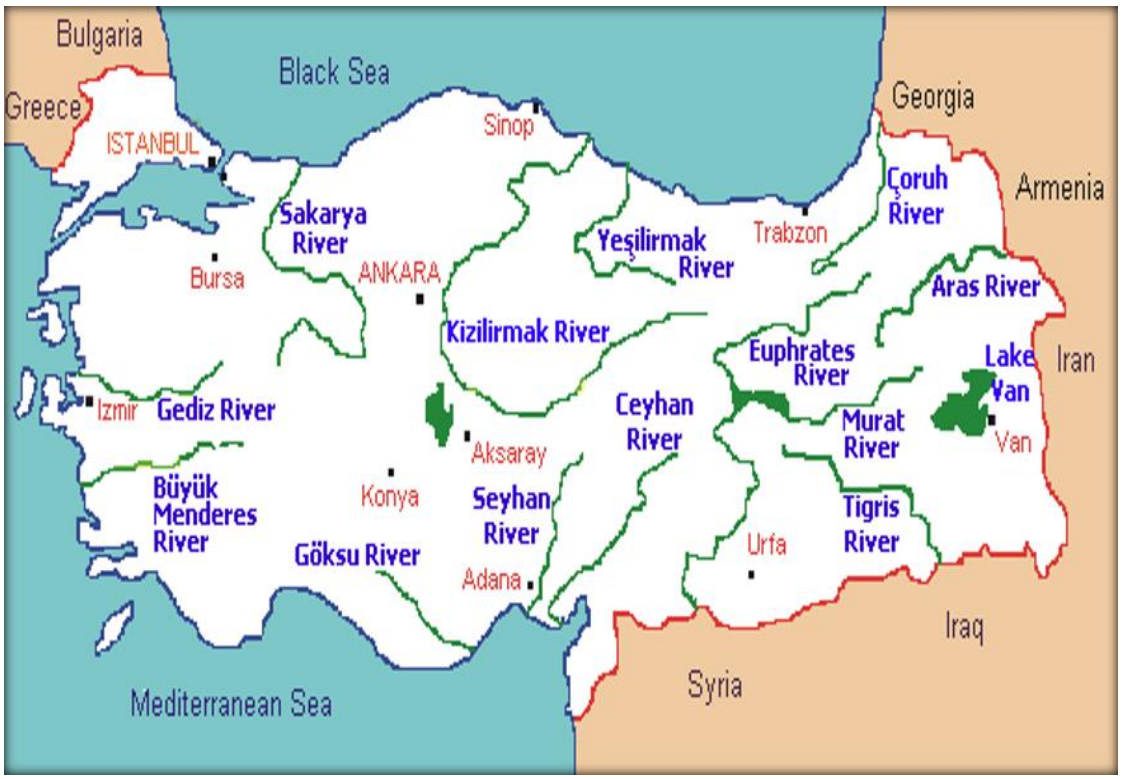

Figure 4.3 Seas in Turkey and rivers running into them [175]

Table 4.3 Flow rate of rivers running into the seas in Turkey [176]

River streams	Discharged sea	Maximum Flow Rate (m^3/s)	Minimum Flow Rate (m^3/s)
Sakarya	Black Sea	285.29	58.438
Filyos (Çaycuma)	Black Sea	223.18	21.982
Çoruh	Black Sea	569	53.09
Yeşilırmak	Black Sea	237.107	97.255
Kızılırmak	Black Sea	184	184
Bartın	Black Sea	41.477	1.513
Simav (Susurluk)	Marmara Sea	109.58	0.773
Gönen	Marmara Sea	911	0.024
Biga Çayı	Marmara Sea	42.774	0.683
Gediz	Egean Sea	77.238	18.283
Bakırçay	Egean Sea	40.408	0.208
Büyük Menderes	Egean Sea	157.93	38.696
Küçük Menderes	Egean Sea	11.45	11.45
Manavgat Çayı	Mediterranean Sea	202.28	53.837
Göksu	Mediterranean Sea	201.3	35.525
Dalaman	Mediterranean Sea	94.711	0.189
Aksu	Mediterranean Sea	24.299	2.346
Seyhan	Mediterranean Sea	165.859	8.632
Ceyhan	Mediterranean Sea	356.426	91.689
Asi	Mediterranean Sea	163.192	0.406

Using Equation 3.5, the membrane area (A) required when the Ceyhan, Seyhan and Göksu rivers streams run into the Mediterranean Sea is calculated considering 1/3 of the minimum flow of the water of these rivers. 1/3 of the water is considered in the RED entrance to avoid major disturbance in the water's natural flow. With a power density of 0.705 W/m^2, Equation 3.6 and 3.4 were used to determine the total power and energy production potential by RED. The results are presented in Table

4.4. Taking into consideration rains and snows that affect the rivers for almost two months a year, 300 days a year can be considered for power generation and the minimum electrical energy generable by RED with 1/3 water from the Ceyhan river is up to 17.18 $x10^6$ kWh electrical energy per year. This electrical energy can be tripled with an optimal RED stack and improved IEM. Also, the present study was performed using feed solutions at 18 ^oC temperature. Studies demonstrated that high temperature is favorable for the RED process [108], [127], [128]. when the temperature of the feed solutions increases, the resistance of the RED stack decreases [128], consequently the conductivity increases, and ionic mobilities are facilitated, ohmic losses are reduced resulting in higher power output [127]. The present study was conducted with 18 ^oC feed temperature which is the average temperature of the different rivers. The temperature ranges of Ceyhan, Göksu and Seyhan rivers are 9-27 ^oC, 10-27 ^oC and 9-32 ^oC, respectively [176]. The lowest temperatures of the rivers are in the winter period and the energy production by the RED will decrease in the cold season. The energy generation will be higher during summer when the feed solutions are at their hottest state. The RED process can generate much higher energy during summer and will present a higher power density and energy efficiency in tropical countries where the water bodies are warmer. These are facts that support a much higher energy output than we found in the present study with the optimization of the process and operation conditions.

Table 4.4 Estimated power and energy generation of Ceyhan, Göksu and Seyhan rivers when 1/3 of their water flow is used in RED at the contact point with the Mediterranean Sea

Rivers	Minimum Flow rate ($m^3.m^{-2}.h^{-1}$)	(1/3) x Minimum Flow rate ($m^3.m^{-2}.h^{-1}$)	Membrane Area (m^2)	Power (kW)	Energy (kWh) per day
Ceyhan	330080	110027	3385440	2387	57281
Göksu	127890	42630	1311693	925	22194
Seyhan	31075	10358	318720	225	5393

4.1.4 Results' Evaluation

Power generation by RED processes could be a life-changing technology in the near future by converting the salinity gradient power into useful energy. The flow rate and the feed solutions salinity are among many parameters that affect the performance of the process. This study revealed that at low feed solution concentration, the optimal flow rate of 30 to 45 mL/min is required to operate the RED system efficiently. The results also showed that the NaCl concentration of the LC solution is more sensible and can be optimal for the process between 4 and 6 mM, while HC is optimal at concentrations over around 600 and 684 mM. The results suggest that one should operate the RED system by using an LC solution with low salinity instead of just using a high saline HC solution without taking into consideration the real impact of the LC solution. The Mediterranean Sea and the Aegean Sea in Turkey are suitable for RED along with Ceyhan, Göksu and Seyhan rivers. 1/3 of the minimum water flow rate from the Ceyhan river is estimated to generate over 17.18×10^6 kWh electrical energy per year by RED when it runs into the Mediterranean Sea.

4.2 The Effects of Increasing Cell-Pairs Number in Reverse Electrodialysis Power Efficiency

SGP has a lot of benefits, however, it is mostly available for coastal countries, and many limits still need to be overcome to make the process viable and implementable in real life. The performance of the RED process can be affected by many parameters among which the membrane cost and properties, the geometry and structure of the spacer, the feed solution ions content and concentration are very important. Tong et al. (2016) stated that ''Low energy efficiency, low power density, and membrane fouling problems are major issues that prevent the commercialization of RED.'' [102]. Besides the anti-fouling property required by the membrane, its high affinity for the ions of interest can enhance the efficiency of the RED process. Power loss due to the system resistance can contribute to lower the energy output. The membranes and the spacers can significantly contribute to the resistance. Mehdizadeh et al. (2019) reported that the spacers equipped between the membranes to keep their

intermediate distance do have a significant effect on RED stack resistance and this effect is called the spacer shadow effect [118]. Membrane electrical resistance and permselectivity are known to be the key membrane parameters determining the performance of RED. An ideal IEM should have a very low electrical resistance and high permselectivity. With low resistance membranes, the power output is enhanced in the RED stack because ohmic losses are reduced. The spacers alone can be a source of resistance and could lead to a large decrease in efficiency by up to 60%, resulting in a significant reduction in the power density of RED based on theoretical calculations [108].

An RED module consists of several repetitive units of ''cell-pairs''. Each cell-pair consists of an CEM, an AEM, interposed between two channels and separated by a spacer, allowing the two solutions of different salinity to flow but not mix one another in the RED stack. Each unit of cell-pair generates a given power which accumulates with the number of cell-pairs in the stack. As a result, the power output in an RED process is proportional to the number of cell-pairs. Since the IEMs and the spacers in the RED stack are responsible for the biggest part of the stack resistance, it is right to assume that the increase of the cell-pairs unit may also result in an increase of the resistance and disrupt the expected proportional increase of the power density. To fully understand the resistance caused by the membranes and the spacers, the present study investigated the power losses with the increasing cell-pairs in the module with various spacers. A lab-scale RED module was fed with synthetic saline solutions, 257 mM and 4 mM for HC and LC solutions, respectively, to investigate the resistance effects in the module caused by the IEMs and the spacers.

The RED process was operated by increasing the number of cell-pairs from 1 to 10 with each cell-pair operated for 15 minutes. The increases of the voltage, the intensity and the power density were monitored and the resistance effect of the increasing cell-pairs was investigated. Four different spacers were used during the study to investigate the effect of the spacer geometry, thickness and structure. An ED woven spacer purchased from pccell, Germany (Spacer 1), a handmade woven spacer (Spacer 2), a handmade PVC spacer (polymerizing vinyl chloride) with less

surface contact (Spacer 3) and a handmade PVC spacer with more opening (Spacer 4).

4.2.1 The Effects of Increasing Cell-Pairs on the Intensity, Voltage and Power Density

Increasing the number of cell-pairs similarly increases the voltage and the intensity in the RED module, consequently increases the power density as depicted in Figure 4.4. The RED process exploits the chemical potential difference between volumes of water different in their NaCl concentration and separated by IEMs. The difference in concentration across the membrane creates a voltage difference across each membrane. If several CEMs and AEMs are lined, with alternately two solutions different in salinity supplied in the compartments between the IEMs, there is an accumulation of the membranes voltages, resulting in higher voltages. The total voltage of the stack is proportional to the number of cell units in the RED module [63], [66], [78]. From this point of view, a linear increase in the voltage is expected with a linear increase in the number of cell-pairs. However, the voltage increases but deviated from the linear trend and declined with the increasing number of cell-pair. The voltage values illustrated by Figure 4.4 declined from the linear curve with the increasing number of cell-pairs. This nonlinear trend of the voltage illustrated by Figure 4.4 is the result of the stack resistance induced either by the spacers, the membranes, or both. Concerning the intensity, the number of cell-pairs plays an important role as well. The fist cell-pair resulted in a very low intensity which highly increased with the increased number of cell-pairs, but rapidly reached a first breaking point where the increase of intensity was low with the increasing number of cell-pairs. The present study was limited to 10 cell-pairs, not reaching the total breaking point of the intensity, a point where the increase of the number of cell-pairs will not induce a significant change of the intensity value. At such a point, the power density will be more controlled by the process voltage. The behavior of the intensity is connected to the resistance which increased with the number of cell-pair, but, similar to the voltage behavior, the increase declined from the linear trend. As a result, the power density increased with an increasing number of cell-pair but

does not show a linear trend since power is the product of voltage and intensity. This result points out the importance of operating the RED process with a high number of cell-pairs to benefit from the optimal intensity values, but the number of cell-pair should be controlled not to surpass the optimal intensity, after such a point the resistance values will continue pulling the voltage down, resulting in less optimal power density.

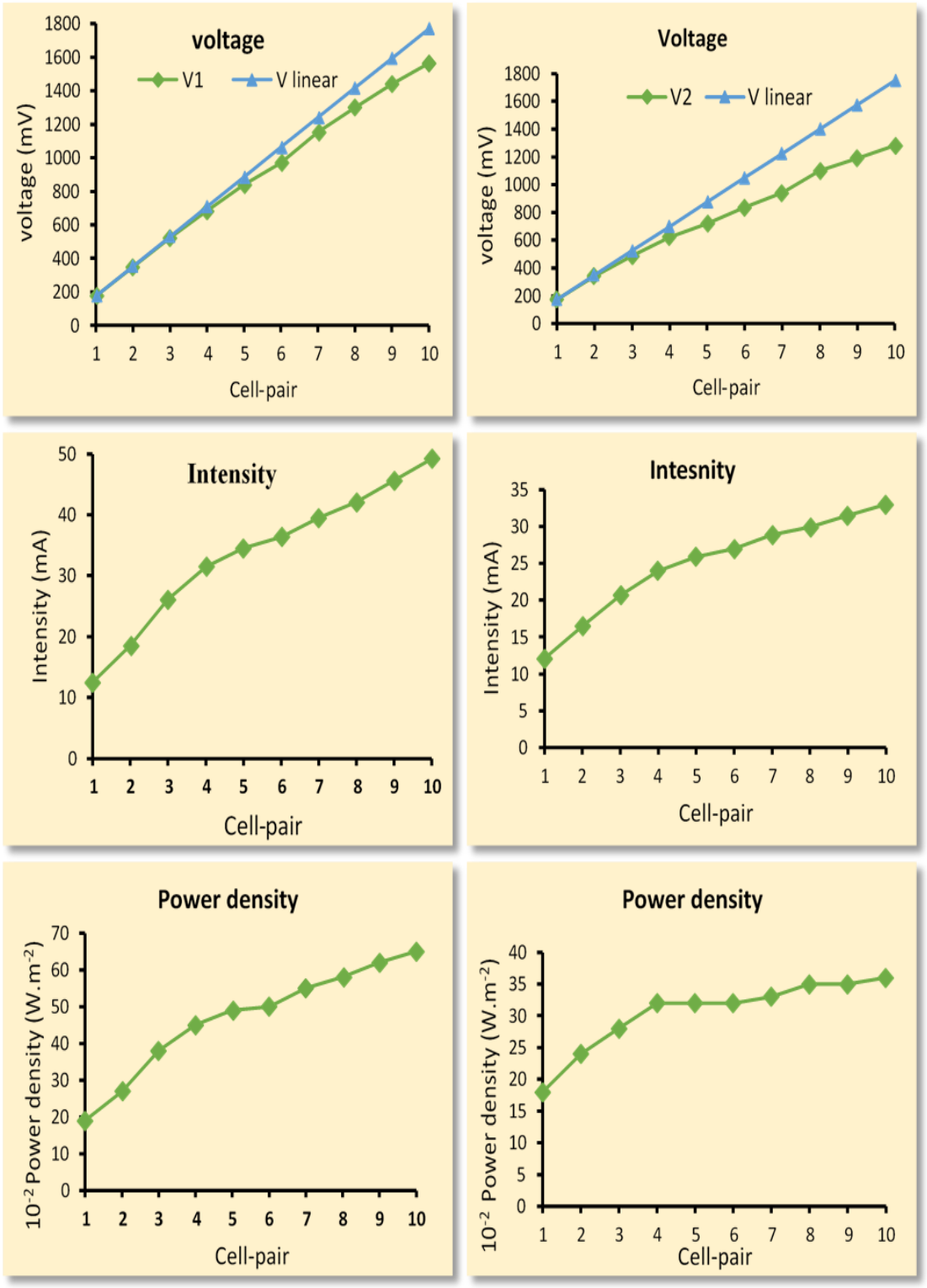

Figure 4.4 The effects of increasing the number of RED cell-pairs on voltage, intensity and power density, Left curves with Spacer 1 and right curves with Spacer 2

4.2.2 Stack Resistance

The electrical resistance is an important parameter that may affect the efficiency of the energy output in an RED process and is as important in other electro-separation processes [140]. The resistance of an RED stack should be minimal to maximize the energy output. The stack resistance with Spacer 1 and Spacer 2 was monitored during the study and is depicted in Figure 4.5. The electrical resistance of the stack is one of the most important parameters that affect the performance of the RED process. The resistance was higher with Spacer 2 compared to Spacer 1. Also, the resistance increased with both spacers with the increasing number of cell-pairs. The presence of non-conducting mesh in the spacer-filled channels increases the electrical resistance of the cell-pairs, and this spacer effect is called the shadow effect. The presence of the spacer mesh in the flow compartments obstructs the space available for the movement of ions and inhibits the current passing through the two streams [143]. This explains the difference in resistance with 2 different spacers. The spacer material, structure, and angles affect differently the process. Even though the spacer is sometimes responsible for most part of the resistance in the RED stack, a wide number of parameters are accountable. The RED stack resistance is theoretically the summation of the resistances of the individual components in series (or spacer-filled channels), in this case, the resistances of the AEM and CEM, diluted solution compartment and concentrated solution compartment [130], and the resistance of the spacers. CEM and AEM used in the study presented an electrical resistance of 5-8 $\Omega.cm^2$ and 6-8 $\Omega.cm^2$, respectively, at 0.1 M NaCl. These values are high since the resistance of IEMs in an RED module is expected to be as low as possible, a maximum of 3 $\Omega.cm^2$ [8], [13]. The feed solution concentration [141] and composition (Mg^{2+}, Ca^{2+}, SO_4^{2-}) affect membrane resistance [142]. Długołecki (2010) reported that the resistance of IEMs is highly connected to the solution concentration. The resistance effect is stronger with low salinity solutions, especially when operating at low concentrations with NaCl below 0.1 M, the membrane resistance becomes significant [141]. The resistance is also affected by the feed stream temperature. It decreases when the temperature increases [111]. Since the same solution was used in the present study, the effect of the solution was

not observed, but it does not mean it did not occur. The high resistance with Spacer 2 is the reason of the achievement of lower power density (Figure 4.5) and a negative effect on the whole process performance.

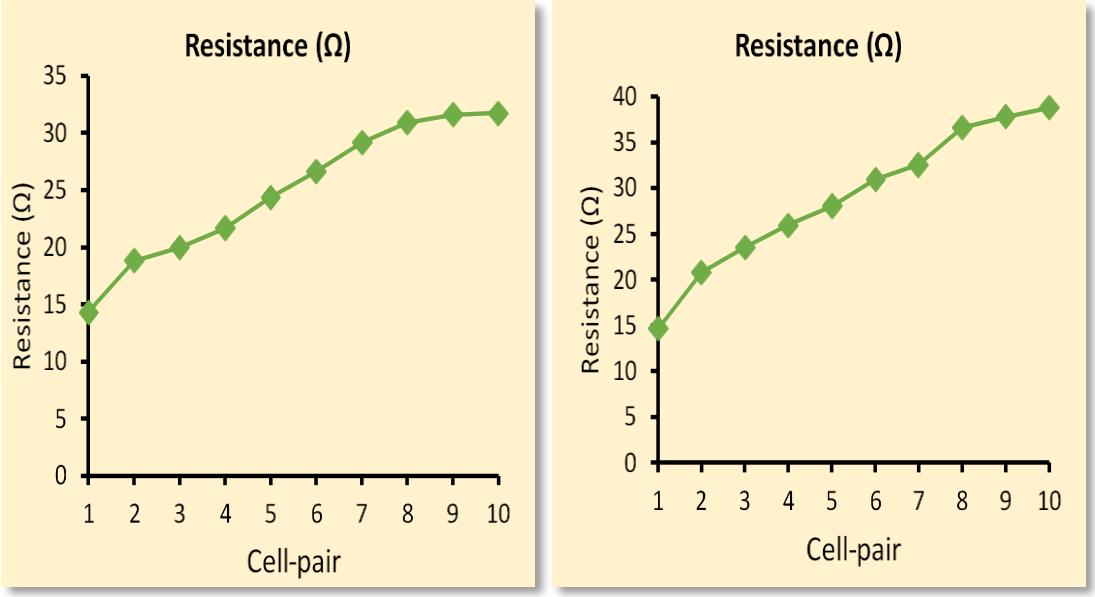

Figure 4.5 The effects of increasing the number of RED cell-pairs on the stack resistance, Left curves with Spacer 1 and right curves with Spacer 2

4.2.3 Membranes Resistivity Effects on RED Stack Efficiency

Due to the similarity between ED and RED, most of the membranes used for RED process investigations are commercial membranes specifically developed for ED processes. These membranes do not reflect exactly the exigence of RED [61], [107]. Membrane electrical resistance, IEC, and permselectivity are known to be the key membrane parameters controlling the performance of RED. The IEMs used in the present study presented a high resistance; 5-8 Ω.cm^2 and 6-8 Ω.cm^2 at 0.1 M NaCl for CEM and AEM, respectively. Długołecki et al. (2008) reported that the charge density of IEMs strongly impacts the permselectivity and membrane resistance. By comparison, CEMs have a higher charge density than AEM, resulting in higher permselectivity of CEMs [111]. The ideal RED membrane should have a very low resistance, a maximum of 3 Ω·cm^2 [8], [13], and highly permselective. With low resistance membranes, the power output is enhanced in the RED stack because ohmic losses are reduced [108]. The membranes in an RED stack are placed in series,

so the voltage and resistance induced by the membranes follow the same trend. This creates a cumulative resistance with the increasing number of cell-pairs. To reduce the resistance effect, the membrane should be highly selective for monovalent ions (Na^+, Cl^-), which are the ions of interest in the RED process. Veerman et al. (2009) performed a comparative study of 6 commercial membrane pairs (CEMs and AEMs) based on their thermodynamic efficiency and reported varied power densities from 0.5 to 1.2 W/m^2 when operated at similar conditions [113]. Their results confirmed the importance of the membrane structure and characteristics in the RED power output efficiency.

4.2.4 Spacers Effects

The spacers between the membranes are designed to preserve their intermediate distance [127] and enhance the mass transfer by facilitating turbulence in the system [108]. They are usually made of non-conductive materials such as woven. Because the mesh used as spacer material is made of non-conducting elements, they contribute to additional stack resistance which reduces the RED performance and is known as the spacer shadow effect [108], [118]. Four different spacers were used in the present study and their effect on the intensity, the voltage, the power density, and the stack resistance were monitored and depicted in the graph in Figure 4.6. The voltage, intensity, and power density increased while the resistance decreased with the RED stack operated at similar conditions with PVC1, PVC2, handmade woven, and woven spacers. Purchased woven spacer resulted in three times higher power density than PVC1. The spacer geometry and thickness have dramatic effects on RED process efficiency. The resistance of the flow channel is proportional to the thickness of the spacer and inversely proportional to the conductivity of the solution [143]. The spacers highly contribute to the RED stack resistance by a phenomenon called the spacer shadow effect which can cause up to 60% efficiency drop of the RED process [118]. Veerman et al. [130] and Danidilis et al. [103] reported in different experiments, 45%, and 66% respectively, as the contributions of the resistances of the spacer-filled dilute channel to the resistances of the cell pair. Mehdizadeh et al. (2019) investigated the spacer shadow effects and solution

compartment resistances with 16 different spacers with various geometries, having porosity and thickness between 56% - 84 % and 0.100 - 0.564 mm, respectively. They reported that the spacer geometry influences the spacer shadow effect [118]. A similar observation was performed in the present study with the four spacers used. The increase of resistance with different spacers is proof that the spacers can be a source of resistance and could result in a huge decline of the RED efficiency causing an important decrease in the produced energy efficiency, as reported through theoretical projections [108] and experimental works [118]. It is reported that thicker spacers impact enormously the resistance of the cell-pair while thinner spacers can significantly decrease the resistance (specifically when operating with very low NaCl concentrations of a dilute solution) [130]. However, the design of the spacer is very important as well, a very smooth and thin spacer (PVC) can reduce the water flow in the stack and affect the process performance, similarly, a spacer with less contact space of the water (PVC1 compared to PVC2) may reduce the ions migration by reducing the water contact with the IEMs, though reducing the whole process efficiency. Not adequate spacer geometry (PVC1 and handmade spacer) contributes to hindering the feed solution circulation over time, thus reducing the power output over time [128].

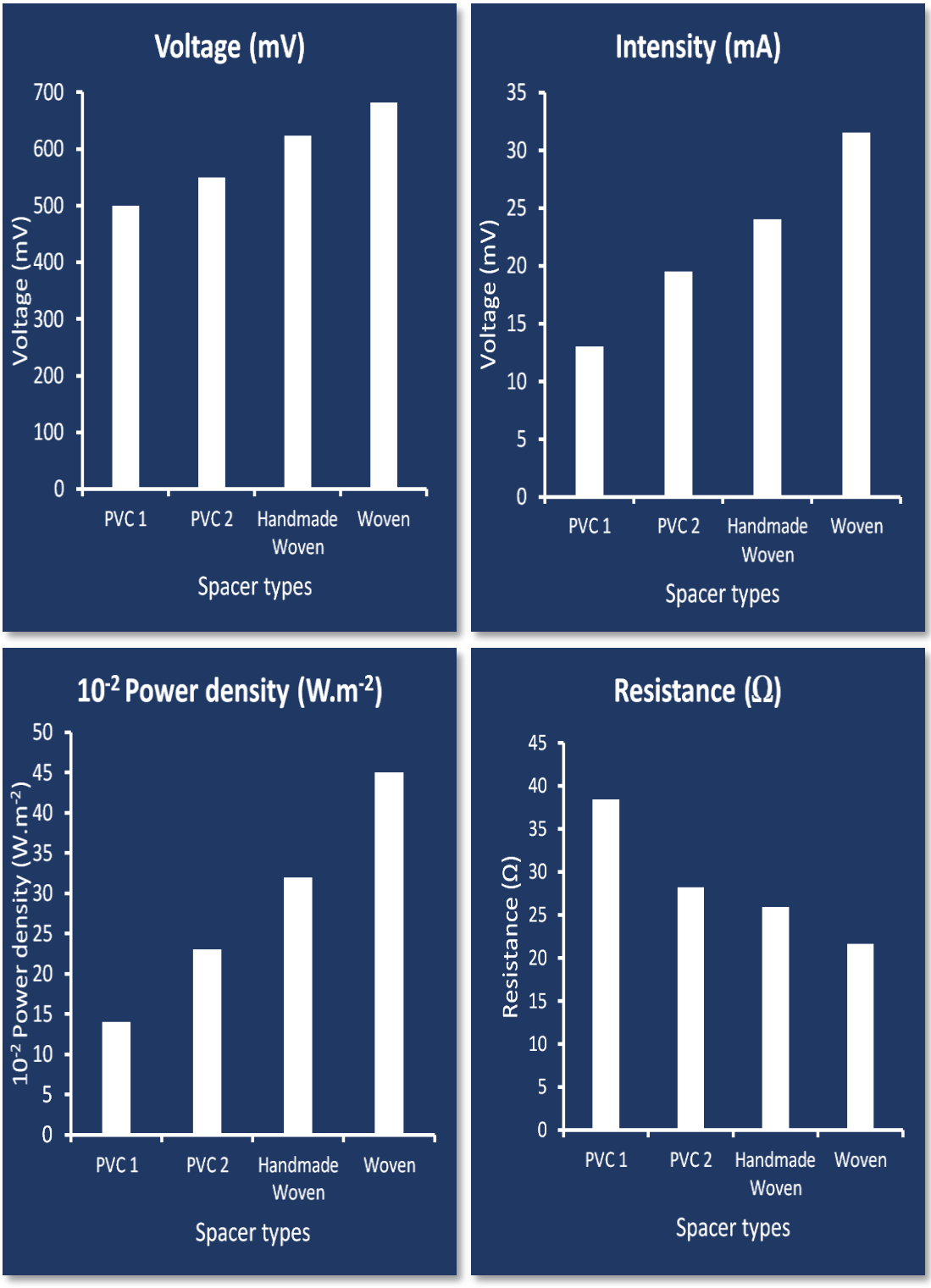

Figure 4.6 The effect of different spacers on the RED performance

4.2.5 The Effect of Increasing the Stack Cell-pairs in the RED Process Performance

Increasing the RED stack cell-pairs is necessary to optimize the energy output firstly due to the accumulative effect of the generated power, and secondly due to the reduction of the end membranes. For each stack, an extra membrane is required to close the stack and these membranes are directly in contact with the ERS. The ERS is known to negatively affect the end membranes over time, such a point that they become useless. As illustrated by Figure 4.7A, Figure 4.7B and Figure 4.8, the end CEM autopsy by SEM, SEM-EDX, and FTIR analysis, respectively, shows some membrane structural destruction. By increasing the cell-pair number, the need for a membrane (which is expensive) is reduced in the RED operation, economizing in the membrane. End membranes are the most sensible in the process which will require replacement much faster than the other membranes do. Increasing the number of cell-pairs will reduce the number of end membranes needed for the whole operation. SEM and SEM-EDX results unanimously reported a stressed end CEM due to the ERS. There is a high deposition of Fe^{+2}, Na^{+}, K^{+} on the membrane. The FTIR results show a structural modification of the CEMs used as end membranes. The modification was intensive on the side of the membrane facing the ERS. This effect may induce a need for membrane change in a short period.

On the other end, increasing the number of cell-pair contributes to an increase of the whole RED stack resistance which affects the expected linear increase in power density. This is the result of the cımulative resistance of the membranes and the spacers in series. Also, the nature, structure, geometry, and thickness of the spacer play an important role in the resistance of the RED stack by inducing the shadow effect. The effect of the spacer is higher with an increasing number of cell-pair. Some researchers proposed different spacer materials such as conductive spacers or spacers made of IEMs, others tried to improve the spacer geometry and thickness, and recently spacer-less RED units have been investigated. Ion conductive spacers and spacer-less RED stack are under development to offset the negative effects induced by the spacer effect. Vermaas et al. (2011) proposed a spacer-less RED stack by introducing profiles in the form of ridges (230–245 μm) on one side of the IEMs

by hot pressing [120], which reduced the ohmic resistance and increased the power density. However, profiled membranes require engineering skills to produce and operate successfully. Further studies emphasizing large scale applications will enlighten our understanding and the behavior of such membrane in long-term large processes.

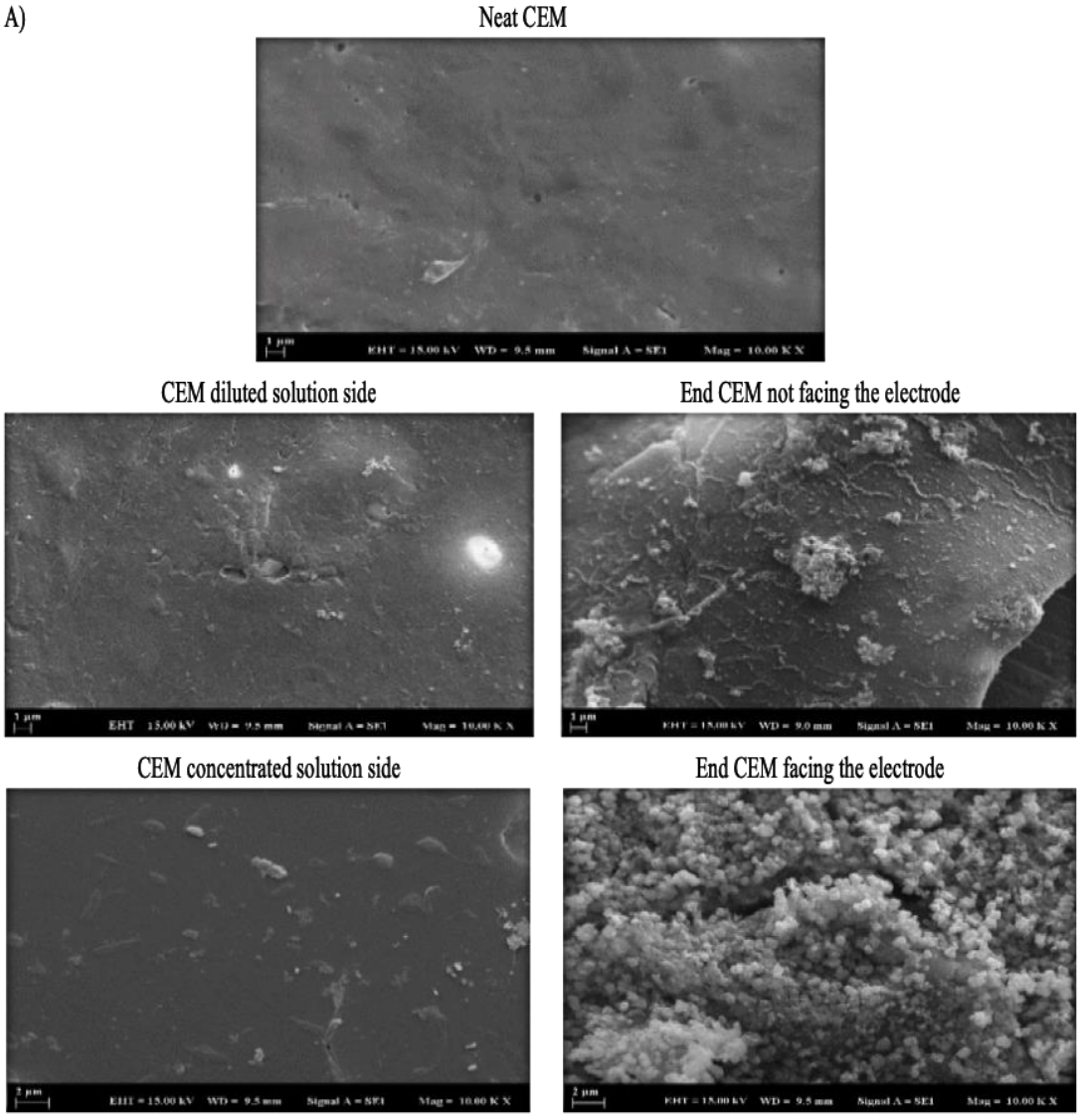

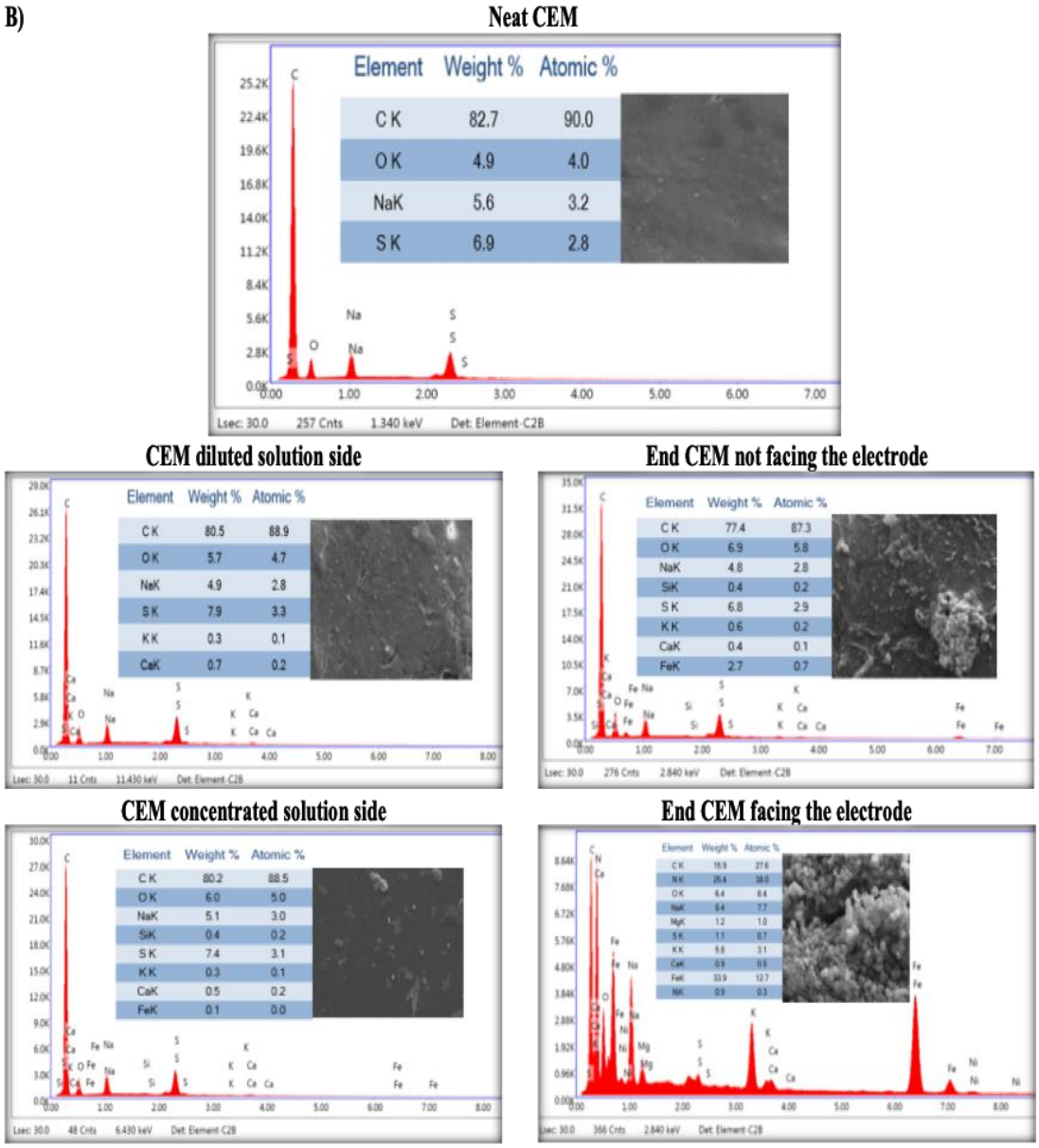

Figure 4.7 10000x magnification SEM (A) and SEM-EDX spectrums (B) results of Neat CEM, CEM diluted solution side, CEM concentrated solution side, End CEM not facing the electrode, End CEM facing the electrode

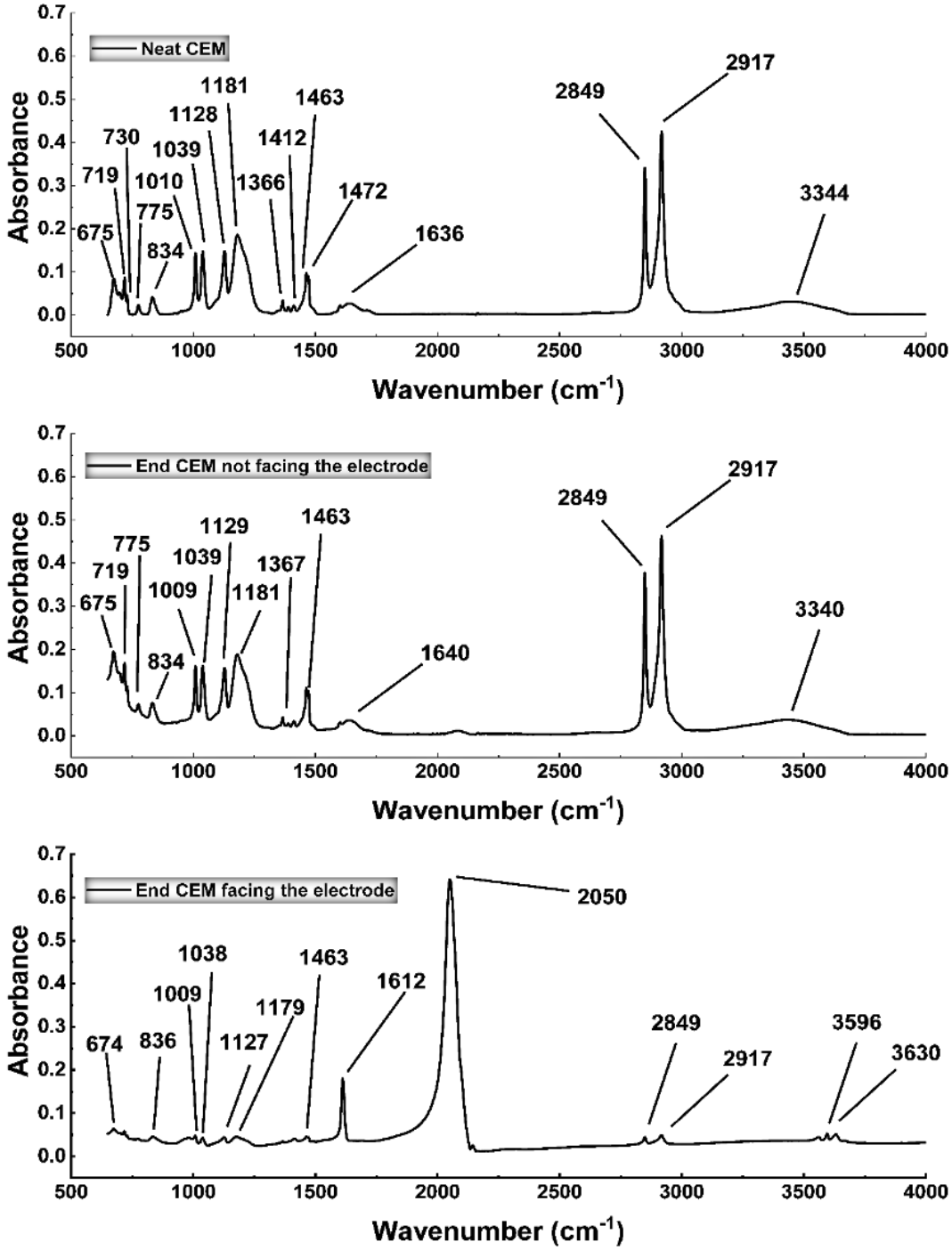

Figure 4.8 FTIR results of Neat CEM, CEM diluted solution side, CEM concentrated solution side, End CEM not facing the electrode, End CEM facing the electrode

4.2.6 Results' Evaluation

The performance of the RED unit can be affected by many parameters among which the resistance plays an important part. The present study demonstrated that the increase in the number of cell-pairs of the RED stack is beneficial since it causes an increase in the voltage and the intensity resulting in a higher power density. However, the increase of the voltage is not linear as the result of the increasing resistance which deviated from the increasing trend of the voltage. This resistance was mostly due to the spacers and the IEMs. Different spacers used proved that the spacer structure, geometry, and opening affects the stack resistance by inducing the spacer shadow effect. SEM, SEM-EDX, and FTIR analyses proved that the ERS is harmful to the end IEMs, and operating an RED unit with a high number of cell-pair reduces the need for end membranes.

4.3 SGP Potential of Red Fed with Treated Municipal Wastewaters and the Marmara Sea

As reported in the literature, the chemical potential difference between water bodies with different salinities releases chemical energy known as SGP [10], and this energy can be converted into electricity by using specific systems that perform a controlled mixing of the solutions. Pattle developed and proposed the first concept of extracting SGP in 1954 by introducing a technique known as a hydroelectric pile that could be used to extract electric power from mixing fresh and saltwater [12]. Today, high worldwide SGP is theoretically available [15] as a gigantesque source of clean and renewable energy able to contribute to the global energy demand but is lost in nature [15], [16]. In the principle of SGP, when two solutions with different salt concentrations are mixed, there is an increase of the entropy of the system, a dissipation of a chemical potential gradient which can be converted into electricity [9], [13], [14].

RED utilizes a flow system between electrodes and alternating CEMs and AEMs [63] to extract the SGP by the transport of ions through IEMs during the mixing of two solutions with different salinity [18]. It is a non-polluting, sustainable technology to generate power from the mixing of solutions with different salinity [9], [10], [13]–

[16]. In its operation principle, the ions (mostly Na^+ and Cl^-) in the concentrated solution (HC) migrate across the membranes toward the diluted solution (LC); Na^+ ions migrate through the CEM toward the cathode while Cl^- ions migrate through the AEM toward the anode, as depicted by Figure 3.2. The opposite ion flow will create a chemical potential, resulting in chemical energy which is converted into electrical current, by using an appropriate redox couple at the electrodes [63], [66], [78].

Due to its complexity, few investigations have been conducted in the field of SGP extraction by the RED process using natural feed solutions. Natural water bodies contain divalent ions, dissolved matter, and suspended solids which make the process difficult and highly affect its feasibility. As a result, most of the studies focused on lab-scale investigations of synthetic solutions mimicking sea and river water. The results from synthetic studies, although necessary, investigations on the performance of reverse electrodialysis unit in the real environment by using real solutions are crucial to identify the actual potential of this renewable energy source, current limitations, and future perspectives. Seawaters and rivers are great natural stream candidates for SGP generation, however, some attention has been devoted recently to alternative feed solutions such as wastewaters and brines from desalination plants. Targeting different feed solutions such as brines concentrates from different desalination processes and wastewaters can diversify the potentiality of RED. Membrane fouling [144], uphill transport of multivalents ions [147], and the low power density are among the main challenges with natural water sources. Avci et al. (2018) compared natural feed streams salinity gradient power harvesting by RED with synthetic equivalent ionic strength and reported approximately 2/3 loss in power density. They attributed this result to increased membrane resistance, reduced open-circuit voltage (OCV) and the occurrence of uphill transport for Ca^{2+}, $Mg^{2+,}$ and SO_4^{2-} in the RED stack operated with natural feed streams [147]. Many researchers reported up to 50% decrease in the power density within the first-hour of RED operation with natural feed streams [144], [148],[149].

The present study investigates the SGP production potential of RED feed with seawater (Marmara Sea) and different treated municipal wastewater effluents (advanced biological treatment, ultrafiltration, membrane bioreactor) used as a

diluted solution. The importance of wastewater in energy generation can lead to zero waste management and optimize the interest of SGP by RED. The influence of the different natural solutions compared to synthetic feed solutions has been evaluated based on the process power density drop over time and the effect on the IEMs. The stack contained 10 cell pairs, consisted of 11 CEMs and 10 AEMs. Each membrane dimension was 0.077 m x 0.077 m, resulting in a total active membrane area of 0.11858 m^2. The HC and LC solutions were circulated in a single pass with a fixed flow rate of around 30 ml/min for the LC solution (treated wastewater) and 20 ml/min for the HC solution (the Marmara Sea). The Marmara Sea and treated municipal wastewaters were collected in Istanbul, Turkey. However, synthetic solutions mimicking the wastewater and the Marmara Sea by their conductivities have been investigated as well to understand the effect of the wastewater and seawater on the RED performance.

Electrochemical impedance spectroscopy demonstrated that the decrease of the system performance is prevalently due to the significant increase of CEM resistance due to the presence of negatively charged organic matters in natural water bodies. As a membrane process, membrane fouling and concentration polarization could be some major challenges with natural feed solutions in RED. In addition to antifouling strategies such as periodic feedwater reversal and air sparging [148] or the use of CO_2 saturated feed water as two-phase flow cleaning for fouling mitigation [149], membrane modification to improve its properties and the fouling resistance [152], profiled membranes [144], stack water feeding pattern improvement by additional water inlet and outlet [180] are alternatives to reduce the fouling effects and improve the RED performance. On the other hand, using feed solutions with good quality could prevent fouling. In this study, the influence of the quality of the wastewaters in the process performance was assessed and the importance of wastewater in RED energy generation was investigated to highlight an opportunity for zero waste management and enlarge the scope of SGP by RED. Using Ataköy and Ambarlı WWTP as models, for being among the biggest WWTP of the city of Istanbul, the study also investigated their total power and energy output and projected by

simulation with optimal conditions the net RED energy output in Ataköy and Amabarlı WWTP.

4.3.1 Operation Conditions and Behavior of the Feed Solutions

The lab-scale RED process was operated for 6 days (4 hours continuous running/day) for 24 hours total operation time. Three tanks with 2 L volume each were used as reservoirs. The first tank was filled with the Marmara Seawater, the second tank with treated wastewater, while the third tank carried the ERS.

The study investigated 7 combinations of feed solutions, each set for 24 hours in the RED operation, and the behavior of each feed solution combination was monitored. The voltages of the seven combinations are represented by V1, V2, V3, V4, V5, V6, V7, and the power densities by PD1, PD2, PD3, PD4, PD5, PD6, PD7, which depict the feed solution combinations AB2-Marmara Sea, AB1-Marmara Sea, UF-Marmara Sea, MBR-Marmara sea, Synthetic diluted Solution-Marmara Sea, UF-Synthetic concentrated solution and Synthetic diluted solution-Synthetic concentrated solution, respectively.

The feed solutions (Marmara sea and treated municipal wastewaters) presented high harness, a result of the high concentration of calcium and magnesium. The total hardness for all feed solutions was higher compared to the total alkalinity; some of Ca^{2+} and Mg^{2+} in the solutions are associated with SO_4^{2-}, Cl^-, SiO_3^{2-} or NO_3^- but not with HCO_3^- and CO_3^{2-}.

4.3.2 Voltage and Power Density

The voltages and power densities of the different feed solution combinations are portrayed by the graphs in Figure 4.9 and Figure 4.10, respectively for 24 hours RED operation. The process was continuously operated for 4 hours each day for 6 days. As shown in Figure 4.9, the highest voltage was obtained with V7 which used only synthetic solutions as feed stream, followed by V6 which combined UF effluent and synthetic concentrated solution, and V5 with a combination of synthetic diluted solution and the Marmara Sea. The remaining 4 combinations depicted the lowest voltage with V3 and V4 relatively higher than V1 and V2. These results demonstrate

the advantage of the synthetic solution in terms of RED performance. On the other hand, replacing synthetic diluted solution with the UF effluent (V6) affected very little the voltage compared to the replacement of the synthetic concentrated solution by the Marmara Sea (V5), showing that concentrated solutions are more prone to affect the process performance than diluted solutions. Also, the results revealed a sharp decrease of all the voltages for all the combinations in the first 2 days of operation from 0 to 8 hours continuous operation, except for V7 and V6 where the voltage decreased slightly. The decrease was even sharper in the first hour of operation.

The present study operated with the Marmara Sea (conductivity of 33.2 mS/cm) and synthetic solutions with equivalent ionic strength as high saline feed solutions. Since the wastewater was collected at the vicinity of this sea, the advantage of operating at elevated HC salinity which would increase the driving force and process power density [106] was not possible. Figure 4.10 depicted the power density values of the RED process fed with different wastewater effluents mixed with the Marmara Sea and synthetic solutions. Similar to the voltage, PD7 appears to be the highest power density followed by PD6 and PD5. There was a sharp decrease of power densities PD1, PD2, PD3, PD4 and PD5 within the first 2 days but the decrease was shaper in the first hour of operation, including PD6. PD7 remained steady for the 24 hours operation with a very slight decrease. Although synthetic solutions resulted in better power densities and less affected over time, when we compare PD7 and PD3 which are only synthetic and real UF-Marmara Sea combinations, respectively, the average power density for 24 hours operation did not show a significant difference. These average power densities were 0.57 $W.m^{-2}$ and 0.52 $W.m^{-2}$ for PD7 and PD3, respectively. The lowest power densities observed in the present study were PD1 and PD2 which reported a similar average power density of 0.48 $W.m^{-2}$, 15.8% lower than the power density of synthetic solutions PD7. These results were surprisingly interesting since it has been reported in the literature over 50% power density reduction with natural streams compared to synthetic solutions [144], [148], [149]. All the treated wastewaters used in this study presented a high quality, assimilable to synthetic solutions, and this might explain the reported results.

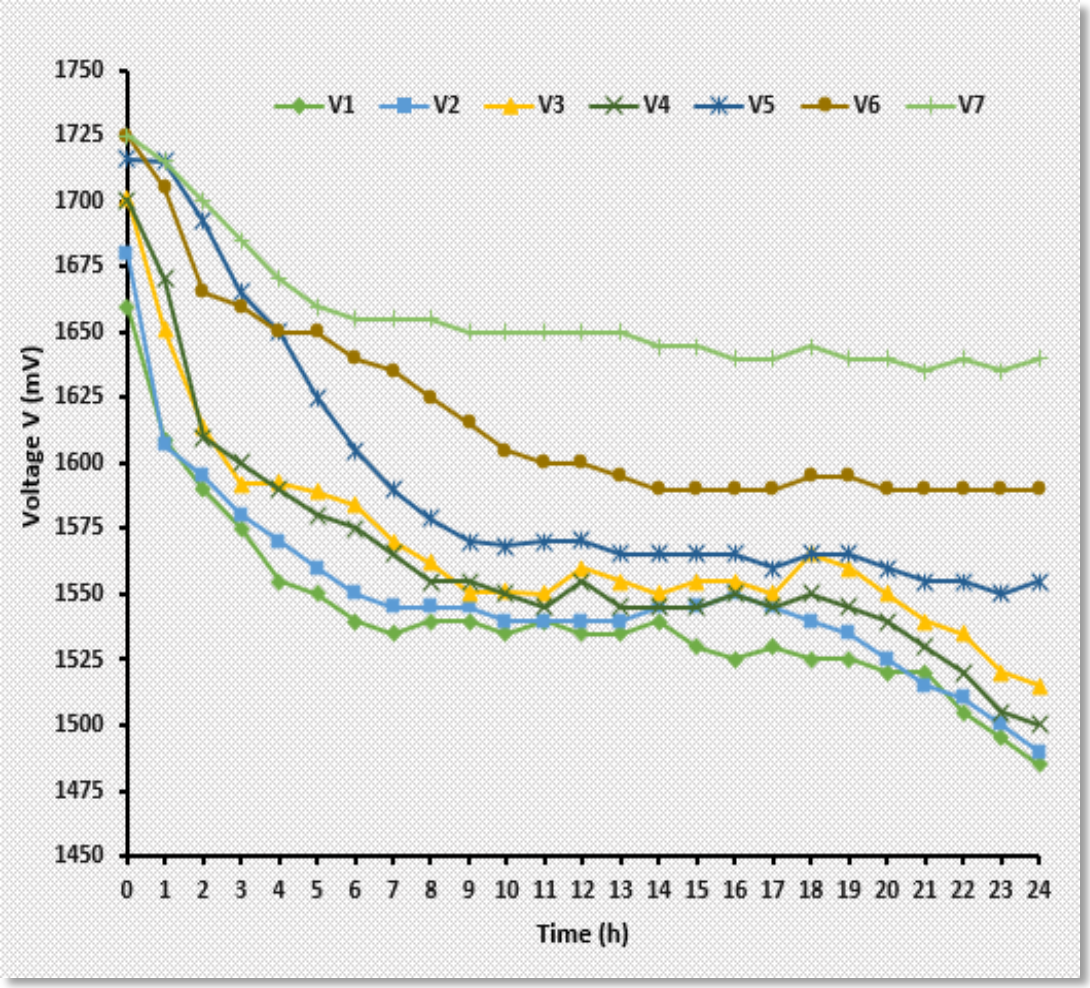

Figure 4.9 Voltage values of the RED process with Ataköy and Ambarlı WWTP effluents, the Marmara Sea and synthetic solutions

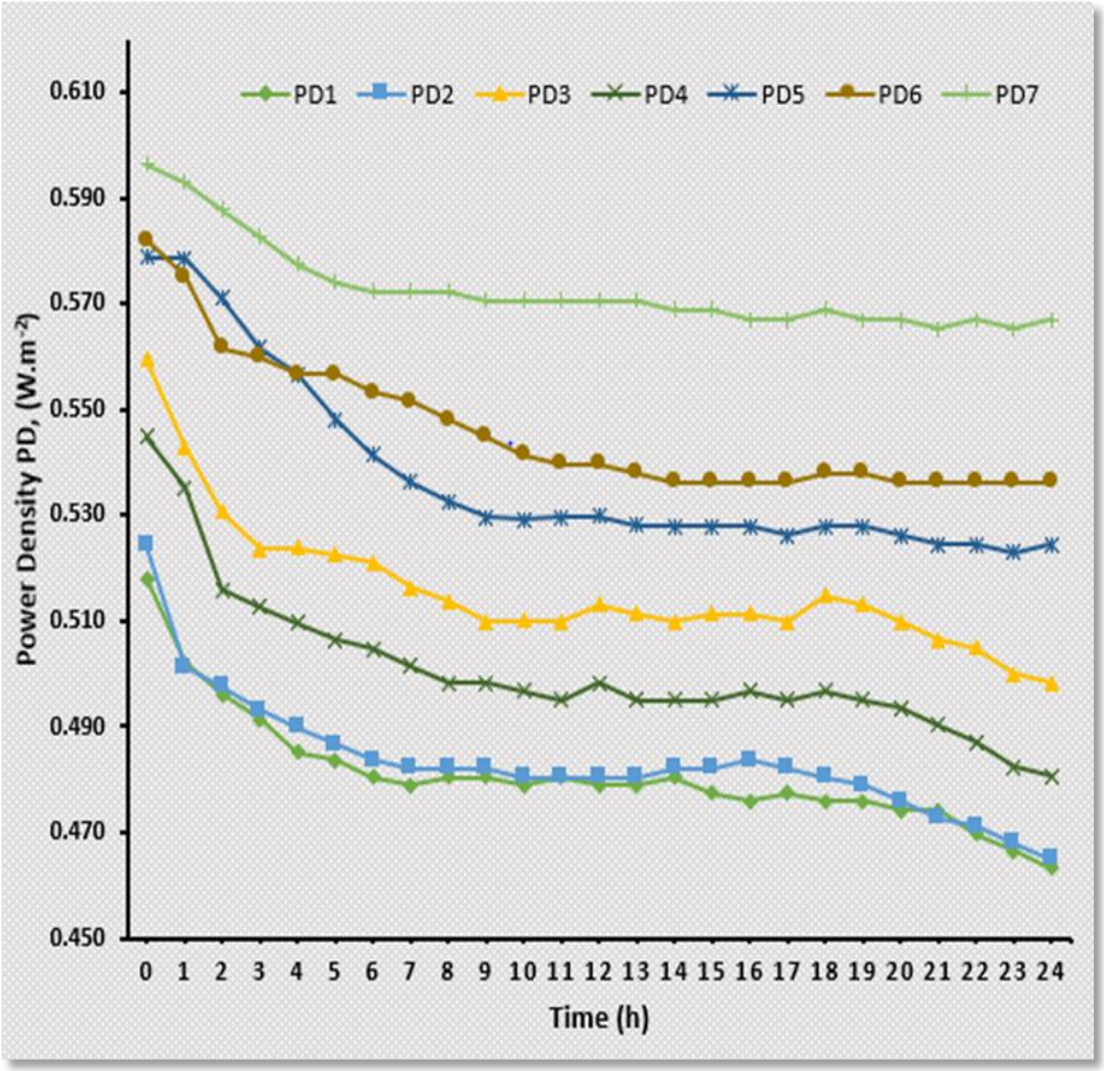

Figure 4.10 Power density values of the RED process with Ataköy and Ambarlı WWTP effluents, the Marmara Sea and synthetic solutions

4.3.3 Real feed solutions

In the first minutes of RED operation, the natural feed solutions resulted in power densities of 0.52 $W.m^{-2}$, 0.52 $W.m^{-2}$, 0.54 $W.m^{-2}$ which decreased gradually over time and resulted in 24 hours average power densities of 0.48 $W.m^{-2}$, 0.48 $W.m^{-2}$, 0.50 $W.m^{-2}$ and 0.52 $W.m^{-2}$ for PD1, PD2, PD4, and PD3, respectively, as depicted by Table 4.5 PD1 and PD2 are the results of feed solutions with the same quality (ABT effluent) but from a different treatment plant (Ataköy and Ambarlı WWTP). They presented the same power density throughout the process, indicating that the low

power density obtained with PD1 and PD2 compared to PD3 and PD4 was due to the poor quality (higher COD) and to the higher ionic strength (higher conductivity) of AB1 and AB2 effluents compared to UF and MBR effluents used as diluted solutions. PD3 showed the highest power density among the treated wastewaters thanks to the quality of UF effluent (lower conductivity and COD) which was close to tape water used as a synthetic solution. The effluent from UF and MBR presented better power densities compared to ABT effluents. Although all treated wastewaters depicted high quality, the salt content was low in UF effluent (around 1050 $\mu m.cm^{-1}$ conductivity) compared to MDR (around 1180 cm^{-1} conductivity) and ABT effluents (average 1270 cm^{-1} conductivity). The salinity of the diluted solution is more sensible for the RED process. It is however worth mentioning that neither UF nor MBR are suitable for the removal of water conductivity, but they might have slightly reduced the conductivity by removing some of the bounded matters to conductivity causing ions. A slight variation of the LC salinity can affect the process performance and might have resulted in lower power densities with AB1 and AB2 compared to UF and MBR effluents. By operating the process for 24 hours, a very low decrease in the power density was observed with all the feed solutions. It is a common belief that the presence of multivalent ions and NOMs in the feed solution causes a lower power density by reducing the OCV of the RED process. Negatively charged NOMs such as humic acids shield the positively charged groups in AEMs reducing the membrane permselectivity and increasing its resistance [117]. All the wastewaters used in this study presented a high quality, minimizing membrane fouling and scaling. Vanoppen et al. (2019) investigated pretreatment techniques for WWTP effluent used in an RED unit and supported that adequate pretreatment is required to efficiently run the RED system. They found that 100 µm filters and rapid sand filtration can significantly reduce membrane fouling, and can prevent pressure drops, high frequency of cleanings, and low permselectivity [153]. Nam et al. (2018) investigated a pilot-scale RED fed with sea and wastewaters and achieved a power density of 0.38 $W.m^{-2}$ [156]. Although they worked with elevated HC salinity (52.9-53.8 mS/cm), the quality of their wastewater effluent was low, resulting in lower power density compared to the present study. The high effluent quality from

advanced municipal WWTPs together with the clean seawater surrounding the treatment plant can successfully be used as feed solutions in an RED stack.

Table 4.5 Power densities of RED with differently treated wastewaters

	Power densities ($W.m^{-2}$)				
	PD1	PD2	PD3	PD4	PD6
First min	0.52	0.52	0.56	0.54	0.58
24^{th} hour	0.46	0.46	50	0.48	0.54
24 hours average	0.48±0.02	0.48±0.02	0.52±0.02	0.50±0.02	0.55±0.02

4.3.4 Power Density lost rate within 24 hours RED process

Within the 24 hours of operation, the power density sharply decreased in the first hour of operation and gradually continues to decrease slightly over time. The power density percentage that is lost for each feed solution combination is computed and exhibited in Figure 4.11. While PD1 and PD2 showed the highest power loss (11.54%) within 24 hours, PD7 lost only 5%, which is the lowest. Synthetic solutions operated for hours with no significant reduction of the power density. Using feed solutions combination of synthetic and natural waters resulted in higher power loss compared to only synthetic solutions but lower compared to only natural solutions. Among the natural feed streams, UF followed by MBR wastewater effluent presented the lowest power lost over time. The presence of trace organic matters in natural feed streams participated in slightly reducing the achieved power density by affecting the ion transport efficiency and by deposing on the membrane surface causing some fouling [117], [153]. But the results remained satisfactory since the power loss was insignificant and no remarkable difference was observed between synthetic and natural wastewaters power loss over time, which was the concern of many scientists [144], [148], [149] in the application of natural water streams in RED processes. For effective use of wastewater or natural feed streams in an RED stack, it is recommended in the literature that appropriate pretreatment techniques

been applied to improve the process performance [153]. Considering ABT, MBR, and UF, which are more advanced wastewater treatment techniques, these effluents are, without any doubt, a good alternative in RED.

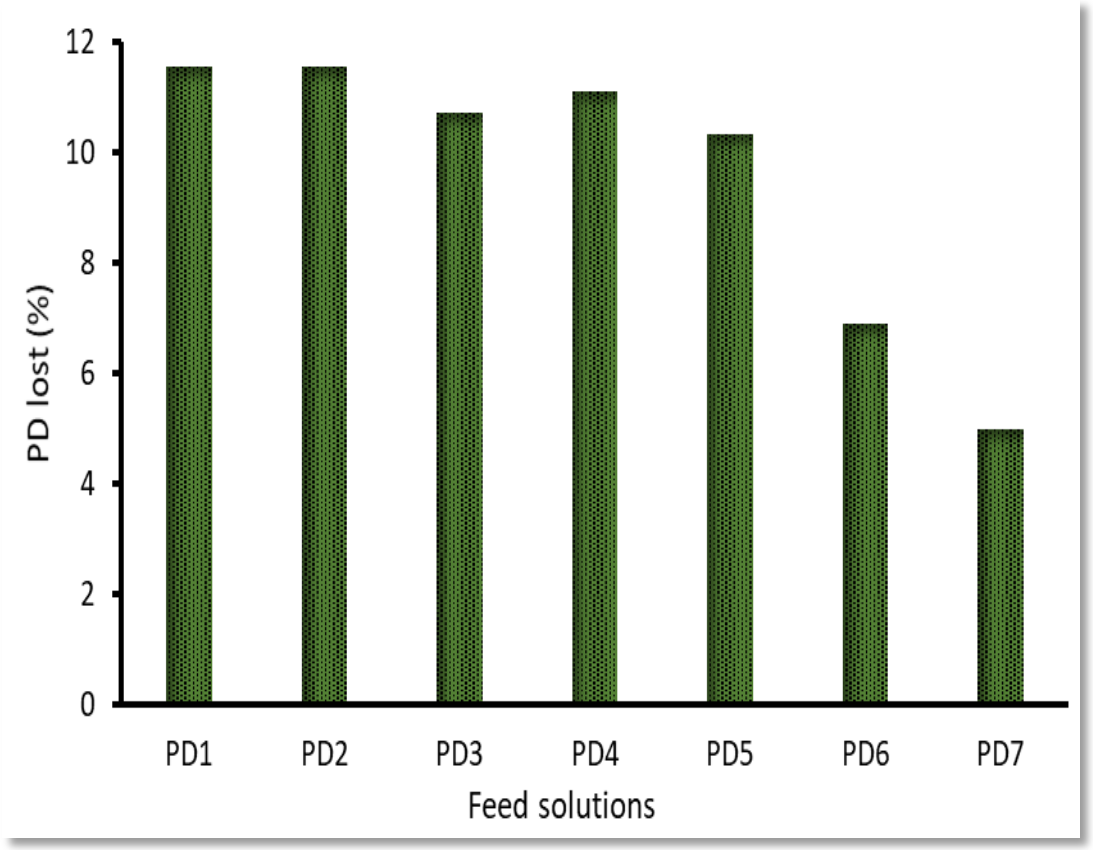

Figure 4.11 Power density lost rate within 24 hours operation of RED

4.3.5 Synthetic and Natural Feed Solutions

The results summarized in Figure 4.9, Figure 4.10, and Figure 4.11 imply that synthetic solutions presented the best results and are more efficient compared to natural feed solutions in the RED process. The few investigations conducted with the RED process using real sea and river waters reported a low power density. It is supported that natural feed solutions are complex and the presence of divalent ions in sea waters, dissolved matters and suspended solids found in natural water [144] make the process difficult and results in low power output. The SEM results in Figure 4.12 showed the presence of minerals, while the SEM-EDX spectra depicted in Figure 4.13 confirmed the presence of divalent ions such as Ca^{2+} and Mg^{2+} with

high concentration and may behave like a shield, reducing the movement of Na^+ and Cl^- responsible for energy generation in RED. Using a synthetic solution equivalent ionic strength of natural solutions, Avci et al. (2018) achieved 3 times higher power density and reported that the low performance with natural feed solutions was the result of high membrane resistance, low OCV and the transport of Ca^{2+}, $Mg^{2+,}$ and SO_4^{2-} through the membrane [147]. Tedesco et al. (2016) reported similar results with 60% higher power density with synthetic NaCl solutions at similar operating conditions with natural streams [76]. In the present study, the performance reduction with natural streams was likely caused by non-NaCl ions, especially Mg^{2+}, in relatively large concentrations, which adversely affected both the electromotive force and stack resistance. Replacing the Marmara Sea by synthetic solution with similar ionic strength while using UF effluent as the diluted solution (PD6), resulted in a power output very close to an only synthetic concentrated and diluted solution (PD7). Divalent ions in the sea and river water or treated wastewaters, ideal candidates for real RED implementation, remained one of the strong limiters of RED performance due to both induced uphill transport and increased membrane resistance. To mitigate those divalent ions effects, novel and tailor-made membranes are being investigated [167]. To improve the electrochemical properties of the IEMs among which high permselectivity and low resistance, many attempts have been made such as organic-inorganic nanocomposite membranes from polyphenylene oxide (PPO) [168], halogenated polyethers, such as polyepichlorohydrin (PECH) [169], sulfonated polyethersulfone (sPES) cation CEM [61]. Improving membrane properties [152], increasing their permselectivity, and reducing their resistance or eliminating the spacers [119], [120] in the RED stack are among many attempts that will improve the power density and the LCOE generated by an RED process.

4.3.6 Autopsy of the IEMs After 24 Hours RED Process with Various Feed Solutions

Although it is generally accepted that IEMs in RED are less subjected to fouling than typical pressure-driven membrane processes such as RO or UF, the main issues encountered by all membrane processes are membrane fouling, wetting, clogging and damage. These influence the integrity of the membranes and cut down the performance of the membrane process over time [181], [182]. To understand the fate of the IEMs after the RED operation, SEM, SEM-EDX, and FTIR analyses were performed. The SEM images, SEM-EDX and the FTIR spectra are depicted in Figure 4.12, Figure 4.13 and Figure 4.14, respectively, and they enlighten the behavior of the IEMs after 24 hours of operation in an RED process using synthetic solutions, treated municipal wastewaters, and the Marmara Sea as feed solutions. In Figure 4.12, the SEM images with 10000x magnifications show the morphology of the neat CEM and AEM as well as their morphologies on the HC side (the Marmara Sea and Synthetic concentrated solution) and LC sides (UF, MBR, AB1, AB2 effluents, and synthetic diluted solution) after 24 hours RED operation, consequently depicting the structural modification and the pollutants trapped on the surfaces of the membranes during the RED process. The neat membranes showed a non-porous morphology, on the other hand, the surfaces of the used membranes were affected by the deposition of crystals and debris. There was a high deposition of salt crystals on both CEM and AEM facing the seawater side, however, fewer crystals were observed on the LC sides of the membranes. The LC sides of the membranes for UF, MBR, AB1, AB2 municipal wastewater effluents seem to be slightly affected by the deposition of some materials. These are tiny organic and inorganic matters which were not removed during the advanced treatment processes, and some debris was deposited in the water during the stagnation phase after the treatment processes. The debris may not be a substantial problem since adequate care will be taken to avoid such deposition if any advanced treated wastewater is to be used in an RED process.

EDX analysis was performed to identify the elemental composition (chemical nature) of the material on the membrane surface. The corresponding peaks of the different area focused during the EDX measurements are shown in Figure 4.13. Multivalent ions such as Mg^{2+}, $Ca^{2+,}$ and Fe^{2+} were observed on the surface of the CEM and AEM facing the natural feed solutions, especially with the Marmara Sea. Only negligible amounts of multivalent ions were observed on the membranes facing the synthetic concentrated side. In addition to traces Mg^{2+} and Ca^{2+}, Si^{2+}, Fe^{2+}, and K^{+} were present in the treated wastewaters and were deposited on the surfaces of the membranes. It is worth mentioning that none of the municipal wastewater treatment techniques used (ABT, MBR, UF) was able to remove ions from the wastewaters. Detailed information of substances present in the feed solutions and their atomic and weight percentages are depicted by the EDX spectra in Figure 4.13. The presence of the divalent ions (mostly Mg^{2+} and Ca^{2+}) highlighted by the SEM-EDX results might have contributed to lowering the RED performance in terms of power density when the natural solutions were used [147].

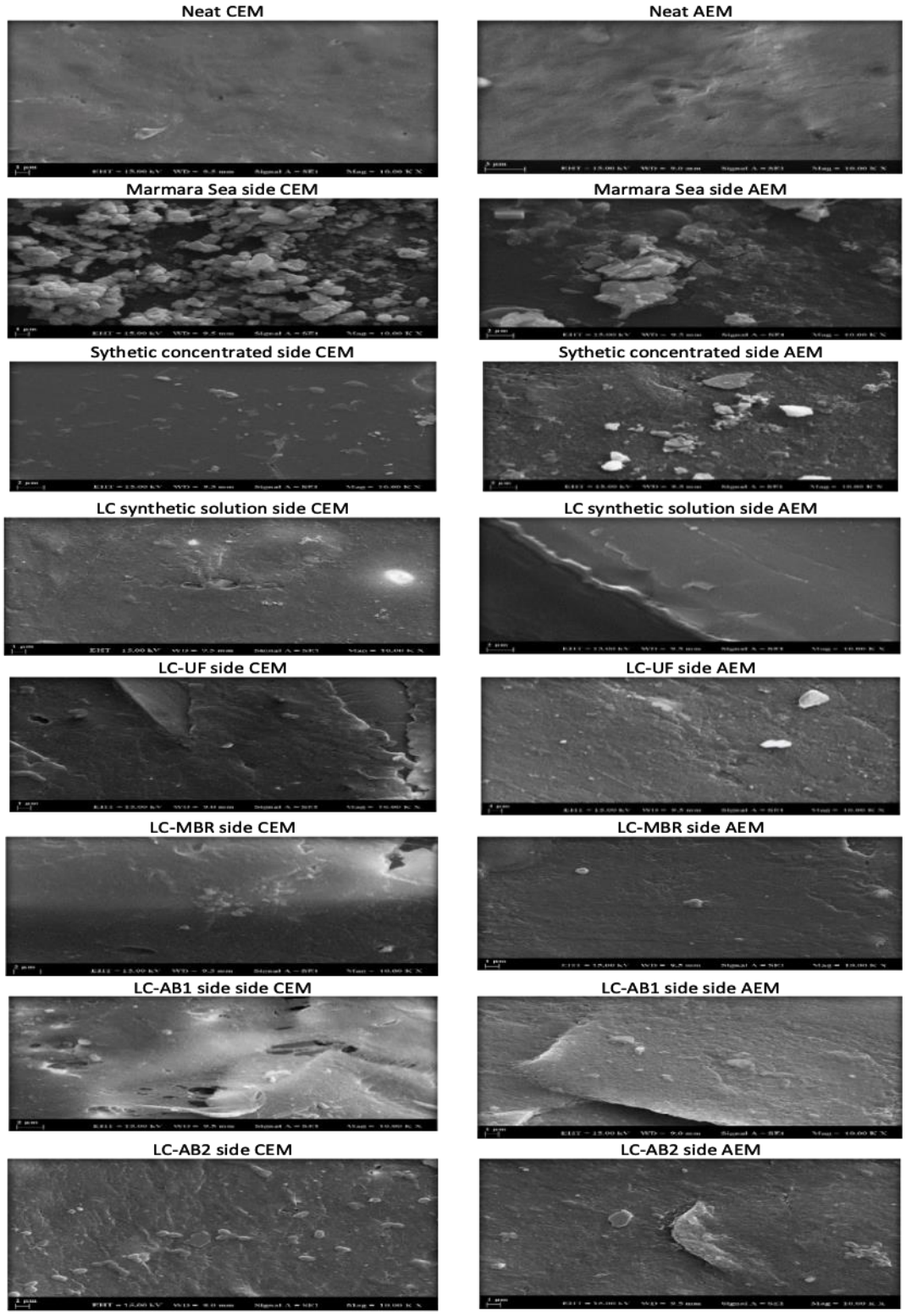

Figure 4.12 10000x magnification SEM images of Neat, HC side and LC side of UF, MBR, AB1, AB2 and synthetic feed solutions of CEM and AEM after 7 days RED process operation

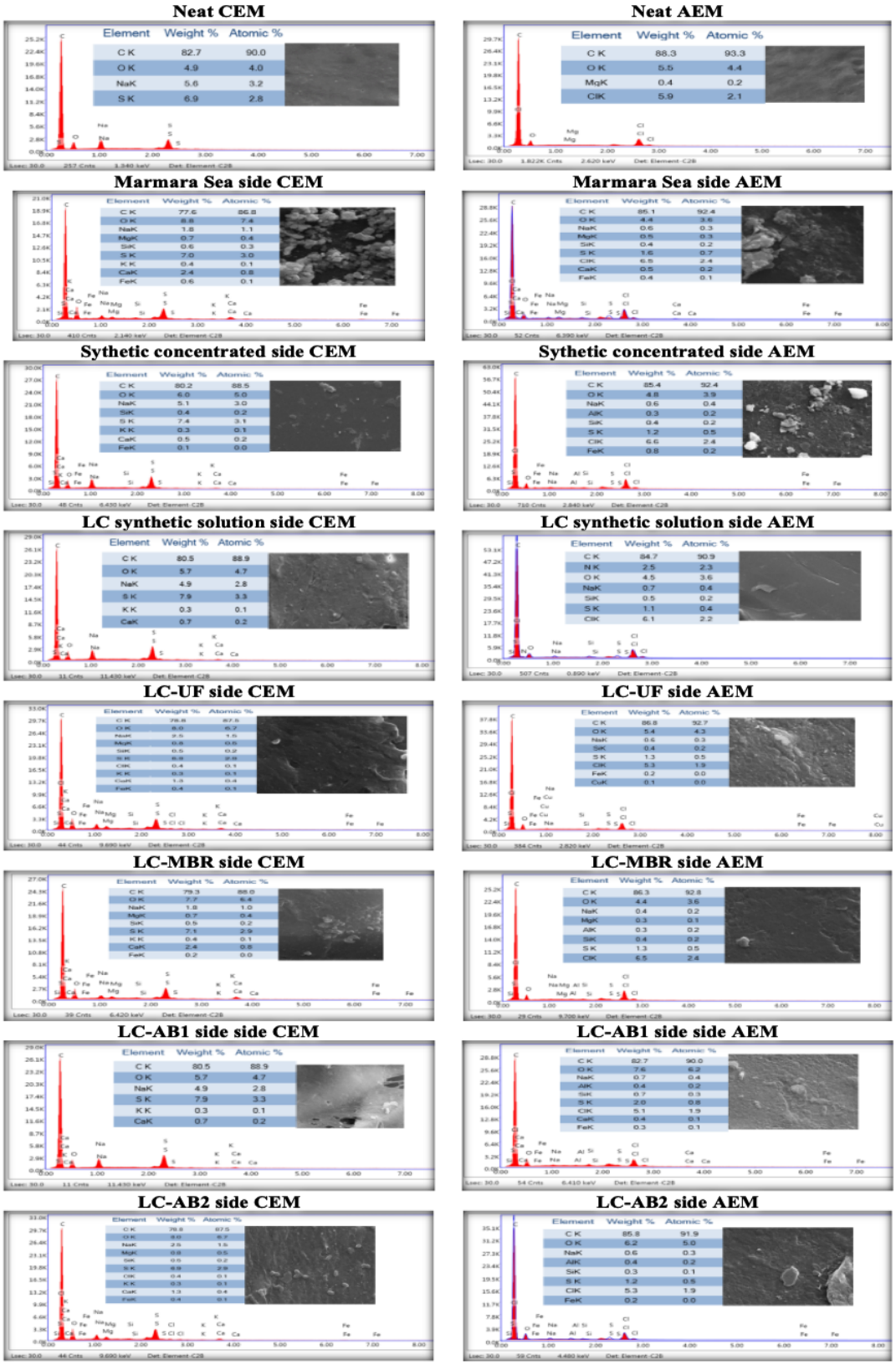

Figure 4.13 EDX spectrums of Neat, HC side and LC side of UF, MBR, AB1, AB2 and synthetic feed solutions of CEM and AEM after 7 days RED process operation

The changes that occurred in the membrane structures after 24 hours of RED operation were examined with FTIR and depicted in Figure 4.14. Both neat AEM and CEM showed a major pick at 2849 cm^{-1} and 2917 cm^{-1} which are related to the stretching vibration C-H groups present in the membranes' backbone. They also have a stretching O-H group exhibited by 3444 cm^{-1} and 3381 cm^{-1} peaks. A cloud of peaks from 675 cm^{-1} to 1636 cm^{-1} characterizing the functional groups of the CEM associated with polysulfones and from 719 cm^{-1} to 1711 cm^{-1} characterizing the functional groups of the AEM associated with quaternary ammonium were also presented by the FTIR spectra. The aromatic ring stretch is also represented in these clouds of peaks [183], [184]. Considering the FTIR spectra, there is no change or almost no noticeable changes in the peaks observed between neat and used membranes; no peaks removed, none added after 24 hours RED operation. Their wavenumbers and wavelengths remained almost similar for all the membranes with the same nature (CEMs or AEMs) regardless of the feed solutions. The spectra remain unchanged, they showed no sign of distortion from the RED process. This result suggests that none of the membranes lost their properties after 24 hours of operation in RED with synthetic solutions, the Marmara Sea, and the different advanced treated wastewater (UF, MBR, and ABT solutions). A similar result was observed by Tedesco et al. (2016) who claimed that no membrane fouling, scaling nor aging occurred during 5 months RED operation in their study [76]. This result was supported by D'Angelo et al. (2017) who reported that only a small decrease in the RED performance was observed after 4 months of operation in a real environment with the same redox solution [158].

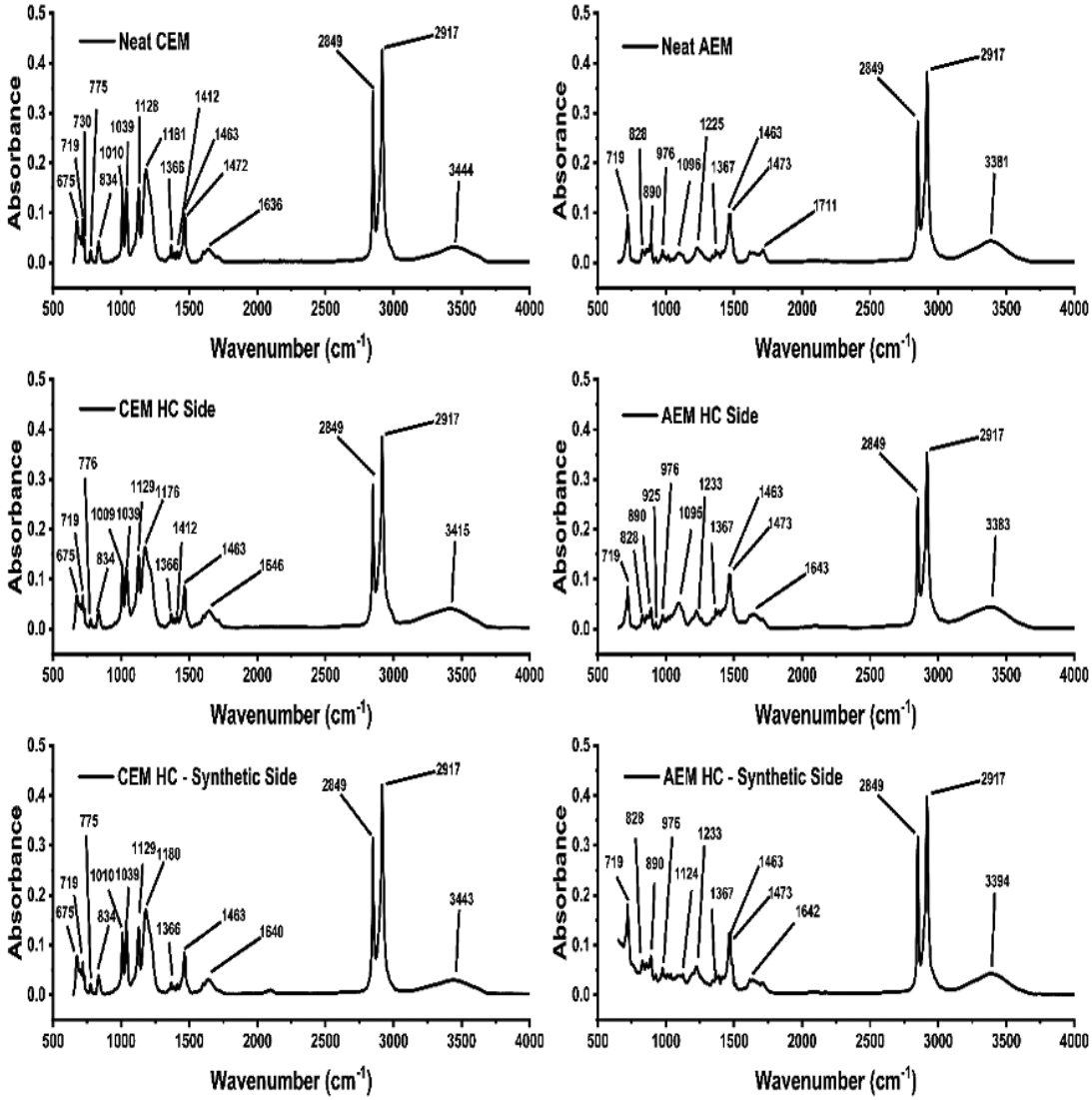

A- FTIR of the IEM's surface facing the high compartment (HC) side

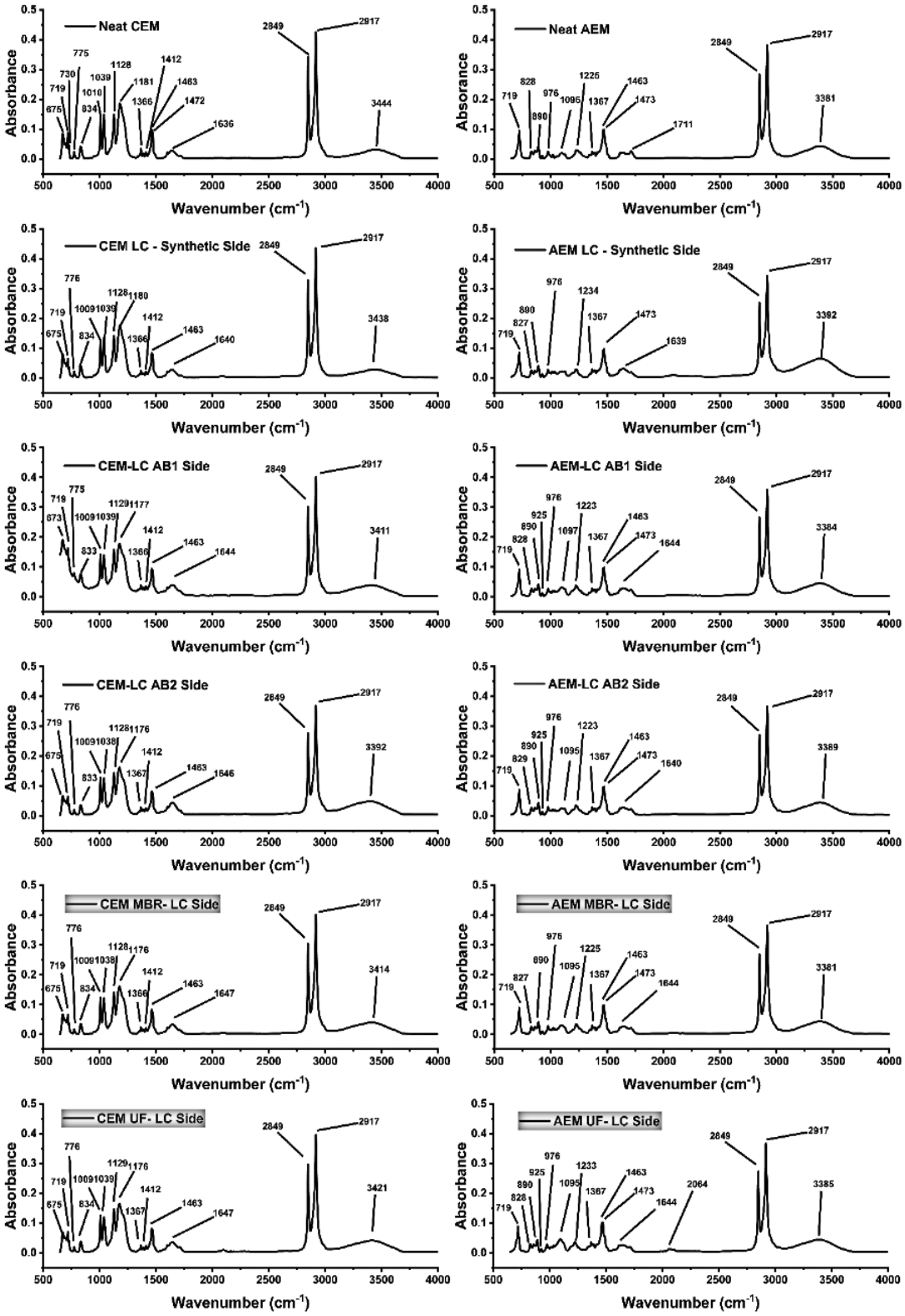

B- FTIR of the IEM's surface facing the low compartment (LC) side

Figure 4.14 FTIR results of Neat, HC side and LC side of UF, MBR AB1 of CEM and AEM after 24 hours RED process operation

The effect of fouling induced by organics, multivalent ions, and biomaterials on the RED performance especially in the application of natural waters (real river or saline waters) contributes to postponing the commercial application of RED process [116]. These particles are mainly composed of remnants of diatoms, clay minerals, organic fouling, and scaling [144]. The present study confirmed that the fouling of IEMs is negligible in an RED process as claimed by Tedesco et al. [76] and D'Angelo et al. [158]. Therefore, no performance losses due to membrane fouling or scaling were observed. This does not exclude the negative effects of debris and NOMs in the feed solution which can shield the membrane surface and prevent the adequate movement of the ions, consequently reducing the RED performance, and can be accounted for fouling. Also, fouling may take time to occur, for a longer period of RED operation, in real plants, the IEMS can experience fouling and scaling over time. To prevent this, some measures such as membrane modification to improve its properties and the fouling resistance [152] and profiled membranes [144] are alternatives to reduce the fouling effects. Some antifouling strategies have recently been proposed among which, periodic inversion of the feedwater and air sparging [148] or by using CO_2 saturated feed water as two-phase flow cleaning to reduce membrane fouling [149]. Recent studies on antifouling techniques also include the use of finer pre-filtration and the increase of the inter-membrane distance.

4.3.7 Design of RED Plant Installation at Ataköy and Ambarlı WWTP

Istanbul disposes of 89 municipal wastewater treatment plants (MWWTP), 8 pretreatment and 81 advanced biological treatment plants, with a total capacity of 5,815,260 $m^3.day^{-1}$, receiving around 3,927,030 $m^3.day^{-1}$ wastewater [172]. Both located in the European side, Ataköy and Ambarlı are among the high capacity treatment plant of the city with a total capacity of 600,000 $m^3.day^{-1}$ and 400,000 m^3/day, respectively, and receives 411,250 $m^3.day^{-1}$ and 336,820 $m^3.day^{-1}$, respectively. Ataköy WWTP includes an MBR unit with a capacity of 30,000 $m^3.day^{-1}$, and Ambarlı WWTP contains an UF unit with a capacity of 25,000 $m^3.day^{-1}$ expected to reach 50,000 $m^3.day^{-1}$ soon [172]. Ambarlı and Ataköy WWTP are located at the vicinity of the Marmara Sea, 5 m and 10 m altitude, respectively. The

treated wastewaters are discharged into the sea by gravitation. An appropriate RED stack can be installed underground allowing both feed solutions to flow by gravity into the stack. The brackish solution from the stack will then be stored at about 5 m down sea level before being pumped to the surface of the Marmara Sea, as schematically depicted by Figure 4.15.

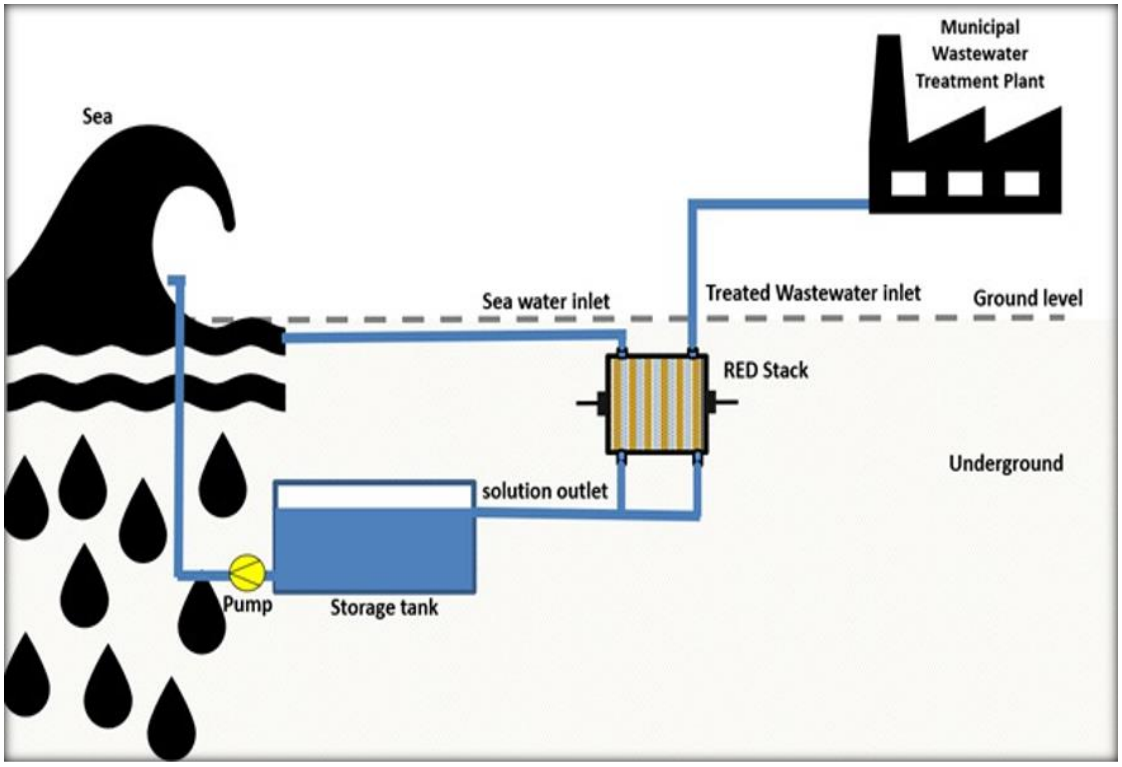

Figure 4.15 Proposed simplified scheme of RED plant layout for Ataköy and Ambarlı

4.3.8 RED Power Density Potential of Ataköy and Ambarlı wastewaters

Figure 4.16 below depicted the power density values overtime for 7 days and the average power densities of the RED process operated with Ataköy and Ambarlı WWTP effluents and the Marmara Sea. The effluent solutions from UF and MBR presented better power densities compared to advanced biological treatment effluents, with the 7 days average power densities of UF effluent solutions of 0.49 $W.m^{-2}$ being the maximum power density, Figure 4.8B. By operating the process for 7 days, they were a sharp decrease in the power densities in the first 3 days and it stabilized to an insignificant decrease for the remaining days with all feed solutions.

As reported in the previous sections, multivalent ions, NOMs and membrane fouling might affect the RED process performance by reducing the membrane permselectivity and increasing its resistance [117]. Many researchers reported up to 50% decrease in the power density within the first hour of the RED operation with natural feed streams [144], [148], [149]. However, All the wastewaters used in this study and the Marmara Sea presented a high quality, minimizing membrane fouling and scaling, and resulting in a low decrease in the power densities, less than 10% in the first 2 days which is the highest slope of power density loss, Figure 5.8A. As reported by Goa et al., increasing the membrane selectivity and anti-organic fouling potential would maximize the energy output and the membrane life when natural feed solutions are used. But, above all, feed solution with fewer pollutants is important, since membrane fouling is not the only issue, but the low inter-membrane space provided by the spacers for the circulation of the feed solutions can be clogged with untreated feed solutions and can lead to a pressure drop and a dramatical decrease of the flow rate. Vanoppen et al. (2019) investigated different pretreated municipal wastewaters in an RED unit and pointed out the influence of the treatment technique and effluent water quality on the RED performance. [153]. Nam et al. (2018) resulted in a power density of 0.38 m^2/W [156], lower than the power density achieved in the present study, even though they operated the RED stack with much high salinity gradients. The high effluent quality from Ataköy and Ambarlı WWTP together with the clean Marmara Sea surrounding the treatment plant cut off the need for a pretreatment process when these solutions are fed to an RED stack. The present study may have presented a better result compared to former studies using similar feed solutions, however, the obtained power densities are still below optimal values for the process to be viable and accepted in the energy market, due to the use of a stack with a very low number of cell-pairs and membranes which are less suitable for RED (low permselectivity, high resistance, and thickness). Besides, the HC was filled with the Marmara Sea with a conductivity of 33.2 mS/cm. Increasing the HC salinity would increase the driving force and contribute to optimizing the power density [106], but this option is not possible for Ataköy and Ambarlı WWTP since they are located at the vicinity of the Marmara Sea,

but can be considered for other treatment plants located nearby high saline solution such as the Mediterranean Sea.

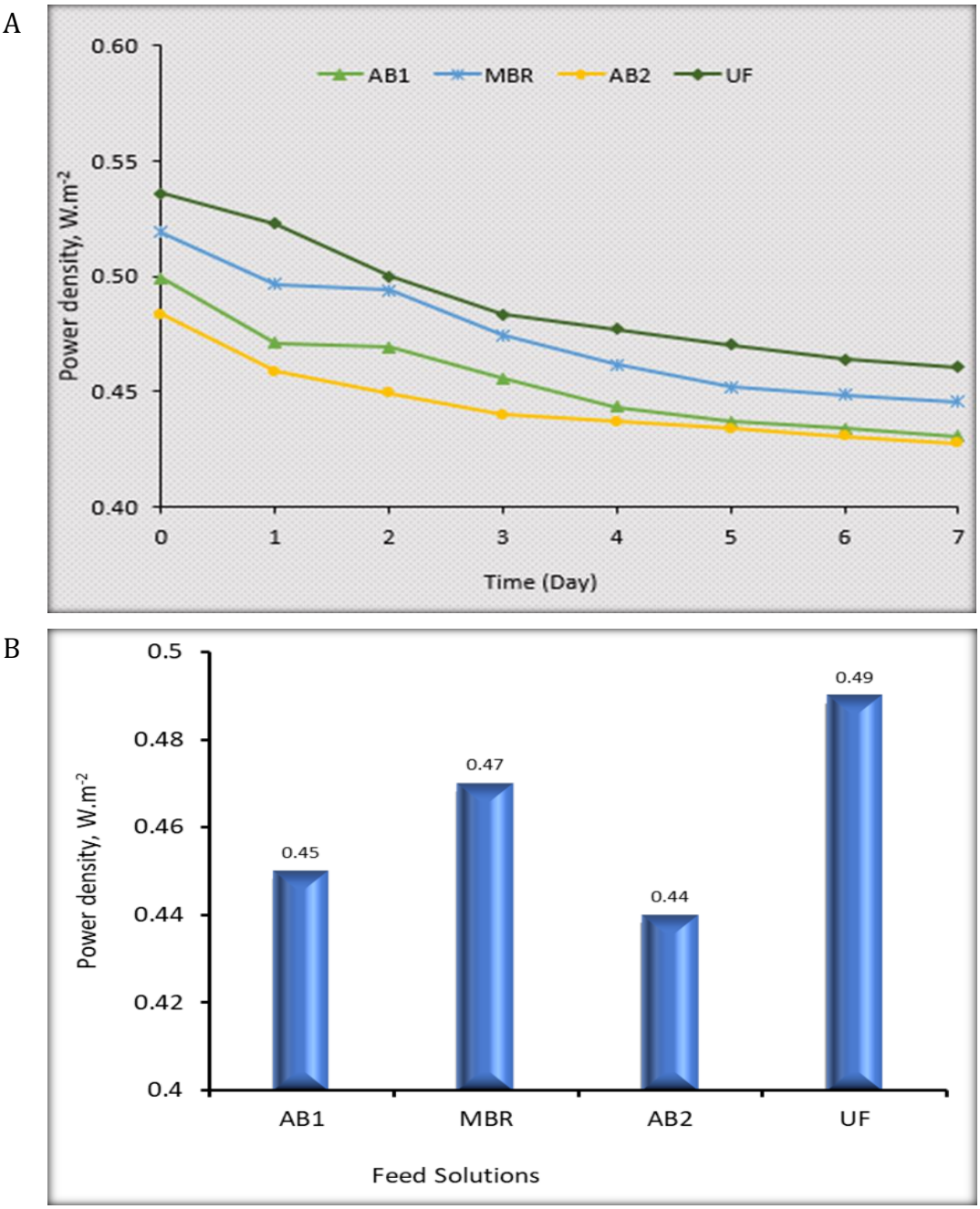

Figure 4.16 Power density values of the RED process with Ataköy and Ambarlı WWTP effluents and the Marmara Sea: A) PD over time, B) Average PD for 7 days

4.3.9 Energy Generated by RED with Ataköy and Ambarlı Wastewater Discharged in the Marmara Sea

Ataköy WWTP discharges a daily average of 411,250 m^3 treated wastewater at the Marmara Sea; 381,250 $m^3.day^{-1}$ from the advanced biological treatment (AB1) and 30,000 $m^3.day^{-1}$ from the MBR process (MBR). A 7 days average power density of 0.45 $W.m^{-2}$ and 0.47 $W.m^{-2}$, was achieved with the RED process when AB1 and MBR are discharged respectively in the Marmara Sea. The effluent from MBR is relatively clean compared to AB1. The presence of trace organic matters in AB1 participated in slightly reducing the achieved power density by affecting the ion transport efficiency and by deposing on the membrane surface (Figure 4.12) causing some fouling [117], [153]. However, not a big difference is observed, showing that the AB1 solution can effectively be used in the RED process and result in high power density when operating at optimal conditions. Discharging all these treated wastewaters into the Marmara Sea through the RED process resulted in total energy production of 18,566.25 $kWh.day^{-1}$, subdivided as 17,156.25 $kWh.day^{-1}$ with the effluent from AB1 and 1410 $kWh.day^{-1}$ with effluent from MBR, as presented by Table 4.6. In Table 4.7 similar results were observed with Ambarlı WWTP. In this case, the power density was 0.44 $W.m^{-2}$ and 0.49 $W.m^{-2}$ with advanced biological treatment effluent (AB2) and UF effluent (UF) respectively. As observed with the MBR process in Ataköy treatment plant effluent, UF effluent presented the highest power density due to the high effluent quality resulted from the treatment performance which mainly removed particulate organic and inorganic matters during the filtration process. Discharging the treated wastewaters effluent from Ambarlı WWTP into the Marmara Sea through the RED process resulted in total energy production of 16,045 $kWh.day^{-1}$, subdivided as 14,820 $kWh.day^{-1}$ with the effluent from AB2 and 1,225 $kWh.day^{-1}$ with effluent from UF. The effluent from UF treatment achieved the highest power density between the four diluted solutions studied, but with the total amount of water from UF being very low, the daily energy generation is limited. It is obvious that the wastewater treatment method affects the RED performance due to the treated wastewater quality [153] but advanced biological treatment, being the

less effective treatment in the present study, still resulted in good power densities when compared to advanced treatment such as MBR and UF.

Table 4.6 Power and energy generation, and estimated membrane area by an RED process fed with Ataköy WWTP effluent mixed with the Marmara Sea

Parameters	Flow ($m^3.day^{-1}$)	Power (kW)	Energy/day (kWh)	Energy/day (kWh)	Membrane Area (m^2)
AB1	381,250	714.844	17,156.25	6,262,031.25	1,588,542
MBR	30,000	58,750	1410	514,650	125,000
Total	411,250	773.6	18,566.25	6,776,681.25	1,713,542

Table 4.7 Power and energy generation, and estimated area by an RED process fed with Ambarlı WWTP effluent mixed with the Marmara Sea

Parameters	Flow ($m^3.day^{-1}$)	Power (kW)	Energy/day (kWh)	Energy/year (kWh)	Membrane Area (m^2)
AB2	311820	617.5	14,820	5,409,300	1,299,250
UF	25000	51.04	1,225	447,125	104,167
Total	336820	668.54	16,045	5,856,425	1,403,417

4.3.10 Optimized RED and Energy Return On Investment (EROI)

The achieved power density in the present study was relatively low, with 0.49 $W.m^{-2}$ as the maximum power density achieved by UF effluent and the Marmara Sea. The reason for low power output is mainly due to the low cell-pairs used, low HC salinity, module, and spacer geometry as well as the properties of the membrane [106], rather than the feed solution characteristics. To confirm this assumption, the same module with similar conditions was operated using a synthetic concentrated and diluted solution containing only NaCl with salinity like the Marmara Sea and UF effluent solution, respectively. The average power density for 7 days operation was

0.54 $W.m^{-2}$ which is close to the one generated by real wastewater and the Marmara Sea. This is proof that the low power density generated with the Marmara Sea and the treated wastewater effluents was not due to the feed solutions, but the aforementioned parameters and it is worth mentioning that the low salinity of the Marmara Sea contributed as well to yielding low energy output. By optimizing these parameters, literature supported a power density over 2.5 $W.m^{-2}$ [106], [166], [185], achievable. This is not to account for the RED process optimization predicted as the result of highly selective and effective membranes and spacer-less or suitable spacer, predicted to boost the energy output of the RED process in the future. Many options to improve power density are currently being investigated, including membrane profiling conductive spacers and alternative modes of operation.

To estimate the EROI, the energy consumed by the pump to ensure the transport of the feed solutions has been determined. Considering a stack with 2000 CEMs and 2000 AEMs, a total of 429 stacks and 351 stacks are required to operate the effluent from Ataköy WWTP and Ambarlı WWTP, respectively. The energy consumption in the RED process is entirely based on the pumping of the feed solutions. Energy use for pumping is estimated to reach 25% of the total energy generated by the RED system [130], and it affects both the net energy recovery and the operational costs of the process. By using Equations 2.3 and 2.4, the energy consumption for pumping the feed solutions through the projected RED plant is 10,584 $kWh.day^{-1}$ and 8,668.4 $kWh.day^{-1}$ for Ataköy and Ambarlı WWTP, respectively as depicted by Table 4.8. With the current energy output, the pump seems to consume more than 50% of the total energy generated by each plant. The energy required to pump the HC and LC solutions through the RED stack is affected by the flow rates, which also affects the electrical performance of the RED process. Operating the RED stacks with optimal flow rates is, therefore, crucial [186]. To improve the net power output, it is necessary to use pumps that are versatile and allow maximum energy savings. This keeps energy costs down and considerably reduces the pumping station‘s life cycle costs. More important, feed solutions should be fed to the stack at an optimum flow rate as supported by Zhu et al., (2015) with 10 cell-pairs of a total 0.13 m^2 as membrane-active area, they demonstrated that 10 mL/min and 20 mL/min was the

optimal flow rate for HC and LC, respectively to optimize the RED energy generation and simultaneously reduce the pumping cost [186]. Weiner et al. (2015) investigated optimum RED conditions and reported that an optimal stack design that minimizes the Levelized cost of energy (LCOE) consists of low load resistance and feed flow rate as well as a larger residence time [187]. The residence time is proportional to the flow rate which is proportional to the pumping cost. The present study, after testing different flow rates, optimized the energy pumping cost by operating the process with 14 mL/min for the HC and 20 mL/min for the low LC, found to be the optimal pumping flow rate. As shown in Table 4.9, the pumping energy being constant, optimizing the RED process and considering an average power density of 2.5 $W.m^{-2}$ based on current optimized RED research in the literature [106], [166], [185], 39,911.25 $kWh.day^{1}$ and 36,883 $kWh.day^{1}$ net energy can be generated from the Ataköy and Ambarlı WWTP, respectively.

Table 4.8 Gross energy, pumping energy and net energy of the RED process fed with Ataköy and Ambarlı WWTP effluents mixed with the Marmara Sea

Diluted Feed Solution	Generated Gross Energy/day (kWh)	Pumping Energy/day (kWh)	Generated Net Energy/day (kWh)	Membrane Area (m^2)
Ataköy	18,566.25	10,584	7,982.25	1,713,542
Ambarlı	16,045	8,668.4	7,376.6	1,403,417

Table 4.9 Optimized net energy of the RED process fed with Ataköy and Ambarlı WWTP effluent mixed with the Marmara Sea

Diluted Feed Solution	Generated Net Energy/day (kWh)	Optimized RED Net Energy/day (kWh)	Membrane Area (m^2)
Ataköy	7,982.25	39,911.25	1,713,542
Ambarlı	7,376.6	36,883	1,403,417

4.3.11 Reclamation of the Wastewaters after the RED Process

The treated wastewater effluents from UF and MBR units are used in the watering of the gardens surrounding the treatment plant. A slight increase of the wastewater salinity took place during the RED process resulting in a conductivity close to 2000 µS/cm. This is a moderate salinity and can be tolerated when used in agriculture. Besides, the solution presented a very low COD as a result of the MRB and UF processes which effectively removed the dissolved matters and most pollutants from the solution. As reported by Gómez-Coma et al., (2020) effluent quality and energy consumption are the key parameters restraining wastewater reclamation [188]. RED coupled with WWTPs can significantly reduce the need for fossil fuel consumption in the plant and can contribute to a more sustainable and environmental-friendly process that generates energy for self-operation. The reclaimed water showed a high quality and can still be used after the RED process.

4.3.12 Energy coverage with RED at Ataköy and Ambarlı WWTP

Ataköy and Ambarlı WWTP consume a total of 159,084 $kWh.day^{-1}$ and 148,513 $kWh.day^{-1}$ energy respectively [172], and using the treated wastewater in an RED unit can generate 7,982.25 $kWh.day^{-1}$ and 7,376.6 $kWh.day^{-1}$ net energy, respectively. This represents 5.02% of the daily energy consumed in Ataköy WWTP and 5 % for Ambarlı WWTP for the different wastewater treatment and plant maintenance. The results of the RED energy coverage of both plants are presented in Table 4.10. However, these results were achieved with a low power density around 0.5 $W.m^{-2}$, due to membrane properties, RED module and spacer geometry which contributed to a high resistance and a low power density rather than the process feed solutions properties. At present state of art, the average power density is estimated to be around 2.5 $W.m^{-2}$, and considering this as a simulated value, the optimized energy output for Ataköy and Ambarlı WWTP is estimated to be around 39,911.25 $kWh.day^{-1}$ and 36,883 $kWh.day^{-1}$, respectively. With such power output, the energy generated by RED will cover 25.1% and 25% of the Ataköy and Ambarlı WWTP energy needs, respectively, as shown in Table 4.11. With the expectations of better and specific membranes to RED in the future and high improvement of the

RED-SGP harvesting, this percentage will certainly rise and may lead to the concept of zero energy wastewater treatment plant.

Table 4.10 The rate of energy coverage in Ataköy and Ambarlı WWTP by RED process

Diluted Feed Solutions	Daily Energy consumption (kWh)	RED Daily Net Energy production (kWh)	Percentage Energy coverage (%)
Ataköy	159,084	7,982.25	5.02
Ambarlı	148,513	7,376.6	5

Table 4.11 The rate of energy coverage at the optimal condition in Ataköy and Ambarlı WWTP by RED process

Parameters	Daily Energy consumption (kWh)	Optimized Daily RED Net Energy production (kWh)	Percentage Energy coverage (%)
Ataköy	159,084	39,911.25	25.1
Ambarlı	148,513	36,883	25

4.3.13 Results' Evaluation

Electrical energy harvesting by RED is new under developing process with a lot of challenges to overcome to be accepted in the energy market. IEMs characteristics, membrane costs, suitable spacers, and electrodes are the parameters of interest to make the process economically acceptable. From the sensitivity analysis, Daniilidis et al. (2014) reported that membrane-related parameters (pricing and performance) and inflation are the most important factors in the implementation of RED on a real and large scale [166]. The IEC, selectivity and membrane resistance are the most sensible RED-IEM parameters which should be high for the first two, and low for the last one. The fabrication process and coating or modifications of IEMs should be the focus of new researches to adapt the membranes to the required

RED system to be commercially applicable and economically cost-effective through the vulgarization of the RED process. Many attempts to produce properly designed RED membranes are still under investigation with major signs of progress in the improvement of membrane selectivity and resistance. Divalent ions in the sea and river water, ideal candidates for real RED implementation, remain one of the major constraints of RED performance due to both induced uphill transport and increased membrane resistance. To mitigate those divalent ion effects, novel and tailor-made membranes are being investigated [167]. To improve the electrochemical properties of the IEMs among which high permselectivity and low resistance, many attempts have been made such as organic-inorganic nanocomposite membranes from polyphenylene oxide (PPO) [168], halogenated polyethers, such as polyepichlorohydrin (PECH) [169], sulfonated polyethersulfone (sPES) cation CEM [61]. These attempts aimed to improve the power density and the LCOE of RED. Membrane modification to improve its properties and reduce its vulnerability to fouling has been performed with success, as an example study of Güler et al. (2014) who successfully coated a standard commercial AEM and improved the membrane antifouling properties and monovalent-ion selectivity [152]. Another perspective is to produce a membrane with a relatively thin thickness, to reduce membrane resistance, and spacer-less membrane carrying straight-ridges named profiled membrane and fabricated to eliminate the use of non-conductive spacers in RED stack [119], [120]. The preparation of ultrathin (approximately 500 nm thickness) and ion-selective Janus membranes will allow a low fluidic resistance and rapid mass transport which will improve the conversion of the SGP [170], and the need for understanding nanofluidics and nanoconfinement, therefore ionic transport in confined nano-environment will open a new way in membrane design and application in SGP production [171].

The current state of technology results in high LCOE in RED compared to other currently available energy technologies, but the projection with the improvement of the power density (2.7 W/m^2) and membrane price (less than EUR $4/m^2$) in near future, can make RED competitive in term of electricity production compared to conventional and established renewable technologies, with a projected lower LCOE

index of 0.16 EUR /kW h [166]. A low cost and easy to produce tailor-made IEMs suitable for RED with low resistance, high permselectivity, high IEC, resistant to fouling, chemically and mechanically stable will win the race to a low-LCOE RED process that can be competitive in the energy market. Hybrid RED processes which include the combination of desalination processes such as RO and MD as high saline sources, and wastewaters for both concentrated and diluted solution sources are new prospects for a tendency to zero waste management systems with energy extractions and resources recovery.

The costs of IEMs are still high today. These costs are expected to decrease with the increase of IEMs use and the vulgarization of the RED process. On another hand, there is likely a decrease in the intensity of the power with the increasing number of membranes in the RED stack. The energy values depicted in Tables 4.10 and Table 4.11 were calculated taking into account the results obtained in the laboratory experiments. It is recommended to carry out a pilot-scale study on the change of power density with increasing cell-pairs in the RED stack after laboratory work to enlighten and project real energy obtainable from the wastewater treatment plants.

5
RESULTS AND DISCUSSION

Fossil fuel has been for years the main source of energy for humanity, however, due to the negative impacts of fossil fuel-based energy on our environment and the limited amount of this energy source makes it no sustainable and no reliable for the future. The need for new sustainable energy with high potentiality becomes a necessity to keep the economy of the world flourishing and improve humanity's comfort. Renewable energy has been considered with success as alternative energy to fossil. At present, solar and wind energy are leaders in the renewable energy market, but SGP presents a huge potential that can contribute to the energy market. RED has been presented as an effective technique to harvest the SGP normally wasted in nature when two water bodies with different salinity meet. The performance of the RED process can be affected by many parameters among which the membrane cost and properties, the geometry and structure of the spacer, the feed solution ions content and concentration, the system resistance and the characteristics of the electrode are the main parameters to be considered and monitored. The present study monitored and proposed some optimal RED conditions and investigated different synthetic, real and alternative feed solutions for power generation with RED process.

Power generation by RED processes could be a life-changing technology soon by converting the SGP into useful energy. By monitoring the flow rate and the feed solution salinity, it was found that at low feed solution concentration, the optimal flow rate of 30 to 45 mL/min equivalent to 0.0216 to 0.0325 $m^3.m^{-2}.h^{-1}$ is required to operate the RED system efficiently. The results also showed that the LC solution NaCl concentration is more sensible and can be optimal for the process between 4 and 6 mM, while HC is optimal at concentrations over around 600 and 684 mM. The results suggest that one should operate the RED system by using an LC solution with low salinity instead of just using a high saline HC solution without taking into consideration the real impact of the LC solution. This illustrates the importance of

the choice of the area for the installation of an RED plant. The ideal estuary will be the one with the concentrated solution of NaCl concentration above 0.6 M like the Mediterranean Sea and a diluted solution between 4 and 6 mM. The Mediterranean Sea and the Aegean Sea in Turkey were found suitable for RED along with Ceyhan, Göksu, and Seyhan rivers. 1/3 of the minimum flow rate from the Ceyhan river is estimated to generate over 17.18×10^6 kW electrical energy per year by RED when it runs into the Mediterranean Sea.

The study also demonstrated that the increase in the number of cell-pair of the RED stack is beneficial since it causes an increase in the voltage and the intensity resulting in a higher power density. However, the voltage in the present study increased but deviated from the linear trend and declined with the increasing number of cell-pair. This resistance was mostly due to the spacers and the IEMs. Different spacers used proved that the spacer structure, geometry, and opening affects the stack resistance by inducing the spacer shadow effect. SEM, SEM-EDX, and FTIR analyses proved that the ERS is harmful to the end IEMs, and operating an RED unit with a high number of cell-pair will reduce the need for end membranes.

RED can also be operated with alternative feed solutions such as treated municipal wastewaters. The RED stack was operated with treated municipal wastewaters collected from Ambarlı and Ataköy wastewater treatment plant in Istanbul, and the results suggest that municipal wastewater treated by ABT, UF, and MBR can be used effectively as a diluted solution in an RED process. An average power density around 0.48 $W.m^{-2}$ and 0.52 $W.m^{-2}$ was achieved for the lowest (ABT) and the highest (UF) wastewater quality, respectively, for 24 hours days RED operation. The results were almost similar to synthetic solutions which achieved 0.57 $W.m^{-2}$. Although municipal wastewaters are ideal candidates as diluted solutions for RED operation, the quality of the water and the treatment process are important and affect the power output. It is worth mentioning that, although membrane fouling was not a dominant factor in the RED stack, the presence of NOM and divalent ions in the seawater and treated municipal wastewaters may have slightly reduced the power density over time due to the uphill transport of ions such as Ca^{2+} and Mg^{2+} which increased the membrane resistance.

Projecting an RED plant using the Ataköy and Ambarlı WWTP effluents as feed solutions showed that about 5% of the energy need can be covered by RED and considering state of art RED conditions, over 25% of the energy demand can be covered by the RED process.

The study revealed the resistance effect of increasing cell-pairs number and concentrated-diluted feed solutions concentration rate influence on RED performance. It showed that the concentration of NaCl in the diluted solution has a high impact on the RED process as well as the salinity gradient. Salinity gradient is not the only salinity factor; operating RED with a low diluted solution and high concentrated solution salinities should first take into account the minimum NaCl concentration of the diluted solution which was 4 mM in the present study, below this value the RED performance is reduced. The RED-SGP Potential of Ataköy and Ambarlı Municipal wastewaters with the Marmara Sea revealed that the treatment processes of municipal wastewaters together with effluents quality are important to optimize the energy output.

To accelerate the commercial applicability of RED, novel and tailor-made membranes may be investigated to improve the membrane properties and eliminate the NOM and divalent effects in natural feed solutions. A study considering the best IEMs available and optimal operating conditions in a pilot-scale RED stack with a high number of pair cells is required to improve our understanding of how RED can contribute to reducing energy demand in the WWTPs such as Ataköy and Ambarlı which discharge high quality treated effluents into the sea. Also, using the brines from a nearby desalination plant as a concentrated solution would tremendously increase the power output.

The behavior of the RED performance with increasing temperature should be investigated to consider hot wastewaters from industries and membrane distillation concentrates from desalination plants. This will also enlarge our comprehension of seasonal temperature variations and tropical countries' high-temperature water bodies' behavior on RED performance.

The influence of the RED process and the ion exchange membranes at the presence of organic compounds (humic compounds for instance) and the thresholds concentrations of divalent ions which hinder the RED process performance should be investigated to project the influence of different wastewaters and real solutions used in RED process. Hybrid RED with existing desalination processes can be an alternative to cheap symbiotic clean water production and clean RED-SGE generation.

Pilot-scale RED studies taking into consideration the feed flow rate, the impact of the increasing cell-pair, monitoring of the concentrated and diluted solutions ratio, should be investigated to understand the behavior of the RED system at a larger scale.

REFERENCES

[1] Our World in Data, "Energy Production & Changing Energy Sources," 2018. [Online]. Available: https://ourworldindata.org/energy-production-and-changing-energy-sources. [Accessed: 04-Nov-2019].

[2] V. Smil, "Energy Transitions: Global and National Perspectives (Expanded and updated edition)," vol. 30, no. 4, p. 297, 2017.

[3] BP, "BP Statistical Review of World Energy 2019," 2019.

[4] "Energy - Our World in Data." [Online]. Available: https://ourworldindata.org/energy. [Accessed: 15-May-2020].

[5] C. Suresh and R. P. Saini, "Review on solar thermal energy storage technologies and their geometrical configurations," *Int. J. Energy Res.*, no. December 2019, pp. 1–33, 2020.

[6] EPA, "Sources of Greenhouse Gas Emissions."

[7] Eurostat, *The EU in the world 2015*. 2015.

[8] C. Pasten and J. C. Santamarina, "Energy and quality of life," *Energy Policy*, vol. 49, pp. 468–476, 2012.

[9] M. Coleman Gilstrap, "Renewable electricity generation from salinity gradients using reverse electrodialysis," Georgia Institute of Technology, 2013.

[10] S. V. Sylwin Pawlowski, Joao Crespo, "Sustainable Power Generation from Salinity Gradient Energy by Reverse Electrodialysis," no. August 2016, Springer International Publishing Switzerland, 2015, pp. v–vi.

[11] R. S. Norman, "Water salination: A source of energy," *Science (80-.).*, vol. 186, no. 4161, pp. 350–352, 1974.

[12] R.E.Pattle, "Production of electric power by mixing fresh and salt water in the hydroelectric pile," no. 174, p. 660, 1954.

[13] D. A. Vermaas, "Energy Generation From Mixing Salt Water And Fresh Water," 2014.

[14] P. E. Dlugoleci, "Mass Transport In Reverse Electrodialysis For Sustainable Energy Generation," 2009.

[15] J. Veerman, "Reverse Electrodialysis Design And Optimization By Modeling And Experimentation," University of Groningen, 2010.

[16] J. G. Hong *et al.*, "Potential ion exchange membranes and system performance in reverse electrodialysis for power generation: A review," *J. Memb. Sci.*, vol. 486, no. July, pp. 71–88, 2015.

[17] J. W. Post *et al.*, "Salinity-gradient power: Evaluation of pressure-retarded

osmosis and reverse electrodialysis," *J. Memb. Sci.*, vol. 288, no. 1–2, pp. 218–230, 2007.

[18] K. Nijmeijer and S. Metz, "Chapter 5 Salinity Gradient Energy," *Sustain. Sci. Eng.*, vol. 2, no. C, pp. 95–139, 2010.

[19] Statista, "World energy consumption by energy source 2040 | Statista," 2020. [Online]. Available: https://www.statista.com/statistics/222066/projected-global-energy-consumption-by-source/. [Accessed: 21-Jun-2020].

[20] Statista, "Electricity consumption globally 2017 | Statista," *2020*. [Online]. Available: https://www.statista.com/statistics/280704/world-power-consumption/. [Accessed: 21-Jun-2020].

[21] Herman Daly, "Fossil Fuels," *Appl. Energy*, vol. 47, no. 2–3, pp. 101–121, 1994.

[22] J. Wilcox, "Grand challenges in advanced fossil fuel technologies," *Front. Energy Res.*, vol. 2, no. NOV, pp. 2013–2015, 2014.

[23] IEA, "World energy investment 2016. organisation for economic co-operation and development. France, Paris," 2016. [Online]. Available: https://www.iea.org/newsroom/news/2016/september/world-energy-investment-2016.html. [Accessed: 01-Nov-2019].

[24] IEA, "World energy outlook 2017. International Energy Agency, Paris," 2017. [Online]. Available: https://www.iea.org/weo2017/. [Accessed: 01-Nov-2019].

[25] M. Ö. A. Akan, A. A. Selam, and S. Ü. O. Firat, "Renewable energy sources: Comparison of their use and respective policies on a global scale," in *Handbook of Research on Green Economic Development Initiatives and Strategies*, IGI Global, 2016, pp. 238–269.

[26] G. Vitale, "Renewable energies – Future perspectives," *Renew. Energy Environ. Sustain.*, vol. 17, pp. 1–6, 2016.

[27] H. Mikael and X. Tang, "Depletion of fossil fuels and anthropogenic climate change – a review," *Energy Policy*, vol. 52, no. April 2018, pp. 797–809, 2013.

[28] BP, "BP Statistical Review of World Energy 2018," 2018.

[29] R. H. Oldemberg, J., Johansson, T.B., Reddy, A.K.N., Williams, "Basc Needs and Much moree With One Kilowatt," *R. Swedish Acad. Sci.*, vol. 14, no. 4/5, pp. 190–200, 1985.

[30] E. V. Mohammad Mafizur Rahman, "Renewable and non-renewable energy consumption-economic growth nexus: New evidence from South Asia," *Renew. Energy*, 2019.

[31] Statista, "World energy consumption by energy source 2040 | Statista," 2019. [Online]. Available: https://www.statista.com/statistics/222066/projected-global-energy-consumption-by-source/. [Accessed: 02-Nov-2019].

[32] WEC, "World Energy Issues Monitor 2019," 2019.

[33] O. IPCC, Edenhofer *et al.*, *Climate Change 2014: Mitigation of climate change.*

Contribution of Working Group III to the Fifth Assessment Report of the Intergovernmental Panel on Climate Change. Cambridge University Press, Cambridge, UK, and New York, 2014.

[34] M. Lazarus and H. van Asselt, "Fossil fuel supply and climate policy: exploring the road less taken," *Clim. Change*, vol. 150, no. 1–2, pp. 1–13, 2018.

[35] L. Miller and R. Carriveau, "Energy demand curve variables – An overview of individual and systemic effects," *Sustain. Energy Technol. Assessments*, vol. 35, no. August 2018, pp. 172–179, 2019.

[36] J. Rogelj *et al.*, "Paris Agreement climate proposals need a boost to keep warming well below 2 °c," *Nature*, vol. 534, no. 7609, pp. 631–639, 2016.

[37] J. Lee and J.-S. Yang, "Global energy transitions and political systems," *Renew. Sustain. Energy Rev.*, vol. 115, no. August, p. 109370, 2019.

[38] H. Kunz, N. J. Hagens, and S. B. Balogh, "The influence of output variability from renewable electricity generation on net energy calculations," *Energies*, vol. 7, no. 1, pp. 150–172, 2014.

[39] P. E. Brockway, A. Owen, L. I. Brand-correa, and L. Hardt, "Estimation of global final-stage energy-returnon- investment for fossil fuels with comparison to renewable energy sources," *Nat. Energy*, vol. 4, no. July, 2019.

[40] L. C. King and J. C. J. M. Van Den Bergh, "Implications of net energy-return-on-investment for a low-carbon energy transition," *Nat. Energy*, vol. 3, no. April, pp. 334–340, 2018.

[41] C. A. S. Hall, J. G. Lambert, and S. B. Balogh, "EROI of different fuels and the implications for society," *Energy Policy*, vol. 64, pp. 141–152, 2014.

[42] WEC, "World Energy Resources 2016," 2016.

[43] P. A. Owusu and S. Asumadu-Sarkodie, "A review of renewable energy sources, sustainability issues and climate change mitigation," *Cogent Eng.*, vol. 3, no. 1, pp. 1–14, 2016.

[44] T. Kåberger, "Progress of renewable electricity replacing fossil fuels," *Glob. Energy Interconnect.*, vol. 1, no. 1, pp. 48–52, 2018.

[45] GWEC, "New Low for wind Energy Costs: Morocco tender averages USD 30/MWh," 2016. [Online]. Available: https://gwec.net/new-low-for-wind-energy-costs-morocco-tender-averages-us30mwh/. [Accessed: 04-Nov-2019].

[46] M. Darby, "Two 350MW arrays in the Netherlands will supply power at €87/MWh, beating the next cheapest project by miles," 2016. [Online]. Available: https://www.climatechangenews.com/2016/07/06/dong-passes-offshore-wind-cost-milestone-three-years-early/. [Accessed: 04-Nov-2019].

[47] E. Gosden, "New record for cheapest offshore wind farm," 2016. [Online]. Available: https://www.telegraph.co.uk/business/2016/09/14/new-record-for-cheapest-offshore-wind-farm/. [Accessed: 04-Nov-2019].

[48] Vattenfall, “Vattenfall wins tender to build the largest wind farm in the Nordics,” 2016. [Online]. Available: https://group.vattenfall.com/press-and-media/news--press-releases/pressreleases/2016/vattenfall-wins-tender-to-build-the-largest-wind-farm-in-the-nordics. [Accessed: 04-Nov-2019].

[49] G. Media, “Solar Stuns in Mexico’s First Clean Energy Auction: 1,860MW Won at $50.7 per MWh,” 2016. [Online]. Available: https://www.greentechmedia.com/articles/read/solar-stuns-in-mexicos-first-clean-energy-auction-1860-mw-won-at-50-7-p. [Accessed: 04-Nov-2019].

[50] H. Lindon, “Tremendously Low 4.8¢/kWh Solar Price In Peru, Unsubsidized,” 2016. [Online]. Available: https://cleantechnica.com/2016/02/25/tremendously-low-4-8¢kwh-solar-price-in-peru-unsubsidized/. [Accessed: 04-Nov-2019].

[51] Bloomberg, “New Record Set for World’s Cheapest Solar, Now Undercutting Coal,” 2016. [Online]. Available: https://www.bloomberg.com/news/articles/2016-05-03/solar-developers-undercut-coal-with-another-record-set-in-dubai. [Accessed: 04-Nov-2019].

[52] G. Parkinson, “Chile solar auction sets new record low for solar PV,” 2017. [Online]. Available: https://reneweconomy.com.au/chile-solar-auction-sets-new-record-low-for-solar-pv-85114/. [Accessed: 04-Nov-2019].

[53] B. D. LÓPEZ, “Mexico signs lowest-price solar contracts to date,” 2017. [Online]. Available: https://www.pv-magazine.com/2017/02/06/mexico-signs-lowest-price-solar-contracts-in-the-world-to-date/. [Accessed: 04-Nov-2019].

[54] J. F. Weaver, “UPDATED: Cheapest electricity on the planet is Mexican (actually) wind power at 1.77¢/kWh,” 2017. [Online]. Available: https://electrek.co/2017/11/16/cheapest-electricity-on-the-planet-mexican-solar-power/. [Accessed: 04-Nov-2019].

[55] L. Graves, “World’s cheapest prices submitted for Saudi Arabia’s first solar project,” 2017. [Online]. Available: https://www.thenational.ae/business/energy/world-s-cheapest-prices-submitted-for-saudi-arabia-s-first-solar-project-1.663842. [Accessed: 04-Nov-2019].

[56] G. L. Wick and W. R. Schmitt, “PROSPECTS FOR RENEWABLE ENERGY FROM THE SEA.,” *Mar. Technol. Soc. J.*, vol. 11, no. 5–6, pp. 16–21, 1977.

[57] A. Emdadi, P. Gikas, M. Farazaki, and Y. Emami, “Salinity gradient energy potential at the hyper saline Urmia Lake - ZarrinehRud River system in Iran,” *Renew. Energy*, vol. 86, pp. 154–162, 2016.

[58] Y. Mei and C. Y. Tang, “Recent developments and future perspectives of reverse electrodialysis technology: A review,” *Desalination*, vol. 425, no. September 2017, pp. 156–174, 2018.

[59] M. Turek, B. Bandura, and P. Dydo, “Power production from coal-mine brine

utilizing reversed electrodialysis," *Desalination*, vol. 221, no. 1–3, pp. 462–466, Mar. 2008.

[60] N. Y. Yip, D. Brogioli, H. V. M. Hamelers, and K. Nijmeijer, "Salinity gradients for sustainable energy: Primer, progress, and prospects," *Environ. Sci. Technol.*, vol. 50, no. 22, pp. 12072–12094, 2016.

[61] A. H. Avci *et al.*, "Sulfonated polyethersulfone based cation exchange membranes for Reverse Electrodialysis under high salinity gradients," *J. Memb. Sci.*, 2019.

[62] J. W. Post *et al.*, "Salinity-gradient power: Evaluation of pressure-retarded osmosis and reverse electrodialysis," *J. Memb. Sci.*, vol. 288, no. 1–2, pp. 218–230, 2007.

[63] G. Z. Ramon, B. J. Feinberg, and E. M. V. Hoek, "Membrane-based production of salinity-gradient power," *Energy Environ. Sci.*, vol. 4, no. 11, pp. 4423–4434, 2011.

[64] E. Nagy, J. Dudás, and I. Hegedüs, "Improvement of the energy generation by pressure retarded osmosis," *Energy*, vol. 116, pp. 1323–1333, 2016.

[65] A. Altaee, J. Zhou, A. Alhathal Alanezi, and G. Zaragoza, "Pressure retarded osmosis process for power generation: Feasibility, energy balance and controlling parameters," *Appl. Energy*, vol. 206, no. September, pp. 303–311, 2017.

[66] M. Turek and B. Bandura, "Renewable energy by reverse electrodialysis," *Desalination*, vol. 205, no. 1–3, pp. 67–74, 2007.

[67] C. Tristán, M. Fallanza, R. Ibáñez, and I. Ortiz, "Recovery of salinity gradient energy in desalination plants by reverse electrodialysis," *Desalination*, vol. 496, p. 114699, Dec. 2020.

[68] D. Acuña Mora and A. de Rijck, "Blue Energy : Salinity Gradient Power in Practice," 2015.

[69] B. B. Sales, M. Saakes, J. W. Post, C. J. N. Buisman, P. M. Biesheuvel, and H. V. M. Hamelers, "Direct power production from a water salinity difference in a membrane-modified supercapacitor flow cell," *Environ. Sci. Technol.*, vol. 44, no. 14, pp. 5661–5665, 2010.

[70] A. Evans, V. Strezov, and T. J. Evans, "Assessment of sustainability indicators for renewable energy technologies," *Renew. Sustain. Energy Rev.*, vol. 13, no. 5, pp. 1082–1088, 2009.

[71] D. J. Murphy and C. A. S. Hall, "Year in review-EROI or energy return on (energy) invested," *Ann. N. Y. Acad. Sci.*, vol. 1185, pp. 102–118, 2010.

[72] Z. Jalili, K. W. Krakhella, K. E. Einarsrud, and O. S. Burheim, "Energy generation and storage by salinity gradient power: A model-based assessment," *J. Energy Storage*, vol. 24, p. 100755, Aug. 2019.

[73] F. Giacalone, M. Papapetrou, G. Kosmadakis, A. Tamburini, G. Micale, and A. Cipollina, "Application of reverse electrodialysis to site-specific types of saline

solutions: A techno-economic assessment," *Energy*, vol. 181, pp. 532–547, 2019.

[74] X. Zhu *et al.*, "Unique ion rectification in hypersaline environment: A high-performance and sustainable power generator system," *Sci. Adv.*, vol. 4, no. 10, pp. 1–9, 2018.

[75] J. Gao, X. Liu, Y. Jiang, L. Ding, L. Jiang, and W. Guo, "Understanding the Giant Gap between Single-Pore- and Membrane-Based Nanofluidic Osmotic Power Generators," *Small*, vol. 15, no. 11, p. 1804279, Mar. 2019.

[76] M. Tedesco, C. Scalici, D. Vaccari, A. Cipollina, A. Tamburini, and G. Micale, "Performance of the first reverse electrodialysis pilot plant for power production from saline waters and concentrated brines," *J. Memb. Sci.*, vol. 500, pp. 33–45, 2016.

[77] X. Zhu, W. He, and B. E. Logan, "Influence of solution concentration and salt types on the performance of reverse electrodialysis cells," *J. Memb. Sci.*, vol. 494, no. July, pp. 154–160, 2015.

[78] M. Tedesco, H. V. M. Hamelers, and P. M. Biesheuvel, "Nernst-Planck transport theory for (reverse) electrodialysis: I. Effect of co-ion transport through the membranes," *J. Memb. Sci.*, vol. 510, no. March, pp. 370–381, 2016.

[79] B. E. Logan, M. Elimelech, and U. States, "Membrane-based processes for sustainable power generation using water," *Nature*, vol. 488, pp. 313–319, 2012.

[80] IRENA, "Salinity Gradient Energy Technology," 2014.

[81] Ecofys, "Energie uit zout en zoet water met osmose (Energy from Fresh and Salt Water by Osmosis)," 2007. [Online]. Available: https://docplayer.nl/1192330-Energie-uit-zout-en-zoet-water-met-osmose.html. [Accessed: 10-Nov-2019].

[82] P. Stenzel, "Salinity Gradient Power in Europe: State of the Art Sustainable Energy Week Brussels Institute for Infrastructure, Environment and Innovation," 2011.

[83] E. Guler, "ANION EXCHANGE MEMBRANE DESIGN- Thesis Defens," University of Twente, 2014.

[84] R. K. Nagarale, G. S. Gohil, and V. K. Shahi, "Recent developments on ion-exchange membranes and electro-membrane processes," *Adv. Colloid Interface Sci.*, vol. 119, no. 2–3, pp. 97–130, 2006.

[85] M. Y. Kariduraganavar, R. K. Nagarale, A. A. Kittur, and S. S. Kulkarni, "Ion-exchange membranes: preparative methods for electrodialysis and fuel cell applications," *Desalination*, vol. 197, no. 1–3, pp. 225–246, 2006.

[86] T. Sata, *Ion Exchange Membranes Preparation, Characterization, Modification and Application*. The Royal Society of Chemistry, 2004.

[87] T. Xu, "Ion exchange membranes: State of their development and perspective," *J. Memb. Sci.*, vol. 263, no. 1–2, pp. 1–29, 2005.

[88] Y. Tanaka, "Preparation of Ion Exchange Membranes," *Ion Exch. Membr.*, pp. 3–28, 2015.

[89] J. Ran *et al.*, "Ion exchange membranes: New developments and applications," *J. Memb. Sci.*, vol. 522, pp. 267–291, 2017.

[90] T. Sata, "PREPARATION AND CHARACTERIZATION OF ION- EXCHANGE MEMBRANES," in *Encyclopedia of Desalination and Water Resources*, .

[91] B. Tong *et al.*, "Development of heterogeneous cation exchange membranes using functional polymer powders for desalination applications," *J. Taiwan Inst. Chem. Eng.*, vol. 67, pp. 435–442, 2016.

[92] C. Klaysom, S. H. Moon, B. P. Ladewig, G. Q. M. Lu, and L. Wang, "Preparation of porous ion-exchange membranes (IEMs) and their characterizations," *J. Memb. Sci.*, vol. 371, no. 1–2, pp. 37–44, 2011.

[93] J. Balster, O. Krupenko, I. Pünt, D. F. Stamatialis, and M. Wessling, "Preparation and characterisation of monovalent ion selective cation exchange membranes based on sulphonated poly(ether ether ketone)," *J. Memb. Sci.*, vol. 263, no. 1–2, pp. 137–145, 2005.

[94] M. I. Khan *et al.*, "Development of BPPO-based anion exchange membranes for electrodialysis desalination applications," *Desalination*, vol. 391, pp. 61–68, 2016.

[95] W. Garcia-Vasquez, L. Dammak, C. Larchet, V. Nikonenko, N. Pismenskaya, and D. Grande, "Evolution of anion-exchange membrane properties in a full scale electrodialysis stack," *J. Memb. Sci.*, vol. 446, pp. 255–265, 2013.

[96] Y. Liu, Q. Pan, Y. Wang, C. Zheng, L. Wu, and T. Xu, "In-situ crosslinking of anion exchange membrane bearing unsaturated moieties for electrodialysis," *Sep. Purif. Technol.*, vol. 156, pp. 226–233, 2015.

[97] M. I. Khan *et al.*, "Preparation of anion exchange membranes from BPPO and dimethylethanolamine for electrodialysis," *Desalination*, vol. 402, pp. 10–18, 2017.

[98] J. Maiti, N. Kakati, and P. Basumatary, "Imidazolium functionalized poly (vinyl chloride-co- vinyl acetate) -based anion exchange membrane," *Int. J. Hydrogen Energy*, vol. 1, pp. 2–8, 2016.

[99] J. Yang, C. Liu, Y. Hao, X. He, and R. He, "Preparation and investigation of various imidazolium-functionalized poly(2,6-dimethyl-1,4-phenylene oxide) anion exchange membranes," *Electrochim. Acta*, vol. 207, pp. 112–119, 2016.

[100] B. Lin *et al.*, "Preparation and characterization of imidazolium-based membranes for anion exchange membrane fuel cell applications," *Int. J. Hydrogen Energy*, vol. 42, no. 10, pp. 6988–6996, 2017.

[101] Y. Zhao *et al.*, "An anion exchange membrane modified by alternate electro-deposition layers with enhanced monovalent selectivity," *J. Memb. Sci.*, vol. 520, pp. 262–271, 2016.

[102] X. Tong, B. Zhang, and Y. Chen, "Fouling resistant nanocomposite cation

exchange membrane with enhanced power generation for reverse electrodialysis," *J. Memb. Sci.*, vol. 516, pp. 162–171, 2016.

[103] A. Daniilidis, D. A. Vermaas, R. Herber, and K. Nijmeijer, "Experimentally obtainable energy from mixing river water, seawater or brines with reverse electrodialysis," *Renew. Energy*, vol. 64, pp. 123–131, 2014.

[104] M. Tedesco *et al.*, *Reverse electrodialysis with saline waters and concentrated brines: A laboratory investigation towards technology scale-up*, vol. 492, no. May. 2015.

[105] E. Güler and K. Nijmeijer, "Reverse electrodialysis for salinity gradient power generation: Challenges and future perspectives," *J. Membr. Sci. Res.*, vol. 4, no. 3, pp. 108–110, 2018.

[106] M. Ciofalo, M. La Cerva, M. Di Liberto, L. Gurreri, A. Cipollina, and G. Micale, "Optimization of net power density in Reverse Electrodialysis," *Energy*, vol. 181, pp. 576–588, 2019.

[107] J. G. Hong and J. J. Kim, "Salinity Gradient Energy : Current Membrane Development and Challenges for Reverse Electrodialysis System," *New Renew. Energy*, vol. 12, no. 4, p. 53, 2016.

[108] R. A. Tufa, E. Curcio, E. Fontananova, and G. Di Profio, *3.8 Membrane-Based Processes for Sustainable Power Generation Using Water: Pressure-Retarded Osmosis (PRO), Reverse Electrodialysis (RED), and Capacitive Mixing (CAPMIX)*, vol. 3. 2017.

[109] G. M. Geise, M. A. Hickner, and B. E. Logan, "Ionic resistance and permselectivity tradeoffs in anion exchange membranes," *ACS Appl. Mater. Interfaces*, vol. 5, no. 20, pp. 10294–10301, 2013.

[110] L. Villafaña-López, D. M. Reyes-Valadez, O. A. González-Vargas, V. A. Suárez-Toriello, and J. S. Jaime-Ferrer, "Custom-made ion exchange membranes at laboratory scale for reverse electrodialysis," *Membranes (Basel).*, vol. 9, no. 11, pp. 1–19, 2019.

[111] P. Długołecki, K. Nymeijer, S. Metz, and M. Wessling, "Current status of ion exchange membranes for power generation from salinity gradients," *J. Memb. Sci.*, vol. 319, no. 1–2, pp. 214–222, 2008.

[112] A. Zlotorowicz, R. V Strand, O. S. Burheim, and S. Kjelstrup, "The Permselectivity and Water Transference Number of Ion Exchange Membranes in Reverse Electrodialysis," *J. Memb. Sci.*, 2016.

[113] J. Veerman, R. M. de Jong, M. Saakes, S. J. Metz, and G. J. Harmsen, "Reverse electrodialysis: Comparison of six commercial membrane pairs on the thermodynamic efficiency and power density," *J. Memb. Sci.*, vol. 343, no. 1–2, pp. 7–15, 2009.

[114] E. Avci, A.H., Sarkar, P., Tufa, R.A., Messana, D., Argurio, P., Fontananova, E., Profio, D-D., Curcio *et al.*, "Effect of Mg2+ions on energy generation by Reverse Electrodialysis," *J. Memb. Sci.*, vol. 520, no. August, pp. 499–506, 2016.

[115] J. G. Hong and T. W. Park, "Electrochemical characterizations and reverse electrodialysis performance of hybrid anion exchange membranes for salinity gradient energy," *J. Electroanal. Chem.*, vol. 817, no. March, pp. 134–140, 2018.

[116] T. Rijnaarts, J. Moreno, M. Saakes, W. M. de Vos, and K. Nijmeijer, "Role of anion exchange membrane fouling in reverse electrodialysis using natural feed waters," *Colloids Surfaces A Physicochem. Eng. Asp.*, vol. 560, no. October 2018, pp. 198–204, 2019.

[117] H. Gao, B. Zhang, X. Tong, and Y. Chen, "Monovalent-anion selective and antifouling polyelectrolytes multilayer anion exchange membrane for reverse electrodialysis," *J. Memb. Sci.*, vol. 567, no. February, pp. 68–75, 2018.

[118] S. Mehdizadeh, M. Yasukawa, T. Abo, Y. Kakihana, and M. Higa, "Effect of spacer geometry on membrane and solution compartment resistances in reverse electrodialysis," *J. Memb. Sci.*, pp. 271–280, 2019.

[119] E. Güler, R. Elizen, M. Saakes, and K. Nijmeijer, "Micro-structured membranes for electricity generation by reverse electrodialysis," *J. Memb. Sci.*, vol. 458, pp. 136–148, 2014.

[120] D. A. Vermaas, M. Saakes, and K. Nijmeijer, "Power generation using profiled membranes in reverse electrodialysis," *J. Memb. Sci.*, vol. 385–386, no. 1, pp. 234–242, 2011.

[121] J. Veerman, M. Saakes, S. J. Metz, and G. J. Harmsen, "Reverse electrodialysis: Evaluation of suitable electrode systems," *J. Appl. Electrochem.*, vol. 40, no. 8, pp. 1461–1474, 2010.

[122] J. N. Weinstein and F. B. Leitz, "Electric power from differences in salinity: The dialytic battery," *Science (80-.).*, vol. 191, no. 4227, pp. 557–559, 1976.

[123] J. Jagur-Grodzinskr and R. Kramer, "Novel Process for Direct Conversion of Free Energy of Mixing into Electric Power," *Ind. Eng. Chem. Process Des. Dev.*, vol. 25, no. 2, pp. 443–449, 1986.

[124] O. Scialdone and A. G. C. Guarisco, S. Grispo, A. D' Angelo, "Investigation of electrode material – Redox couple systems for reverse electrodialysis processes. Part I: Iron redox couples," *J. Electroanal. Chem.*, vol. 681, pp. 66–75, 2012.

[125] O. S. Burheim, F. Seland, J. G. Pharoah, and S. Kjelstrup, "Improved electrode systems for reverse electro-dialysis and electro-dialysis," *Desalination*, vol. 285, pp. 147–152, 2012.

[126] C. Simões, D. Pintossi, M. Saakes, Z. Borneman, W. Brilman, and K. Nijmeijer, "Electrode segmentation in reverse electrodialysis: Improved power and energy efficiency," *Desalination*, vol. 492, p. 114604, Oct. 2020.

[127] S. Mehdizadeh, M. Yasukawa, T. Abo, M. Kuno, Y. Noguchi, and M. Higa, "The Effect of Feed Solution Temperature on the Power Output Performance of a Pilot-Scale Reverse Electrodialysis (RED) System with Different Intermediate Distance," *Membranes (Basel).*, vol. 9, no. 6, p. 73, 2019.

[128] S. Pawlowski, J. G. Crespo, and S. Velizarov, "Pressure drop in reverse electrodialysis: Experimental and modeling studies for stacks with variable number of cell pairs," *J. Memb. Sci.*, vol. 462, pp. 96–111, 2014.

[129] H. Kang, E. Kim, and S. P. Jung, "Influence of flowrates to a reverse electrodialysis (RED) stack on performance and electrochemistry of a microbial reverse electrodialysis cell (MRC)," *Int. J. Hydrogen Energy*, vol. 42, no. 45, pp. 27685–27692, 2017.

[130] J. Veerman, M. Saakes, S. J. Metz, and G. J. Harmsen, "Reverse electrodialysis: Performance of a stack with 50 cells on the mixing of sea and river water," *J. Memb. Sci.*, vol. 327, no. 1–2, pp. 136–144, 2009.

[131] R. A. Tufa *et al.*, "Potential of brackish water and brine for energy generation by salinity gradient power-reverse electrodialysis (SGP-RE)," *RSC Adv.*, vol. 4, no. 80, pp. 42617–42623, 2014.

[132] P. Długołecki, P. Ogonowski, S. J. Metz, M. Saakes, K. Nijmeijer, and M. Wessling, "On the resistances of membrane, diffusion boundary layer and double layer in ion exchange membrane transport," *J. Memb. Sci.*, vol. 349, no. 1–2, pp. 369–379, 2010.

[133] H. Susanto, M. Fitrianingtyas, A. M. Samsudin, and A. Syakur, "Experimental study of the natural organic matters effect on the power generation of reverse electrodialysis," *Int. J. Energy Res.*, vol. 41, no. 10, pp. 1474–1486, Aug. 2017.

[134] D. A. Vermaas, J. Veerman, M. Saakes, and K. Nijmeijer, "Influence of multivalent ions on renewable energy generation in reverse electrodialysis," *Energy Environ. Sci.*, vol. 7, no. 4, pp. 1434–1445, 2014.

[135] J. W. Post, H. V. M. Hamelers, and C. J. N. Buisman, "Influence of multivalent ions on power production from mixing salt and fresh water with a reverse electrodialysis system," *J. Memb. Sci.*, vol. 330, no. 1–2, pp. 65–72, 2009.

[136] Z. Y. Guo *et al.*, "Effect of ions (K + , Mg 2+ , Ca 2+ and SO 42−) and temperature on energy generation performance of reverse electrodialysis stack," *Electrochim. Acta*, vol. 290, pp. 282–290, 2018.

[137] R. Ortiz-Imedio, L. Gomez-Coma, M. Fallanza, A. Ortiz, R. Ibañez, and I. Ortiz, "Comparative performance of Salinity Gradient Power-Reverse Electrodialysis under different operating conditions," *Desalination*, vol. 457, pp. 8–21, May 2019.

[138] S. Tseng, Y. M. Li, C. Y. Lin, and J. P. Hsu, "Salinity gradient power: Influences of temperature and nanopore size," *Nanoscale*, vol. 8, no. 4, pp. 2350–2357, 2016.

[139] A. M. Benneker, T. Rijnaarts, R. G. H. Lammertink, and J. A. Wood, "Effect of temperature gradients in (reverse) electrodialysis in the Ohmic regime," *J. Memb. Sci.*, vol. 548, pp. 421–428, 2018.

[140] R. Long, B. Li, Z. Liu, and W. Liu, "Performance analysis of reverse electrodialysis stacks: Channel geometry and flow rate optimization," *Energy*, vol. 158, pp. 427–436, 2018.

[141] P. Długołecki, B. Anet, S. J. Metz, K. Nijmeijer, and M. Wessling, "Transport limitations in ion exchange membranes at low salt concentrations," *J. Memb. Sci.*, vol. 346, no. 1, pp. 163–171, 2010.

[142] E. Fontananova *et al.*, "Effect of solution concentration and composition on the electrochemical properties of ion exchange membranes for energy conversion," *J. Power Sources*, vol. 340, pp. 282–293, 2017.

[143] V. V. Wagholikar *et al.*, "Modeling cell pair resistance and spacer shadow factors in electro-separation processes," *J. Memb. Sci.*, vol. 543, no. August, pp. 151–162, 2017.

[144] D. A. Vermaas, D. Kunteng, M. Saakes, and K. Nijmeijer, "Fouling in reverse electrodialysis under natural conditions," *Water Res.*, vol. 47, no. 3, pp. 1289–1298, 2013.

[145] K. Chon, N. Jeong, H. Rho, J. Y. Nam, E. Jwa, and J. Cho, "Fouling characteristics of dissolved organic matter in fresh water and seawater compartments of reverse electrodialysis under natural water conditions," *Desalination*, p. 114478, Jun. 2020.

[146] F. Volpin *et al.*, "Energy recovery through reverse electrodialysis: Harnessing the salinity gradient from the flushing of human urine," *Water Res.*, vol. 186, p. 116320, Aug. 2020.

[147] A. H. Avci, R. A. Tufa, E. Fontananova, G. Di Profio, and E. Curcio, "Reverse Electrodialysis for energy production from natural river water and seawater," *Energy*, vol. 165, pp. 512–521, 2018.

[148] D. A. Vermaas, D. Kunteng, J. Veerman, M. Saakes, and K. Nijmeijer, "Periodic feedwater reversal and air sparging as antifouling strategies in reverse electrodialysis," *Environ. Sci. Technol.*, vol. 48, no. 5, pp. 3065–3073, 2014.

[149] J. Moreno, N. de Hart, M. Saakes, and K. Nijmeijer, "CO2 saturated water as two-phase flow for fouling control in reverse electrodialysis," *Water Res.*, vol. 125, pp. 23–31, 2017.

[150] A. Zoungrana, O. K. Türk, and M. Çakmakci, "Energy coverage of ataköy-ambarlı municipal wastewater treatment plants by salinity gradient power," *J. Water Process Eng.*, vol. 38, Dec. 2020.

[151] J. Luque Di Salvo, A. Cosenza, A. Tamburini, G. Micale, and A. Cipollina, "Long-run operation of a reverse electrodialysis system fed with wastewaters," *J. Environ. Manage.*, vol. 217, pp. 871–887, Jul. 2018.

[152] E. Güler, W. van Baak, M. Saakes, and K. Nijmeijer, "Monovalent-ion-selective membranes for reverse electrodialysis," *J. Memb. Sci.*, vol. 455, pp. 254–270, 2014.

[153] M. Vanoppen *et al.*, "Secondary treated domestic wastewater in reverse electrodialysis: What is the best pre-treatment?," *Sep. Purif. Technol.*, vol. 218, no. October 2018, pp. 25–42, 2019.

[154] S. Mehdizadeh, M. Yasukawa, T. Suzuki, and M. Higa, "Reverse electrodialysis

for power generation using seawater/municipal wastewater: Effect of coagulation pretreatment," *Desalination*, vol. 481, p. 114356, May 2020.

[155] J. Veerman, M. Saakes, S. J. Metz, and G. J. Harmsen, "Electrical power from sea and river water by reverse electrodialysis: A first step from the laboratory to a real power plant," *Environ. Sci. Technol.*, vol. 44, no. 23, pp. 9207–9212, 2010.

[156] N. Nam, J.-Y., Hwang, K.-S., Kim, H.-C., Jeong, H., Kim, H., Jwa, E., Yang, S. Choi, J., Kim, C.-S., Han, J., Jeong, "Assessing the behavior of the feed-water constituents of a pilotscale 1000-cell-pair reverse electrodialysis with seawater and municipal wastewater effluent," *Water Res.*, vol. 148, pp. 261–271, 2018.

[157] M. Tedesco, A. Cipollina, A. Tamburini, and G. Micale, "Towards 1 kW power production in a reverse electrodialysis pilot plant with saline waters and concentrated brines," *J. Memb. Sci.*, vol. 522, pp. 226–236, 2017.

[158] O. S. A. D'Angelo, M. Tedesco, A. Cipollina, A. Galia, G. Micale, "Reverse electrodialysis performed at pilot plant scale: Evaluation of redox processes and simultaneous generation of electric energy and treatment of wastewater," *Water Res.*, vol. 125, pp. 123–131, 2017.

[159] A. Ali, R. A. Tufa, F. Macedonio, E. Curcio, and E. Drioli, "Membrane technology in renewable-energy-driven desalination," vol. 81, no. September 2016, pp. 1–21, 2018.

[160] K. Kwon, J. Han, B. H. Park, Y. Shin, and D. Kim, "Brine recovery using reverse electrodialysis in membrane-based desalination processes," *Desalination*, vol. 362, pp. 1–10, 2015.

[161] R. Ashu, E. Curcio, E. Brauns, W. Van Baak, E. Fontananova, and G. Di, "Membrane Distillation and Reverse Electrodialysis for Near-Zero Liquid Discharge and low energy seawater desalination," *J. ofMembraneScience*, vol. 496, pp. 325–333, 2015.

[162] E. Mercer *et al.*, "Hybrid membrane distillation reverse electrodialysis configuration for water and energy recovery from human urine: An opportunity for off-grid decentralised sanitation," *J. Memb. Sci.*, vol. 584, pp. 343–352, Aug. 2019.

[163] R. A. Tufa *et al.*, "Integrated membrane distillation-reverse electrodialysis system for energy-efficient seawater desalination," *Appl. Energy*, vol. 253, p. 113551, Nov. 2019.

[164] R. Long, B. Li, Z. Liu, and W. Liu, "Hybrid membrane distillation-reverse electrodialysis electricity generation system to harvest low-grade thermal energy," *J. Memb. Sci.*, no. September, 2016.

[165] C. Y. Li, W., Krantz, W.B., Cornelissen, E.R., Post, J.W., Verliefde, A.R.D., Tang, "A novel hybrid process of reverse electrodialysis and reverse osmosis for low energy seawater desalination and brine ...," *Appl. Energy*, vol. 104, no. February, pp. 592–602, 2014.

[166] A. Daniilidis, R. Herber, and D. A. Vermaas, "Upscale potential and financial

feasibility of a reverse electrodialysis power plant," *Appl. Energy*, vol. 119, pp. 257–265, 2014.

[167] T. Rijnaarts, E. Huerta, W. Van Baak, and K. Nijmeijer, "Effect of Divalent Cations on RED Performance and Cation Exchange Membrane Selection to Enhance Power Densities," *Environ. Sci. Technol.*, vol. 51, no. 21, pp. 13028–13035, 2017.

[168] J. G. Hong and Y. Chen, "Nanocomposite reverse electrodialysis (RED) ion-exchange membranes for salinity gradient power generation," *J. Memb. Sci.*, vol. 460, pp. 139–147, 2014.

[169] E. Guler, Y. Zhang, M. Saakes, and K. Nijmeijer, "Tailor-made anion-exchange membranes for salinity gradient power generation using reverse electrodialysis," *ChemSusChem*, vol. 5, no. 11, pp. 2262–2270, 2012.

[170] A. Siria *et al.*, "Giant osmotic energy conversion measured in a single transmembrane boron nitride nanotube," *Nature*, vol. 494, no. 7438, pp. 455–458, 2013.

[171] Z. Zhang *et al.*, "Ultrathin and Ion-Selective Janus Membranes for High-Performance Osmotic Energy Conversion," *J. Am. Chem. Soc.*, vol. 139, no. 26, pp. 8905–8914, 2017.

[172] ISKI, "2018 Activity report," Istanbul, 2018.

[173] R. Audinos, "Electrodialyse inverse. Etude de l'energie electrique obtenue a partir de deux solutions de salinites differentes," *J. Power Sources*, vol. 10, no. 3, pp. 203–217, 1983.

[174] X. Zhu, W. He, and B. E. Logan, "Influence of solution concentration and salt types on the performance of reverse electrodialysis cells," *J. Memb. Sci.*, vol. 494, pp. 154–160, 2015.

[175] "Energy Overview of Turkey." [Online]. Available: https://www.geni.org/globalenergy/library/national_energy_grid/turkey/EnergyOverviewofTurkey.shtml. [Accessed: 21-Feb-2020].

[176] "DSİ - SVT Rasatlar Bilgi Bankası." [Online]. Available: http://svtbilgi.dsi.gov.tr/Sorgu.aspx. [Accessed: 02-Apr-2020].

[177] Ç. Tanriverdi, A. Alp, A. R. Demirkiran, and F. Üçkardeş, "Assessment of surface water quality of the Ceyhan River basin, Turkey," *Environ. Monit. Assess.*, vol. 167, no. 1–4, pp. 175–184, 2010.

[178] Mehmet Ozcelik, "Impact of the cascade hydropower construction (HPC) on water quality of the Seyhan River, Turkey," *Hittite J. Sci. Eng. 2018, 5 125-135*, vol. 2, 2018.

[179] Z. Demirel, Z. Özer, and O. Özer, "Investigation and modeling of water quality of Göksu River (Cleadnos) in an international protected area by using GIS," *J. Geogr. Sci.*, vol. 21, no. 3, pp. 429–440, 2011.

[180] Z. He, X. Gao, Y. Zhang, Y. Wang, and J. Wang, "Revised spacer design to improve hydrodynamics and anti-fouling behavior in reverse electrodialysis

processes," *Desalin. Water Treat.*, vol. 57, no. 58, pp. 28176–28186, 2016.

[181] A. Zoungrana, İ. H. Zengin, O. K. Türk, and M. Çakmakcı, "Ammoniacal nitrogen reclamation by membrane distillation from high ammonia polluted solutions," *Chem. Pap.*, vol. 74, no. 6, pp. 1903–1915, 2020.

[182] A. Zoungrana *et al.*, "The treatability of landfill leachate by direct contact membrane distillation and factors influencing the efficiency of the process," *Desalin. Water Treat.*, vol. 71, 2017.

[183] A. C. S. Talari, M. A. G. Martinez, Z. Movasaghi, S. Rehman, and I. U. Rehman, "Advances in Fourier transform infrared (FTIR) spectroscopy of biological tissues," *Appl. Spectrosc. Rev.*, vol. 52, no. 5, pp. 456–506, 2017.

[184] J. Coates, "Interpretation of Infrared Spectra, A Practical Approach," *Encycl. Anal. Chem.*, pp. 10815–10837, 2006.

[185] D. A. Vermaas, M. Saakes, and K. Nijmeijer, "Doubled power density from salinity gradients at reduced intermembrane distance," *Environ. Sci. Technol.*, vol. 45, no. 16, pp. 7089–7095, 2011.

[186] X. Zhu, W. He, and B. E. Logan, "Reducing pumping energy by using different fl ow rates of high and low concentration solutions in reverse electrodialysis cells," *J. Memb. Sci.*, vol. 486, pp. 215–221, 2015.

[187] A. M. Weiner, R. K. McGovern, and J. H. Lienhard V., "A new reverse electrodialysis design strategy which significantly reduces the levelized cost of electricity," *J. Memb. Sci.*, vol. 493, pp. 605–614, 2015.

[188] I. O. L. Gómez-Coma, V.M. Ortiz-Martínez, M. Fallanza, A. Ortiz, R. Ibañez, "Blue energy for sustainable water reclamation in WWTPs," *J. Water Process Eng.*, vol. 33, no. August 2019, 2020.

PUBLICATIONS FROM THE THESIS

Contact Information: zoungson1@gmail.com

Papers

1. A. Zoungrana, M. Çakmakci, ''Optimization of the Reverse Electrodialysis Power Output through the Ratio of the Feed Solutions Salinity,'' IET Renewable Power Generation., 00:1-9 , 2021.

2. A. Zoungrana, M. Çakmakci, ''From Non-renewable Energy to Renewable by Harvesting Salinity Gradient Power by Reverse Electrodialysis: A Review,'' Int. J. Energy Res., Vol., pp. 1–28, 2020.

3. A. Zoungrana, Ç. Aksel, O. K. Türk, and M. Çakmakci, ''Reverse Electrodialysis Salinity Gradient Power Potential of Treated Municipal Wastewaters Used as Diluted Solution,'' Int. J. Global Warm., Vol., 2021.

4. A. Zoungrana, O. K. Türk, and M. Çakmakci, "Energy coverage of ataköy-ambarlı municipal wastewater treatment plants by salinity gradient power," J. Water Process Eng., vol. 38, Dec. 2020.

Conference Papers

1. A. Zoungrana, O. K. Türk, and M. Çakmakci, ''Energy Production by Reverse Electrodialysis Fed with treated Wastewater by Advanced Biological Process'' 5th Eurasia Waste Management Symposium, Istanbul, 2020.

Projects

1. Energy Generation Potential by Reverse Electrodialysis (Ters Elektrodiyaliz İle Enerji Üretim Potansiyeli), Yildiz Technical University Scientific Research Projects (Grant No: FDK-2020-3860), Researcher, 2020.